COMPUTER SIMULATION FOR STRATIFIED THERMAL STORAGE

By

FRED JOHN OPPEL III

Bachelor Science in Mechanical Engineering

Oklahoma State University

Sitllwater, Oklahoma

1983

Submitted to the Faculty of the Graduate College
of the Oklahoma State University
in partial fulfillment of the requirements
for the Degree of
MASTER OF SCIENCE
July, 1985

COMPUTER SIMULATION FOR STRATIFIED

THERMAL STORAGE

Thesis Approved:

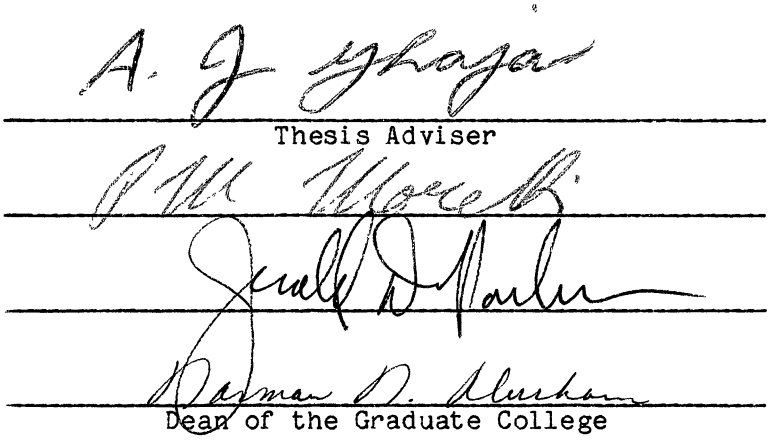

Thesis Adviser

Dean of the Graduate College

PREFACE

I would like to to express my gratification to all the people who assisted my work during my stay at Oklahoma State University. In particular, I am deeply indebted to my major adviser, Dr. A. J. Ghajar, for his invaluable guidance, knowledge, and concern throughout this work. Appreciation is also given to Dr. P. M. Moretti for his helpful suggestions and time. I would also like to thank Dr. J. D. Parker for taking the time to be on my committee.

I must also thank Yousef Zurigat, Cliff Eberle, and Stephen Mitchell for their assistance and encouragement given to me during my study. I would like to thank Mrs. Neisa Lock for helping me to prepare my thesis for the final draft.

Special thanks are due to the School of Mechanical and Aerospace Engineering and to the University Center for Energy Research for the financial assistance that I received during the course of this work.

I would especially like to thank my parents and my fiancee', Susan McCain, for their special love and understanding given to me during this study.

TABLE OF CONTENTS

LIST OF TABLES

LIST OF FIGURES

NOMENCLATURE

ENGLISH SYMBOLS

a	-	above diagonal term in Tridiagonal Matrix, see Eqn. (3.5)
A	-	multiplication coefficient in EDDY equation, see Eqns. (4.1)-(4.3)
AMIX	-	dimensionless mixing parameter, AMIX=(EDDY)(Fo)
b	-	below diagonal term in Tridiagonal Matrix, see Eqn. (3.5)
B	-	intercept ceofficient in EDDY equation, see Eqns. (4.1)-(4.3)
c	-	right side term in Tridiagonal Matrix, see Eqn. (3.5)
C_p	-	constant pressure specific heat
d	-	diagonal term in Tridiagonal Matrix, see Eqn. (3.5)
D	-	inside tank diameter
EDDY	-	dimensionless eddy conductivity factor, EDDY = $(\alpha + \varepsilon)/\alpha$
E_{INLET}	-	inlet value of dimensionless eddy conductivity factor
^oF	-	degrees Fahrenheit
FLOW	-	dimensionless flow parameter, FLOW=$V\Delta t/\Delta x$
Fo	-	dimensionless Fourier number, Fo=$\alpha\Delta t/\Delta x^2$
g	-	gravity constant
ISLAB	-	location at slab I
k	-	thermal conductivity
L	-	effective length between inlet and outlet

M - multiplication coefficient in inlet eddy conductivity equation, see Eqn. (6.1)

N - exponential coefficient in inlet eddy conductivity equation, see Eqn. (6.1)

NSLAB - total number of slabs in tank

Re - Reynolds number, $Re = VD/\nu_{avg}$

Ri - Densimetric Richardson number, $Ri = (\Delta\rho gL)/(\rho_{avg}V^2)$

t - time

T - temperature

V - velocity inside tank

x - vertical direction in tank

X1,X2,X3 - least squares coefficients, see Eqn (C.4)

Y1,Y2,Y3 - least squares coefficients, see Eqn (C.5)

GREEK SYMBOLS

α - thermal diffusivity, $\alpha = k/\rho C_p$

$\Delta\rho$ - density difference between initial and inlet temperatures

Δx - incremental tank height

Δt - incremental time step

ΔT - temperature difference between initial and inlet

ϵ - eddy conductivity factor

ρ - density

ν - kinematic viscosity

SUBSCRIPTS

avg	-	average property between inlet and initial
in	-	inlet property
n	-	north of the point of interest
o	-	initial property
p	-	point of interest
s	-	south of the point of interest
slab	-	slab property
sol	-	solution

SUPERSCRIPT

'	-	value at new time level

CHAPTER I

INTRODUCTION

The efficiency of thermal energy systems can usually be improved by providing for thermal storage of hot and cold water. For example, in solar space heating systems the energy stored during the day can make solar energy available at night for heating. For large air conditioning systems, utility costs may be reduced by operating the equipment at night during low off-peak electricity rates, and using this chilled water that was stored during the night to meet the load demand the next day. With the rising utility costs, the promise of dollar savings with storage is encouraging. Yet acheiving these savings requires investigating the capability of obtaining a storage device to keep the hot and cold fluids from blending.

The design of the device used to store thermal energy is important. The energy placed into this device should be extractable when needed. The simplest model of such a device is the single well-mixed storage tank. This model does not separate the hot and cold fluids in the tank; therefore, this design recovers only a small portion of this energy.

Another approach is the use of multiple storage tanks. This model can improve on the recoverable energy extracted from the system, yet it doubles the tank capacity and requires the cost and complexity of several tanks and many connections.

A third approach is to use a single tank which uses stratification to separate the hot and cold fluids. Here the hot water with the low density is floated directly on top of the cool water with the higher density, resulting in the advantages of the two tank system, but with a single tank. The inlet fluid must be placed within the tank with minimal disturbance with the existing fluid in the tank. The success of this scheme depends upon the design of the inlet; one design of an inlet has been demonstrated in Reference [6].

Some analytical models for a single storage tank are present in the literature, see References [5] and [6]. These models did not accurately predict the temperature profiles inside a single storage tank for the dynamic case of flow through the tank. They both underestimated the mixing occurring inside the tank. They also did not consider the inlet geometry as a function of the mixing occurring inside the tank. Therefore, the general objective of this work is to develop an analytical model which predicts the turbulent mixing occurring inside the tank, and also study the effect of the inlet design on the turbulent mixing. Using this analytical model, a computer program can be developed which will predict the temperature profile in the storage tank as a function of time, if the history of inlet flow and temperatures is provided. These profiles will predict the water temperature at the tank outlet. Such a program is not only a testable end product and an enhancement of our stratification simulation capability, but it is also a useful input into a total system simulation project.

1.1 Objectives

The objectives of this study are as follows:

(1) Determine an analytical model which will correctly predict the change in storage status due to mixing for various through flow situations.

(2) Develop a computer program to simulate the temperature profiles in the tank.

(3) Examine the significant physical parameters of the tank and its inlet configuraion.

(4) Obtain a functional relationship for the mixing inside the tank, represented by an eddy conductivity factor, in terms of the pertinent dimensionless numbers (i.e. Reynolds number, Richardson number) and the inlet configuration.

1.2 Method Of Approach

The problem analysis included the following phases:

(1) Perform a literature survey in order to analyze the pertinent models and experimental data for thermal stratified storage (see Chapter II).

(2) Develop the analytical tools necessary for this model (see Chapter III).

(3) Develop the numerical model (computer program) from the analytical model (see Chapter III).

(4) Simulate the available experimental data in the literature (see Chapter IV).

(5) Build an experimental setup to obtain data and simulate this data (see Chapter V).

(6) Determine the general form of the eddy conductivity factor as a function of dimensionless numbers for the inlets investigated (see Chapter VI).

CHAPTER II

LITERATURE SURVEY

This chapter reviews only the papers pertinent to this work. The analytical models and the available experimental data are discussed for each paper. A listing of other papers, both directly and indirectly related to stratified thermal storage, is presented in Appendix A.

2.1 Pertinent Papers

(1) Sha and Lin [1] have developed a three-dimensional, transient, single-fluid, single-phase mathematical model. In this model, the conservation of energy, mass, and momentum are solved using finite difference implicit techniques. The model is designated as COMMIX-SA (COMponent MIXing-Solar Application). The predictions of this model were in good agreement with the experiments in Reference [1]. Yet, this model is too complex and computationally intensive to be used as part of a total energy simulation package. This paper did not supply enough information on the tank dimensions and flow properties in order to compare our computer model with their model.

(2) Lavan and Thompson [2] did a detailed experimental study of stratified hot water storage tanks and developed an empirical model of tank efficiency as a function of Reynolds number, Grashof number, and height-to-diameter ratio. They systematically studied the effects of geometric and dynamic parameters on thermal stratification. Their

results indicate that stratification improves with increasing L/D, increasing temperature difference between initial temperature and inlet temperature, and increasing the inlet and outlet port diameters; while stratification decreases with increasing flow rates. Their data show that efficiency levels off for L/D ratios greater than 3 or 4. Their study also reveals that stratification is best maintained for tanks with walls made of plastic, concrete, or other materials of low conductivity. All of their experimental results were given in terms of extraction efficiency and parameters discussed above. No temperature profiles inside the tank as a function of time were presented. Thus no simulation runs were executed for the computer model in our work.

(3) Sliwinski [3] attempted to identify a set of dimensionless parameters to predict the degree of stratification during the thermal charging of storage tanks. His results show that the position and sharpness of the thermocline were a function of the Richardson and Peclet numbers. A critical value of Richardson number around 0.25 was observed below which stratification does not occur. His paper did not present sufficient information on temperature profiles and flow rate so that a simulation of his experimental data could be performed.

(4) The paper by Cabelli [4] includes a one-dimensional, transient, semiinfinite, conduction model for adiabatic walls. Geometric configurations include both horizontal and vertical entry into the tank. The effect of the entrance Reynolds number and contribution of buoyancy in promoting stratification were examined. This paper did not present any experimental data.

(5) Han et al. [5] made comparative studies on the thermal performance of three one-dimensional models; a mixed model, a stratified model, and a viscous entrainment model. The Fully Mixed Storage Tank (FMST) model did not allow for temperature stratification inside the tank and therefore, the thermal performance was usually understated. To account for the thermal stratification effects, a Fully Stratified Storage Tank (FSST) model was developed. The FSST model divides the storage tank into N-segments of equal volume and considers an energy balance in each segment. This model tends to understate the thermal stratification by diffusing the temperature profiles. It also tends to overstate the temperature stratification when turbulent mixing occurs at the inlet. To overcome the discrepancies encountered by the FSST model, a Viscous Entrainment Storage Tank (VEST) model was developed. The VEST model incorporated the viscous entrainment effects and turbulent mixing occurring at the inlet. This model utilizes the equations of mass and energy balance at each section of the tank along with the equation of the rate of viscous entrainment. A finite difference method was used to solve these equations. The VEST model was an improvement over the FSST model, but it still did not accurately predict the experimental data presented in the paper as shown in Figure 1. Insufficient information on the tank and flow properties of their experiment for input into the computer model did not allow for simulation of their data and a comparison of their models.

(6) Sharp et al. [6] present a new stratification enhancement device which consists of a porous manifold inlet. This inlet was designed to accommodate a variable inlet temperature while maintaining stratification inside the tank. The porous manifold lets the inlet flow

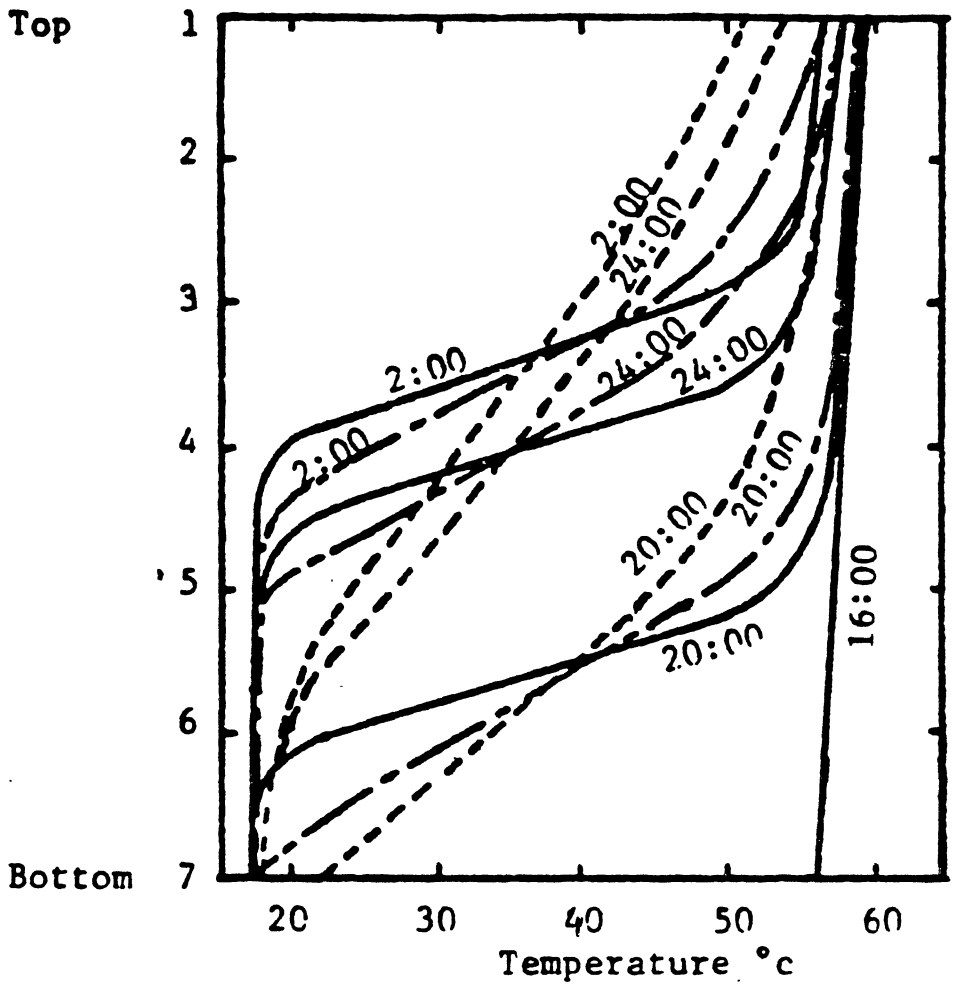

Figure 1. Comparison of the Storage Tank Temperature Profiles During the Load Time, Taken from Reference [5] (—— : Experiment, --- : Fully Stratified Model, —— : Viscous Entrainment Model)

enter at the elevation corresponding to its temperature. Testing of this inlet does show that stratification was preserved for the variable inlet temperature. Yet, results show that better stratification was obtained when the inlet temperature was constant and beyond the extreme temperatures inside the tank. A one-dimensional, explicit, numerical, finite-difference model has been presented. This model divides the tank into N isothermal constant volume segments. An energy balance for each segment was performed consisting of convective energy, conductive energy, and energy loss to the environment. The tank contains two flow loops; a collector loop which charges the tank with hot water collected from the solar panels, and a load loop which extracts the energy for heating purposes. Both loops can operate simultaneously or individually with different flow rates in each loop. This model predicted a temperature profile that was diffused more than the experimental data presented in the paper as shown in Figure 2. The experimental data presented in Reference [6] are depicted in terms of temperature versus tank height at a specific time for the porous inlet. Their paper contains sufficient information so that the present model can be compared with their model.

(7) Adoly [7] presented a model based entirely on conduction. This model produced adequate results for the static (no flow situation) stratified case. When comparing this model for the dynamic stratified case which involved mixing and convection, the model was in error. This paper presents several types of experimental data for both static and dynamic stratified cases. In each case, both insulated and uninsulated experimental data were obtained for a variety of flow rates. The cylindrical test tank contained circular baffles at each end with 561

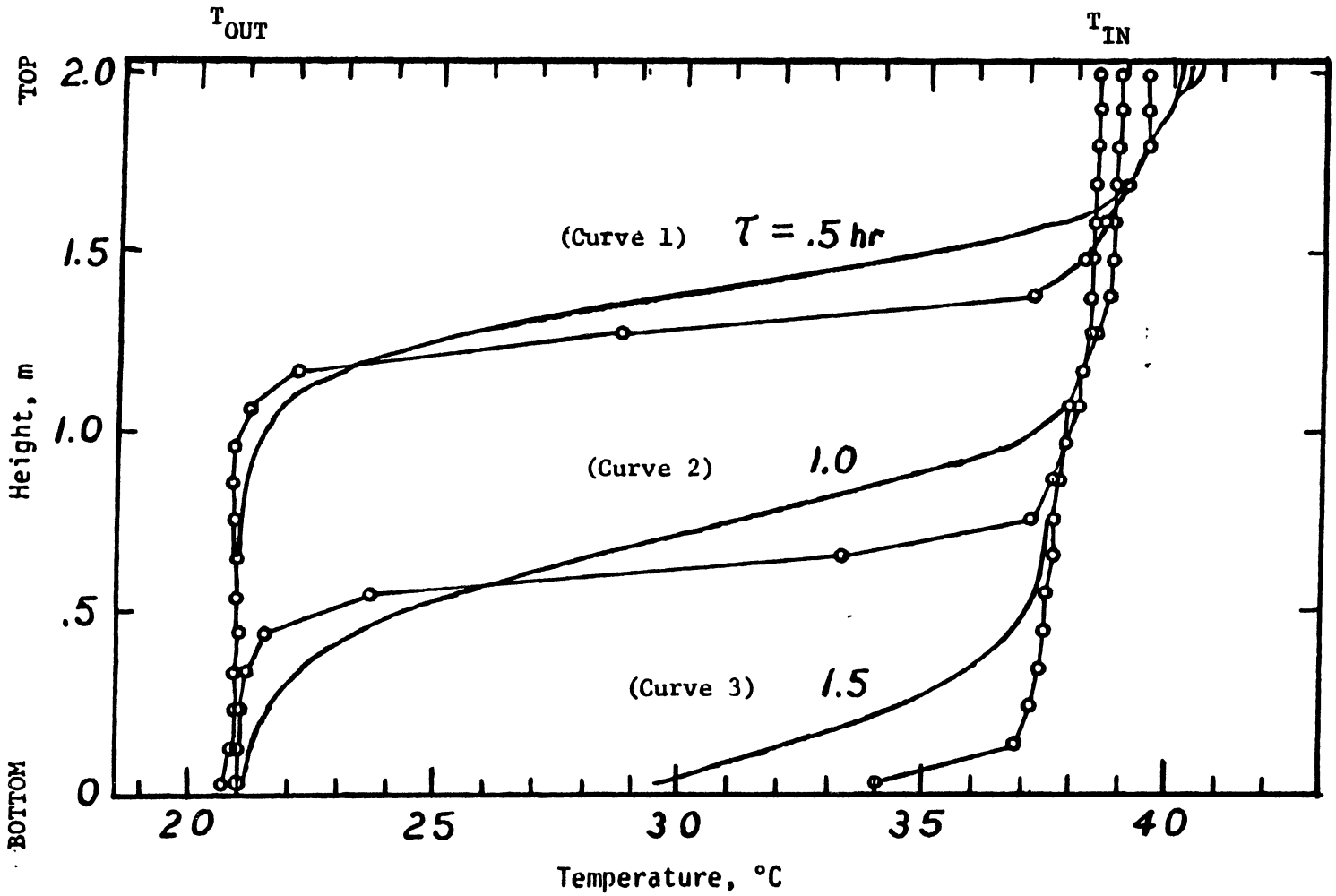

Figure 2. Prototype Manifold, Charging 6 gpm, Taken from Reference [6] (—— : Experiment, —o— : Prediction from [6])

drilled holes for a total opening area of 0.078 square feet per baffle. The percent of recoverable energy and the thermocline thickness were evaluated for each set of data. As the flow rate increased, the percent of recoverable energy decreased, and the thermocline thickness increased. The experimental data presented in this paper contain the information needed for input into our computer model. The data consisted of outlet temperature versus time. All the data obtained were for the tank and inlet design described above.

(8) Cole and Bellinger [8] describe how solar system tanks fail to stratify, and suggest a new solar system control strategy that allows for better stratification. Failure to stratify was explained in terms of the critical Richardson number, which they reported as being below 0.25. They developed a one-dimensional analytical model which was based on the following assumptions: 1) the solution is a function of elevation and time only, 2) plug flow exists, 3) constant flow rate, 4) constant cross-sectional areas of both the tank and tank wall 5) a step change of inlet temperature such that cold water enters the bottom of the tank and hot water enters the top of the tank, 6) heat transfer between the tank wall and the water, and 7) negligible thermal losses from the tank. The empirical constants in their analytical model are determined by using a least squares fit of their experimental data, and correlating the constants with the Fourier and Richardson numbers. The effect of mixing at the inlet can be accounted for by including an empirical constant in the analytical model. They define a stratification index by which the performance of tanks containing various inlet configurations can be compared, where a perfectly stratified tank has an index of 1. They present experimental

data for several different types of baffle and diffuser designs as follows: 1) Side inlet and outlet, 2) Dip tube, 3) Dual concentric baffles, 4) Single horizontal baffle, and 5) Dual radial-flow diffusers. The three best designs were side inlet and outlet, single horizontal baffle, and the dual radial-flow diffusers. They performed tests on each design while keeping the flow rate and temperature difference constant as shown in Figure 3. Thus the functional relationship of eddy conductance with different inlet configurations may be examined. Their experimental data contained sufficient information to compare against a simulation.

(9) Chaney et al. [9] studied the thermocline development through a cubical enclosure with both strongly-conducting and weakly-conducting walls. Flow visualization revealed that a buoyant force occurred for both cases. During the charging period (i.e. hot inlet water) of an energy storage cycle, an upward-directed buoyant force on the fluid next to the wall was established in the colder region of the tank for the strongly-conducting case. This was in contrast to the weakly-conducting walls wherein a downward-directed force on the near-wall fluid occurred through out the entire region of the tank. The motions induced by these forces were relatively weak compared to the main flow. The accummulative influence of buoyant forces was most noticeable for inflows with small Peclet number and stongly-conducting walls. An analytical model of the transient, one-dimensional, energy conservation equation was developed and predicted results similar to the experimental data presented in the paper. The inlet of the rectangular test tank consisted of a 2 inch PVC diffuser pipe projected into the sidewalls of the tank with twenty 1/4 inch holes. Dimensionless plots of temperature

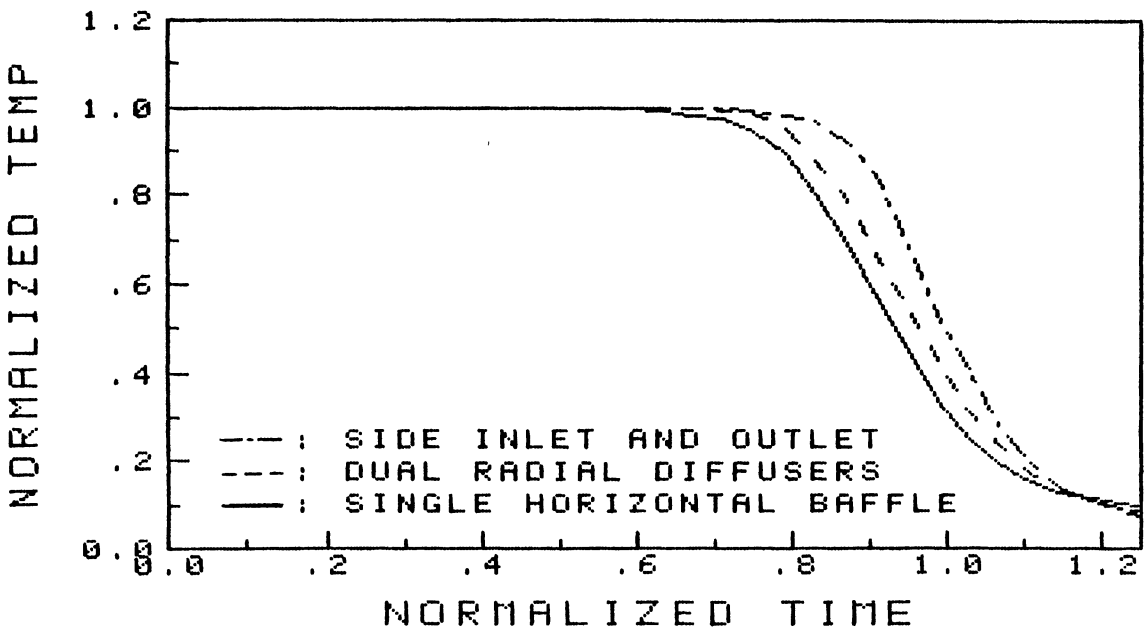

Figure 3. Discharge Tests of Prototype Tank with Different Inlets at 0.75 1/min and 40 ^{0}C Temperature Difference, Taken from Reference [8]

and height were presented along with a Reynolds number and Peclet number. Sufficient information could be obtained from the dimensionless plots and numbers so that a simulation could be performed. This paper was found when the completion of our work was at hand, therefore simulation of this data was not performed at this time.

From this review of the pertinent literature, it can be concluded that the analytical models underpredict the amount of mixing occurring inside the tank. Thus there is a need to develop an analytical model that incorporates the mixing occurring inside the tank.

CHAPTER III

TANK MODEL

This chapter covers the development of the analytical one-dimensional model. The assumptions on which the model is based are presented. The governing differential energy equation for the physical model contains both the conduction and convection terms. Two special cases are examined; namely the conduction-only case and the convection-only case. Both cases are analyzed independently since the results for each case are readily known. The buffer tank concept is introduced to eliminate the artificial viscosity in the convection-only case in order to allow for variable flow rates. The algorithms developed in both cases are combined in a logical fashion to simulate the total effect. The necessary boundary conditions for the computer program and the stability requirements for the convection-only case are also presented.

3.1 Physical Model

The storage geometry modeled is a vertical cylindrical tank. The assumptions on which the model is based are as follows:

(1) One-dimensional fluid flow and heat conduction, which means that the thermocline is axisymmetric and independent of the radial distance. Agreement of this assumption with experiments is acknowledgeed by the authors in [6].

(2) Small losses due to conduction through the walls of the tank, achieved by insulating the tank. This assumption predicts that the changes of the thermocline are dominated by conduction and convection of the fluid instead of conduction through the walls. This is in agreement with authors of [7] if the tank is insulated to obtain maximum efficiency.

(3) The walls of the tank are not overly massive, reducing the tendency of the tank to retain heat within the walls, and minimizing conduction of heat down the walls of the tank. This is in agreement with [7].

(4) The inlet temperature of the flow is beyond the extremes of the temperatures within the tank. That is, the temperature of fluid flowing in the top of the tank must be at least as hot as the temperature of fluid at the top of the tank, and the converse must be true for the cold temperature at the bottom inlet.

The equation governing the stratified thermal model for conduction and convection is the energy equation:

$$\rho \frac{DT}{Dt} = \frac{k}{C_p} \nabla^2 T \tag{3.1}$$

where D/Dt is the substantial derivative. Now applying this to one-dimensional flow in the x-direction which is assumed to be positive upward, Equation (3.1) reduces to:

$$\frac{\partial T}{\partial t} + V \frac{\partial T}{\partial x} = \alpha \frac{\partial^2 T}{\partial x^2} \tag{3.2}$$

Equation (3.2) can be split into two special cases; namely the conduction case (involving only mixing with no flow) and the convection case (involving only flow with no mixing). Numerical procedures will be applied to Equation (3.2) concerning the two special cases in order to verify the simulated results, since the theoretical results for the two cases are known as shown in Figures 4 and 5 for the conduction and convection cases respectively.

3.2 Conduction-Only Model

This special case of only conduction depleting the thermocline occurs when the velocity terms in the governing equation are zero. Thus Equation (3.2) reduces to the following form.

$$\frac{\partial T}{\partial t} = \alpha \frac{\partial^2 T}{\partial x^2} \tag{3.3}$$

The numerical approximation of the derivatives in Equation (3.3) is obtained from the fully implicit finite-difference method (see Reference [10]). By expanding the left hand side (the time derivative) using the first order forward finite-difference formula and expanding the right hand side (the second derivative of temperature) using the second order central finite-difference formula, Equation (3.3) is transferred into the numerical equation shown in Equation (3.4) where the superscript (prime) represents the temperature at the new time step and the subscripts n, p, and s represent the temperature north or above slab p, the temperature in slab p, and the temperature south or below slab p.

$$\frac{T'_p - T_p}{\Delta t} = \alpha \frac{T'_n - 2T'_p + T'_s}{\Delta x^2} \tag{3.4}$$

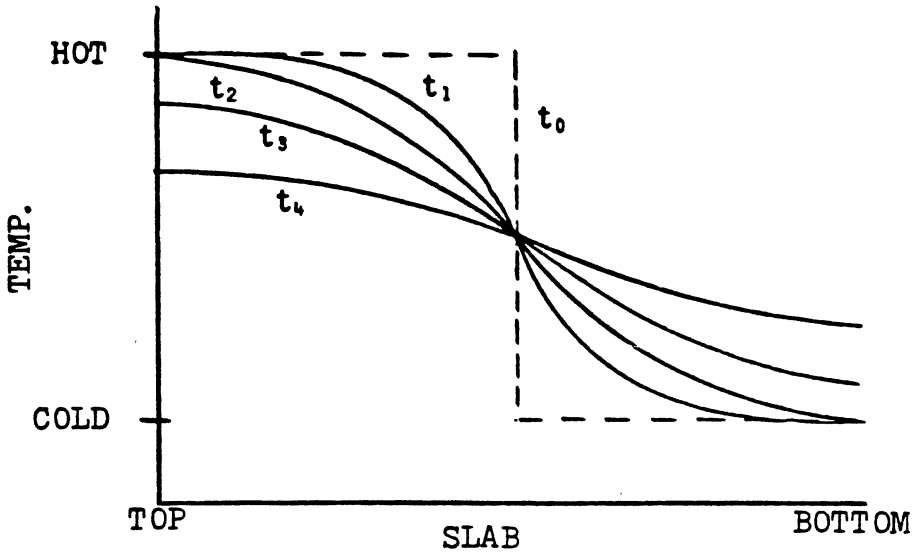

Figure 4. Temperature Profile in the Tank for the Theoretical Conduction-Only Case as Time Increases

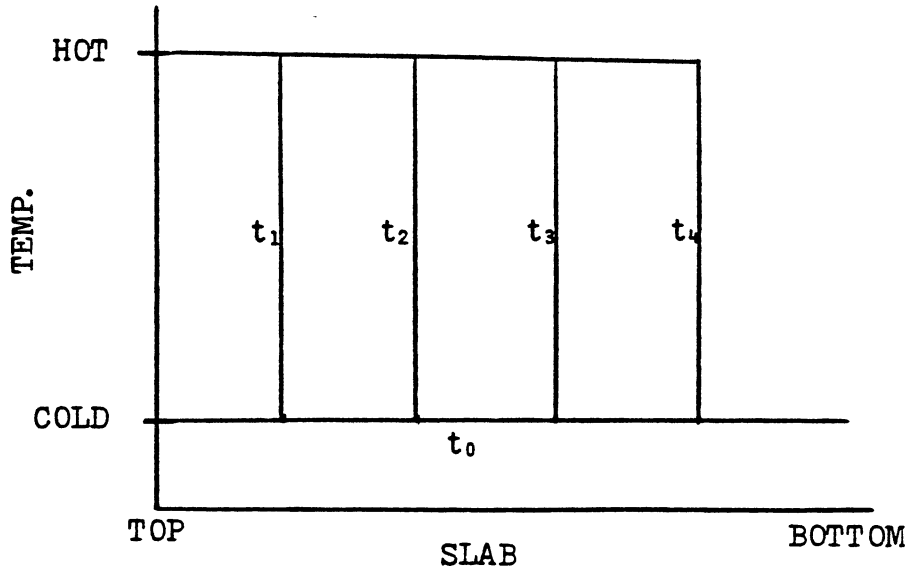

Figure 5. Temperature Profile in the Tank for the Theoretical Convection-Only Case as Time Increases

Define Fo = $\alpha\Delta t/\Delta x^2$ (the "finite-difference" Fourier number) and AMIX = (EDDY)(Fo) (nondimenional mixing parameter), where EDDY is the nondimensional eddy conductivity factor. Let EDDY = $(\alpha + \varepsilon)/\alpha$ where ε depends on mixing and is similar to an eddy conductivity. Laminar mixing contains the following properties: $\varepsilon = 0$, EDDY = 1, and AMIX = Fo. Solve Equation (3.4) for the unknown temperatures on the left and the remaining known temperature on the right to obtain the tridiagonal form. The tridiagonal matrix algorithm will be used to solve Equation (3.4) for the three unknown temperatures at the new time step. Equation (3.5) sufficiently predicted the form of the theoretical curves in Figure 4 for any value of AMIX.

$$b\,T'_s + d\,T'_p + a\,T'_n = c \qquad (3.5)$$

where

$b = -AMIX$

$d = 1 + 2AMIX$

$a = -AMIX$

$c = T_p$

3.3 Convection-Only Model

The convection model, also known as the flow-only model, involves water flowing through the tank with no mixing of temperatures between the water initially in the tank and the incoming water. Thus we obtain perfect stratification in the tank and recover 100 percent of the energy put into the tank. The simplified equation for this situation for the one-dimensional case with the conduction term equal to zero is as

follows:

$$\frac{\partial T}{\partial t} + V \frac{\partial T}{\partial x} = 0 \tag{3.6}$$

To obtain the numerical equation, the upwind differencing technique was used in order to compensate for the directional change of water when flowing either into the top or bottom of the tank (see Reference [10]). Figure 6 depicts the notation used for the tank. Solving for the temperature at the new time level and defining FLOW = $V\Delta t/\Delta x$ (also known as the Courant number in Reference [10]) where V is the velocity magnitude, we obtain Equation (3.7) for water flowing into the top of the tank and Equation (3.8) for water flowing into the bottom of the tank.

$$T'_p = (\text{FLOW})\ T_n + (1 - \text{FLOW})\ T_p \tag{3.7}$$

$$T'_p = (\text{FLOW})\ T_s + (1 - \text{FLOW})\ T_p \tag{3.8}$$

For insuring stability of Equations (3.7) and (3.8), the FLOW parameter cannot be greater than 1. Since the stratified case or convection-only case contains no mixing (i.e. EDDY = 0), the temperature profile should resemble the plot shown in Figure 5. Notice that the temperature of the incoming flow replaces the previous temperature of the slab and continues to march toward the exit of the tank as the time elapses. The equation that would produce the temperature profile for water flowing into the top of the tank as shown in Figure 5 is given by Equation (3.9).

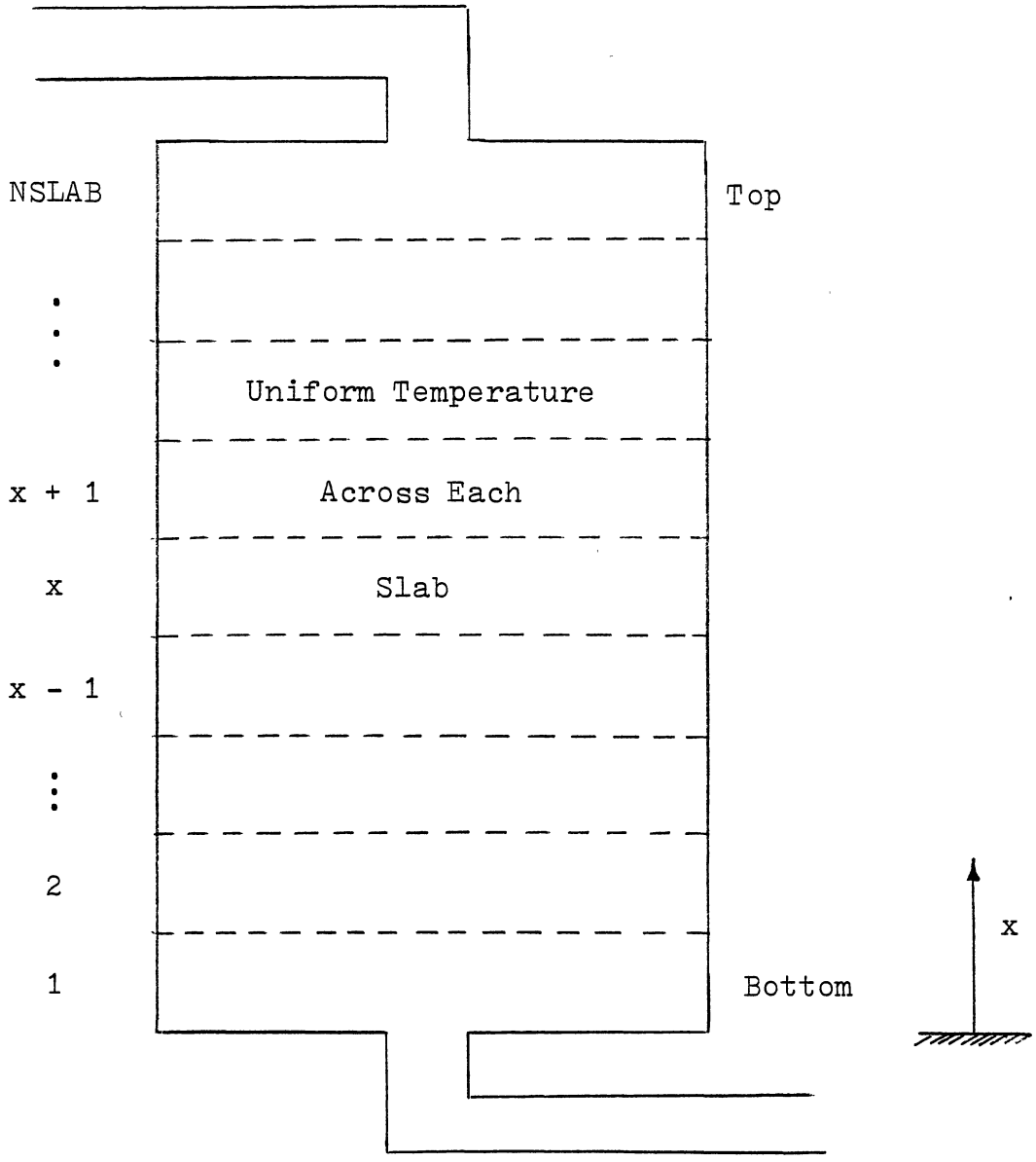

Figure 6. One-dimensional Tank Pictorial

$$T'_p = T_n \tag{3.9}$$

When trying to simulate the temperature profile in Figure 5 with Equation (3.7), we see that the FLOW parameter must equal one. The simulated results with FLOW = 1 are shown in Figure 7. If FLOW is less than 1, our algorithm produces a temperature profile as shown in Figure 8. Notice that this temperature profile is not correct for the stratified flow case. The situation of FLOW = 1 implies that the incoming flow of water must fill up one slab volume in the tank during the time interval of calculation, Δt. Therefore, if Δt and Δx are a fixed value, the velocity of the incoming flow is restricted to $V = \Delta x/\Delta t$ for FLOW = 1. Thus the flow rate must remain constant. If FLOW < 1, then we obtain pseudo-mixing (also known as numerical diffusion or artificial viscosity in Reference [10]). Figure 9 depicts how the artificial viscosity is obtained from the numerical equation. T_{slab} must represent the temperature of the entire slab when the time of calculation is performed. If the flow has not filled up the entire slab during Δt (i.e. FLOW < 1), then T_{slab} must be some average of T_{in} (inlet temperature) and T_o (initial temperature) instead of $T_{slab} = T_{in}$ when FLOW = 1.

To overcome the problem of not being able to vary the flow rate of the incoming flow in the algorithm, two fictitious buffer tanks are placed at the ends of the main tank as shown in Figure 10. The purpose of using the buffer tanks was to allow for a variable flow rate and eliminate the pseudo-mixing in the algorithm when FLOW < 1. The buffer tanks store the incoming flow of water when FLOW < 1 and continue to

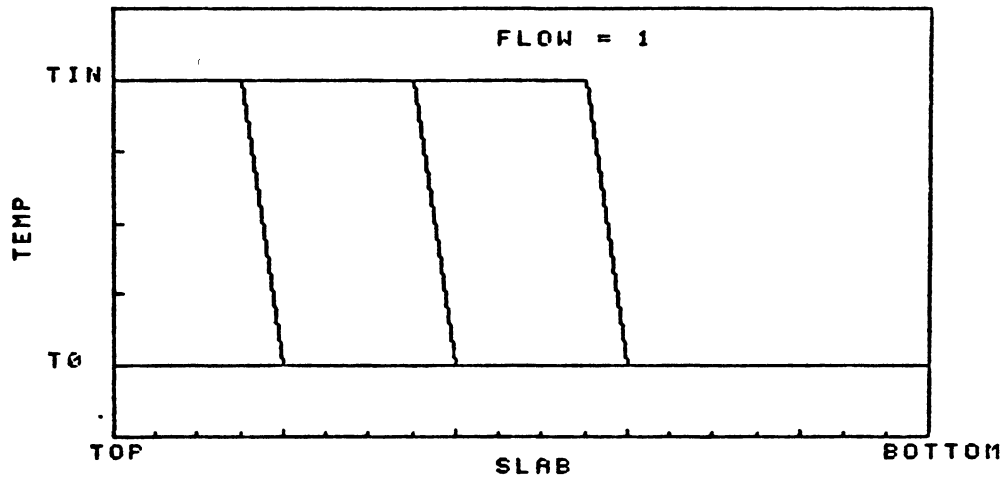

Figure 7. Temperature Profile in the Tank for the Numerical Convection-Only (FLOW=1) Case as Time Increases

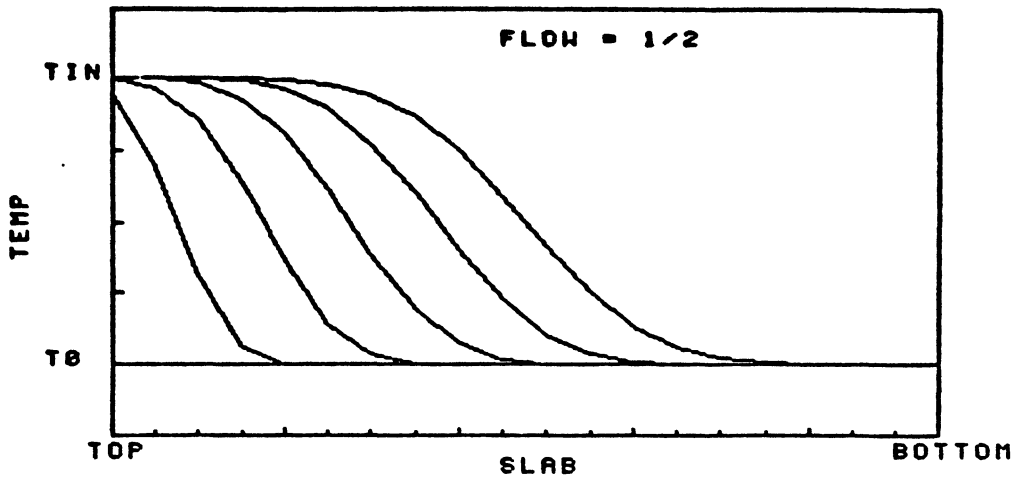

Figure 8. Temperature Profile in the Tank for the Numerical Convection-Only (FLOW=1/2) Case as Time Increases

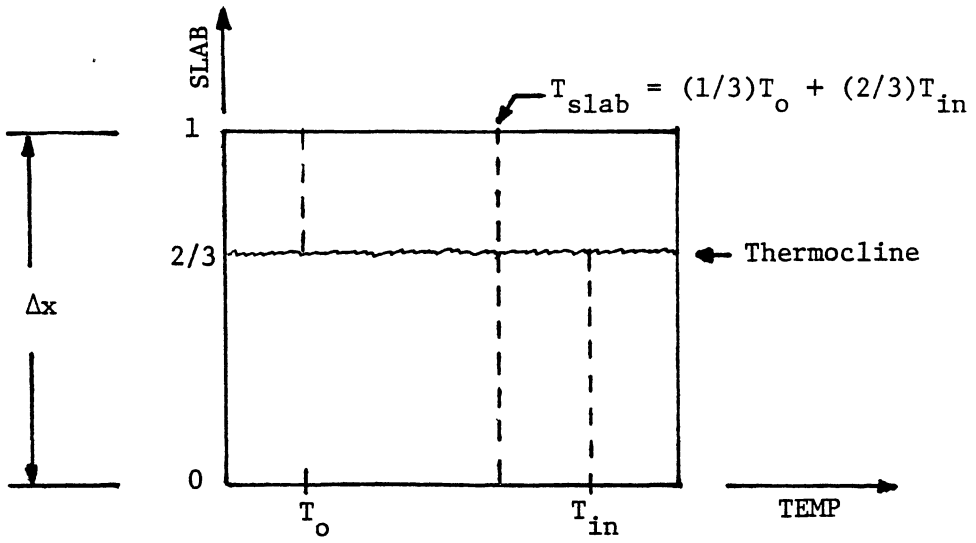

FLOW < 1

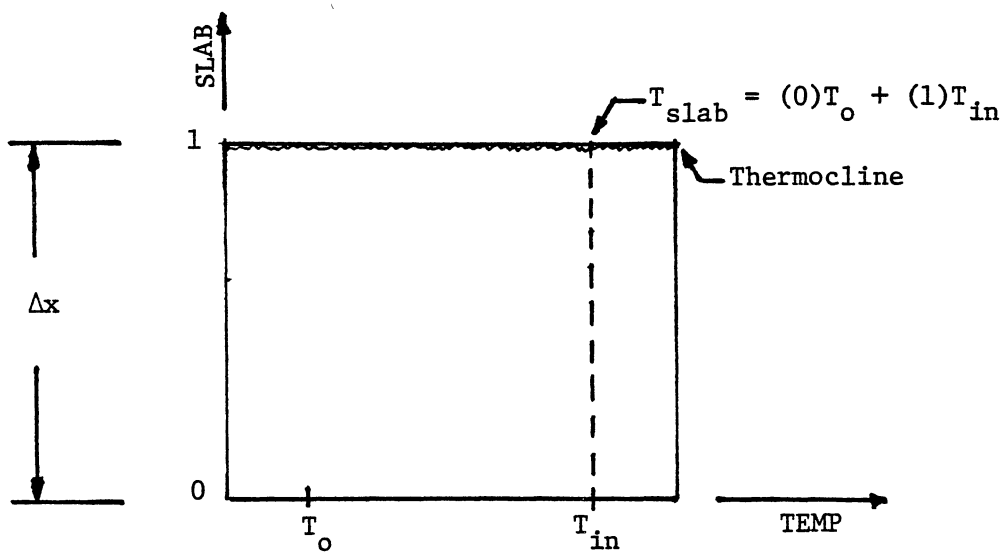

FLOW = 1

Figure 9. Psuedo-Mixing Effect Obtained from the Convection-Only Numerical Algorithm When FLOW < 1

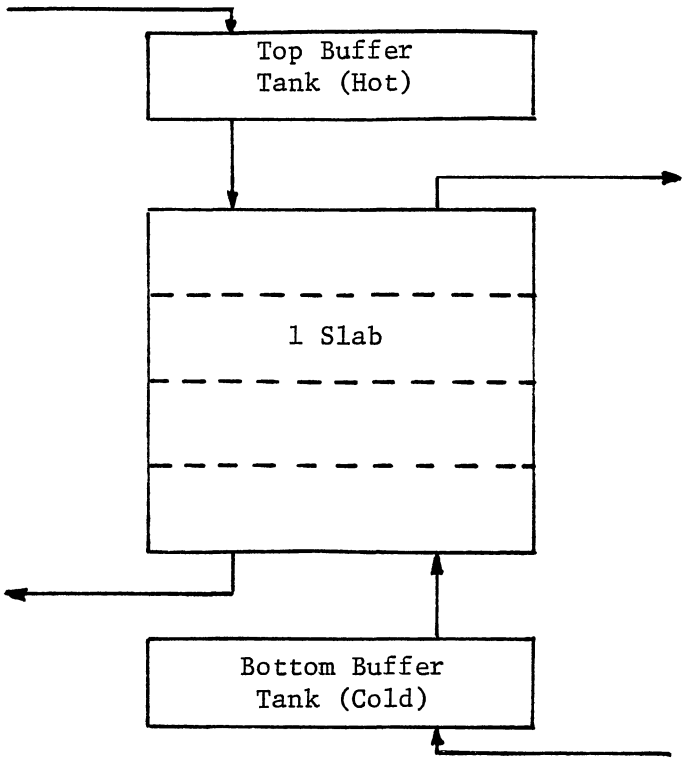

Figure 10. Buffer Tank Concept

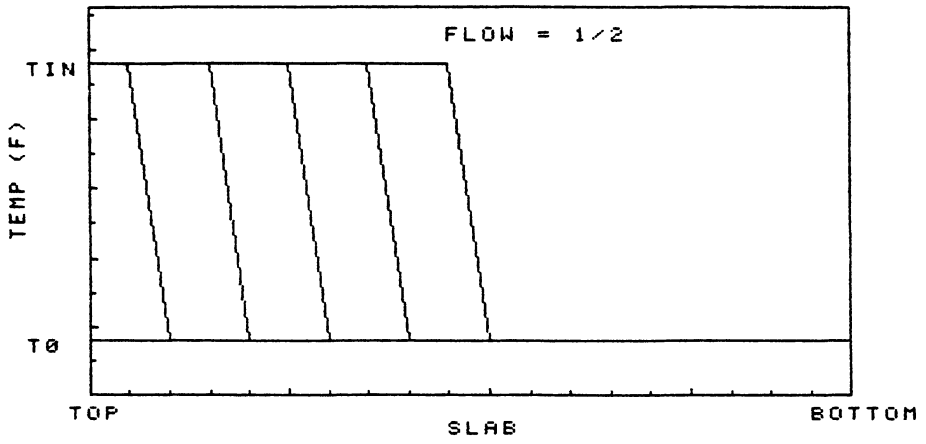

Figure 11. Temperature Profile in the Tank for the Buffer Tank Concept (FLOW=1/2) as Time Increases

accumulate the incoming flow of water until the amount of water in the buffer tank is equal to at least one slab volume in the tank, which is the same as FLOW = 1. Then one slab volume of water in the buffer tank is pulsed into the main tank. Numerically this means that the Equations (3.7) and (3.8) derived for stratified flow are used only when FLOW = 1, leaving the following equations:

For water flowing into the top of the tank

$$T'_p = T_n \tag{3.10}$$

For water flowing into the bottom of the tank

$$T'_p = T_s \tag{3.11}$$

Figure 11 shows the correct temperature profile of the convection-only case when using the buffer-tank concept.

3.4 Combination of Flow and Conduction

To obtain the combined effect, the methods described above can be added together. The conduction-only routine will be applied at each time interval of calculation whereas the convection-only routine will be applied only if there is enough backlog so that we can set FLOW = 1. The convection-only routine might be invoked only occasionally, for example every third or fourth time, depending on the flow rate. Thus we can now simulate a combined condition without introducing pseudo-mixing through numerical procedures, by executing the flow calculations at variable time intervals which are integral multiples of the minimal

times.

3.5 Computer Program Development and Stability Criterion

A listing of the variables used in the computer program is shown in Appendix B. The user of the program must input several variables to the program such as the following: DIA,HEIGHT,QMAX,TO,TIN. One of the two variables, DELT or NSLAB, must be input to the program based upon the choice of the user, while the other one will be calculated from the flow stability criterion. The values of the remaining variables in Appendix B will be either calculated or chosen by the program.

This program will choose the eddy conductivity factor called EDDY in the program. Since EDDY can vary for each slab in the tank, some flexibility is introduced into the one-dimensional flow model. By selecting certain values of EDDY for different slabs, some of the two-dimensional flow properties can be absorbed into this weighting factor EDDY for our one-dimensional flow model.

As mentioned above, DELT or NSLAB will be calculated from the flow stability criterion as stated below in Equation (3.12), where NSLAB = HEIGHT/DELX.

$$\text{FLOW} = \text{VEL} * \text{DELT} / \text{DELX} \leq 1.0 \qquad (3.12)$$

Notice that the maximum velocity, VMAX, must be known. VMAX can be calculated from the input value QMAX. DELT or NSLAB can be calculated from Equations (3.13) and (3.14), respectively.

$$\text{DELT} \leq \text{HEIGHT} / (\text{NSLAB} * \text{VMAX}) \tag{3.13}$$

$$\text{NSLAB} \leq \text{HEIGHT} / (\text{VMAX} * \text{DELT}) \tag{3.14}$$

Appropriate integer values satisfying Equations (3.13) and (3.14) for DELT (calculated from the user supplied NSLAB) or NSLAB (calculated from the user supplied DELT) will be used in the program.

3.6 Boundary Conditions

When trying to develop the computer program with only the information given in the previous sections, difficulty may be encountered in calculating the temperatures at the boundaries. Since the assumption of a well-insulated tank is used in this work, the temperature gradient across the boundaries, that is the top and bottom of the tank, is assumed to be zero. Thus a fictitious slab is introduced outside the end walls of the tank as shown in Figure 12. These fictitious slabs have the same properties as their corresponding interior end slabs as if a mirror image occurred. For the conduction-only case, the boundary conditions at the bottom and top of the tank are given by Equations (3.15) and (3.16), respectively.

$$T'_n = T_p \tag{3.15}$$

$$T'_s = T_p \tag{3.16}$$

With these boundary conditions, the order of sequentially updating the temperature profile should start where the flow enters, and end at the exit. Therefore, the direction of the incoming flow is important in the conduction routine in order to produce the correct order of updating the

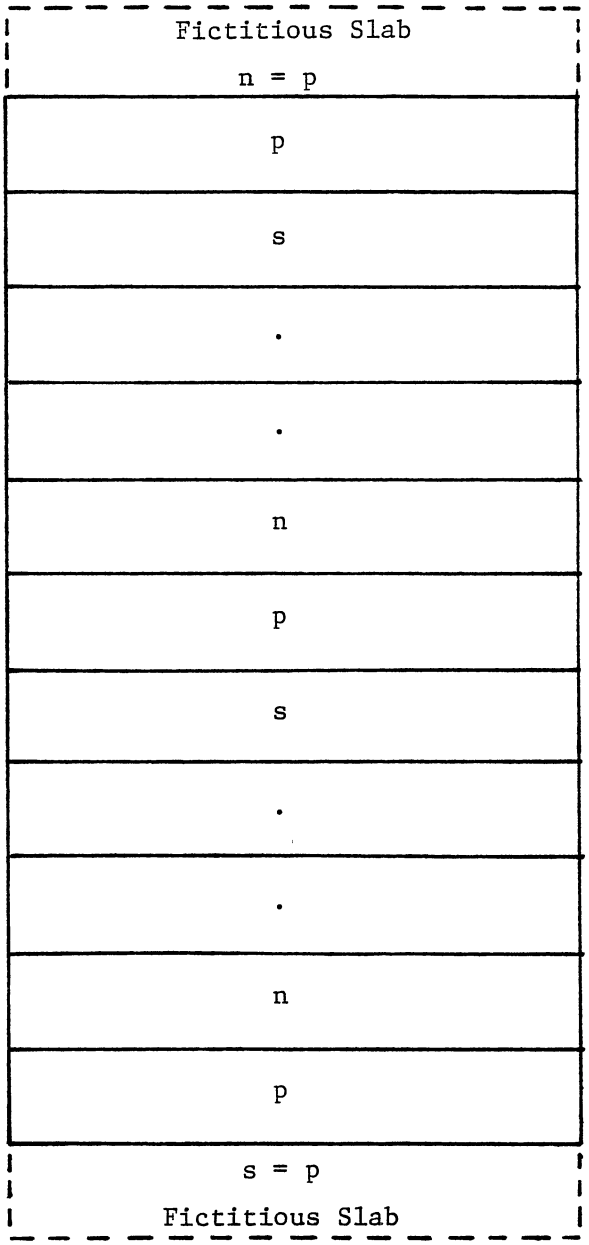

Figure 12. Evaluation of Boundary Conditions for Conduction-Only Case Using the Mirror Image Concept

temperature. The form of the equation at the boundaries is the same as Equation (3.5). The coefficients in Equation (3.5), evaluated at the boundaries, change as follows for both cases of water flowing into the top and bottom of the tank.

For water flowing into the top of the tank

$b = -AMIX$

$d = 1 + 2AMIX$

$a = 0$

$c = (1 + AMIX)\ T_p$

For water flowing into the bottom of the tank

$b = 0$

$d = 1 + 2AMIX$

$a = -AMIX$

$c = (1 + AMIX)\ T_p$

The buffer tank concept resolves the difficulty of handling the boundary conditions in the flow routine by using a top and bottom buffer tank. Conservation of mass is satisfied by this method also. For example, when the inlet flow changes from the top to bottom, the amount of water left in the top buffer is retained until water flows into the top buffer again; likewise for the bottom buffer tank. Also note conservation of energy within the buffer tanks was not considered since the assumption of the inlet temperature flowing into the buffer tanks remains constant; where the top buffer tank remains hot and bottom buffer tank remains cold. Thus the mixing effects in the buffer tanks will be insignificant due to the constant inlet temperature. Even if the inlet temperature does vary somewhat, the mixing effect occurring inside the buffer tank will be insignificant since the volume of the

buffer tanks is very small compared to the volume of the main tank.

With the development of the numerical equations and the employment of the above boundary conditions, an overall program can be produced. Figure 13 shows the flowchart logic of this program. The listing of the Fortran program written for the IBM 3081D computer on the Oklahoma State University campus is presented in Appendix B.

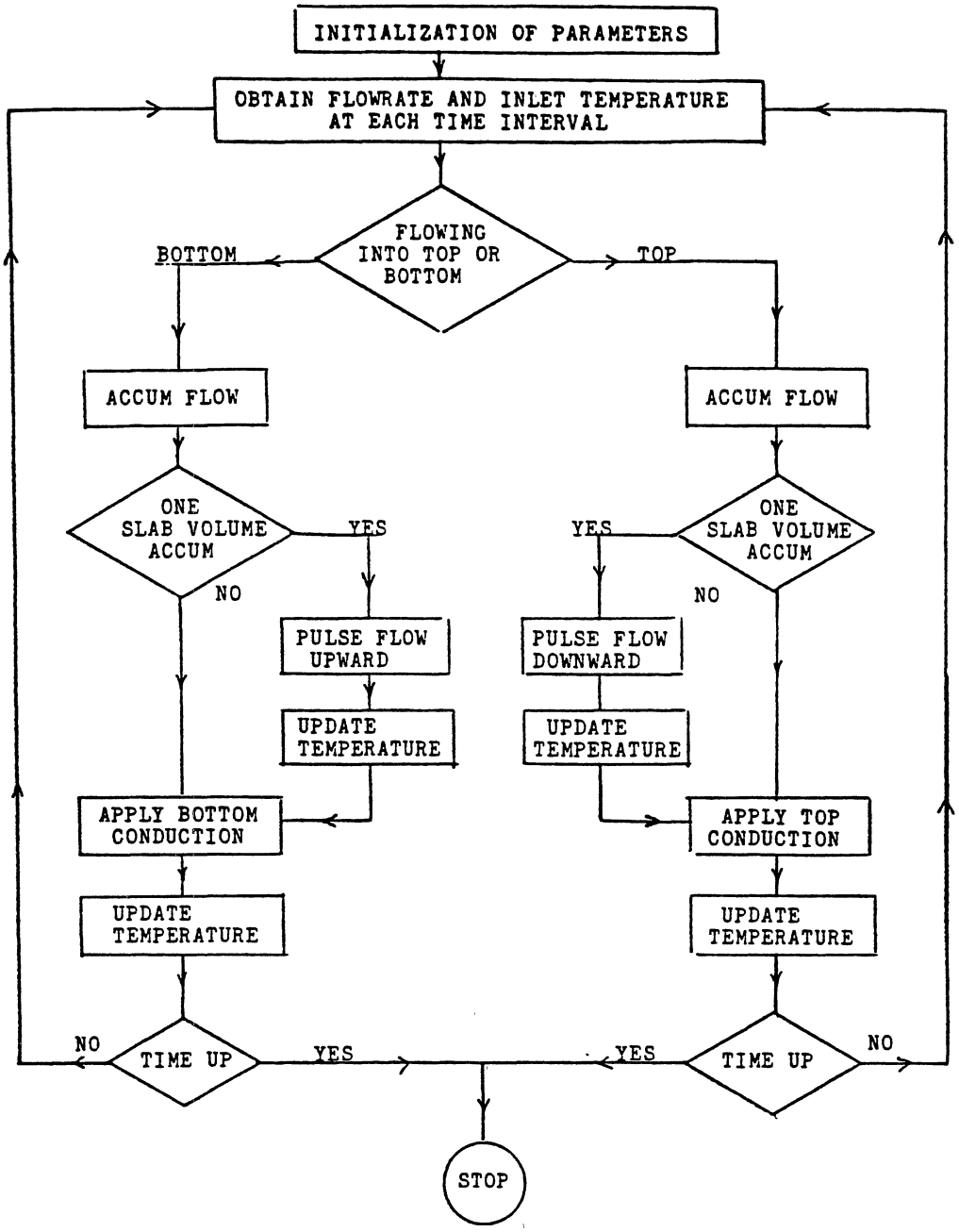

Figure 13. Flowchart

CHAPTER IV

SIMULATION RESULTS

Having developed the computer program in Chapter III, the next step is to simulate the available experimental data found in Chapter II for References [6], [7], and [8]. This chapter concentrates on determining the eddy conductivity factor ε in EDDY required to reproduce the experimental data. Three different cases were examined in the simulation of the experimental data in [6]. They consisted of a laminar, turbulent uniform, and turbulent varying case in order to show that turbulent mixing occurred and varied in some fashion throughout the tank. The data in [7] were used to determine the type of variation from maximum at the inlet to laminar at the exit. Three types of functional variations were examined; linear, hyperbolic, exponential. The dependency of the eddy conductivity factor on the inlet configuration was examined with the experimental data in [8].

4.1 Thermocline Simulation Inside the Tank

In order to simulate the experimental data presented in the papers from the literature survey, the information listed in Table I was required. This information consisted of the tank properties and dimensions; inlet configuration; temperature profile and location in the tank with the corresponding time of measurement; initial conditions;

TABLE I

INFORMATION NEEDED FOR SIMULATION

Tank Dimensions	
Height	Inlet geometry
Inside tank diameter	Tank material
Insulation used	Tank wall thickness
Inlet pipe diameter	Location of inlet and outlet

Fluid Properties
Inlet temperature and flow rate as function of time
Initial temperature of tank
Time of measurements
Temperature profile and location in tank

and the inlet temperature and flow rate as a function of time. Only those papers in the literature survey that provided all the essential information listed in Table I could be used for simulation.

The experimental data provided by Sharp et al. [6] contain temperature data versus slab locations inside the tank, as shown in Figure 2. The type of experiments shown in Figure 2 consisted of charging the initially cold tank with hot water through the inlet at the top of the tank. Notice that the inlet temperature decreased during the operation of the experiment. Each curve will be analyzed individually assuming that the inlet temperature for that curve remains constant. An appropriate eddy conductivity factor, determined from trial and error through simulations, will be chosen for each curve. Thus the variation of the eddy conductivity factor from the inlet to the outlet in the tank may be determined. Only two curves will be simulated (0.5 hr and 1 hr) since the last curve (1.5 hr) does not contain the full thermocline.

The data from [6] that were input into the computer program is listed in Table II. The properties used were evaluated at the average temperature, between T_o and T_{in}. The parameter NSLAB was chosen as 20 since there were 20 thermocouple locations inside the tank. With the parameter NSLAB fixed, DELT must be calculated from the stability criterion. DELT must be less than 4.28 minutes for the FLOW criterion. DELT of 3 minutes was used for ease of comparison with their data. Both curves were simulated for three different cases. The first case contained only laminar conduction with $\varepsilon = 0$ which will show whether turbulent mixing is occurring. The second case considered a uniform eddy conductivity factor throughout the tank. The third case consisted of varying the eddy conductivity factor within four equal

TABLE II

COMPUTER INPUT FOR SIMULATION OF [6]

Tank Specifications	Fluid Properties
HEIGHT = 6.34 ft	T_{in} = 102 F
DIA = 3.8 ft	T_o = 69 F
AREA = 11.34 ft^2	ρ = 62.4 lbm/ft^3
NSLAB = 20	k = 0.355 Btu/hr F ft
DELX = 0.317 ft	C_p = 0.998 Btu/lbm F
Insulated Tank	α = 0.0057 ft^2/hr
Inlet Manifold Designed by [6]	QMAX = 0.84 ft^3/min
	VMAX = 7.44 x 10^{-2} ft/min
Stability Criterion	**Nondimensional Parameters based on DELX, VMAX**
	Pick DELT = 3.0 min
FLOW: DELT $\leq$ 4.28 min	FLOW = 0.70
	Fourier No. = 2.846 x 10^{-3}

regions of the tank. This case was considered in order to see if the eddy conductivity factor varies from the inlet to the outlet. Four equal regions were arbitrarily chosen.

Simulating the first curve (0.5 hr) will help predict the degree of mixing occurring near the inlet. The results of the laminar case shown in Figure 14 dictate that turbulent mixing is occurring as was expected. Figure 15 shows the uniform turbulent case with an eddy conductivity factor of 20. This simulated profile matches the experimental profile better than the model used in Reference [6]. For the varying case, the eddy conductivity factor was maximum at the inlet and decreased toward the outlet. Figure 16 shows the results of the varying case. Notice that the varying profile is nearly the same as the uniform case. This may be attributed to the fact that the eddy conductivity value near the inlet of the tank for the varying case was almost equal to the uniform eddy conductivity value. Thus the eddy conductivity values at the outlet of the tank essentially have no effect since the temperatures have not changed yet.

Simulating the second curve (1.0 hr), which occurs later in time and further down the tank toward the oulet, will determine how the eddy conductivity value changes with time and distance into the tank. The results of the laminar case for the second curve shown in Figure 17 reveal that a smaller amount of turbulence is occurring as the thermocline advances toward the exit. In Figure 18, a uniform eddy conductivity factor of 10 produced a simulated profile similar to the experimental profile. Therefore the turbulent eddy conductivity factor has decreased during the movement of the thermocline toward the outlet. Notice that the experimental temperature above the thermocline

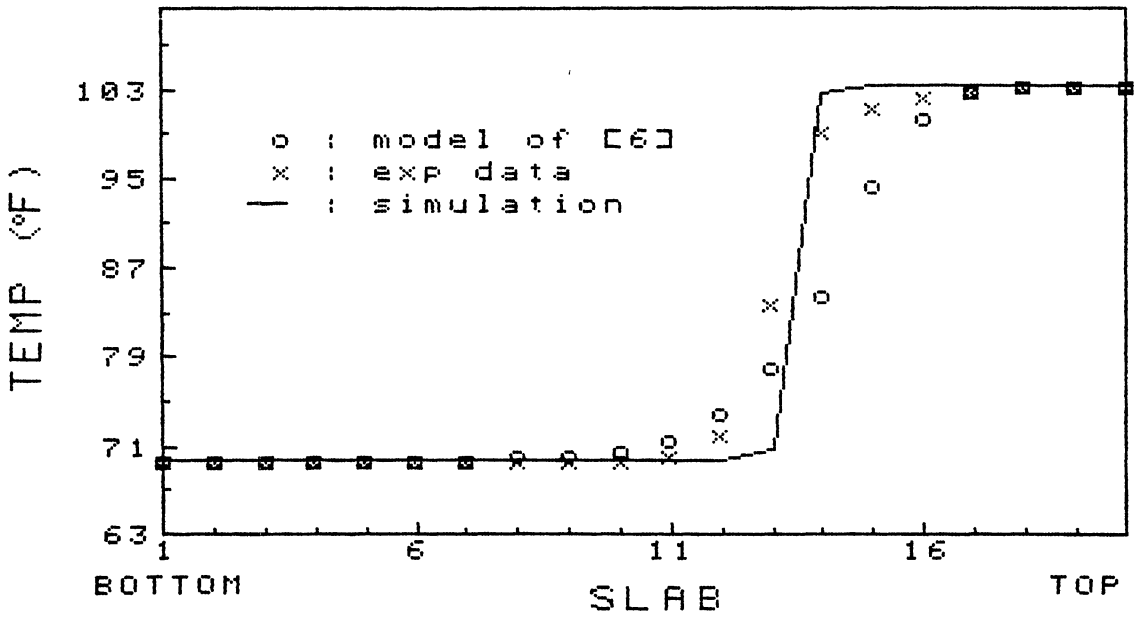

Figure 14. Comparison of Storage Tank Temperature Profiles for the Laminar Case of Curve 1 in Figure 2

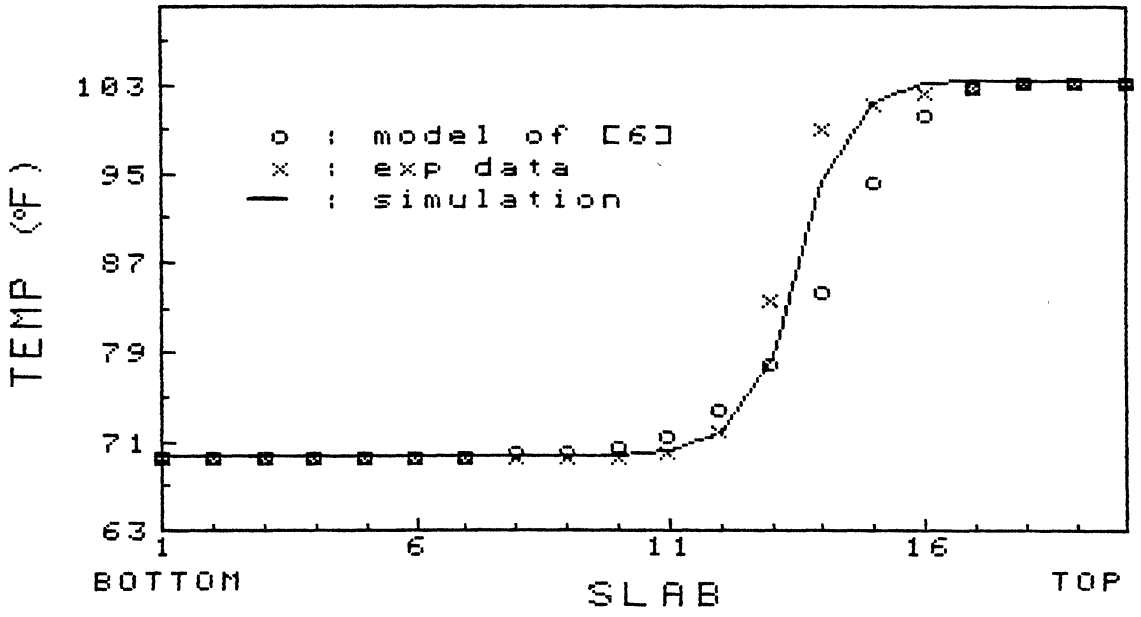

Figure 15. Comparison of Storage Tank Temperature Profiles for the Turbulent Uniform Case of Curve 1 in Figure 2

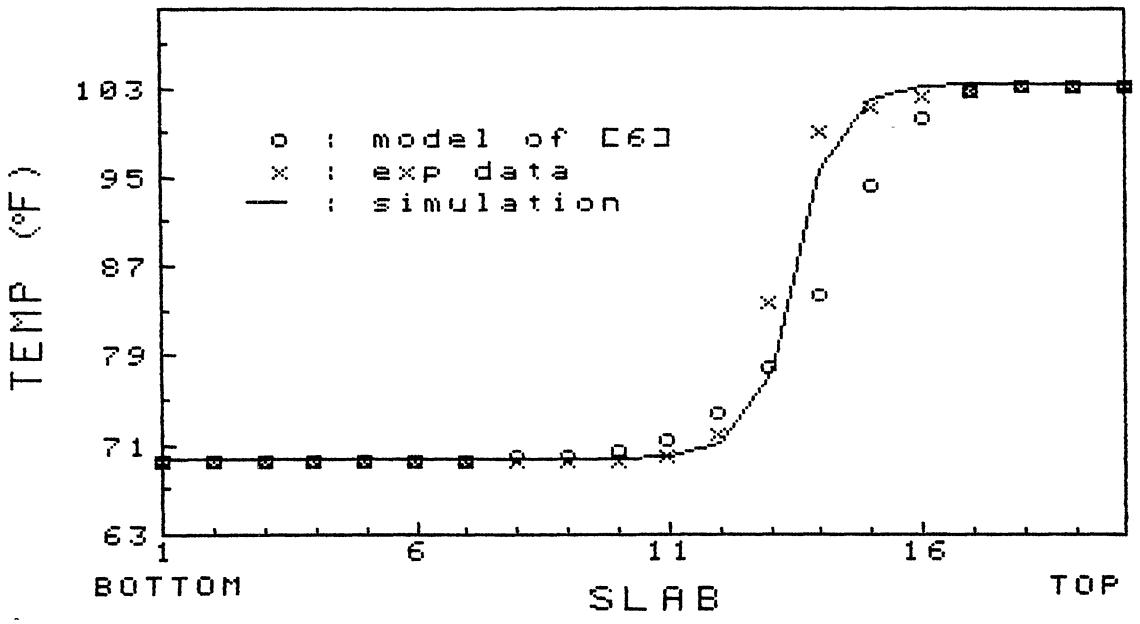

Figure 16. Comparison of Storage Tank Temperature Profiles for the Turbulent Varying Case of Curve 1 in Figure 2

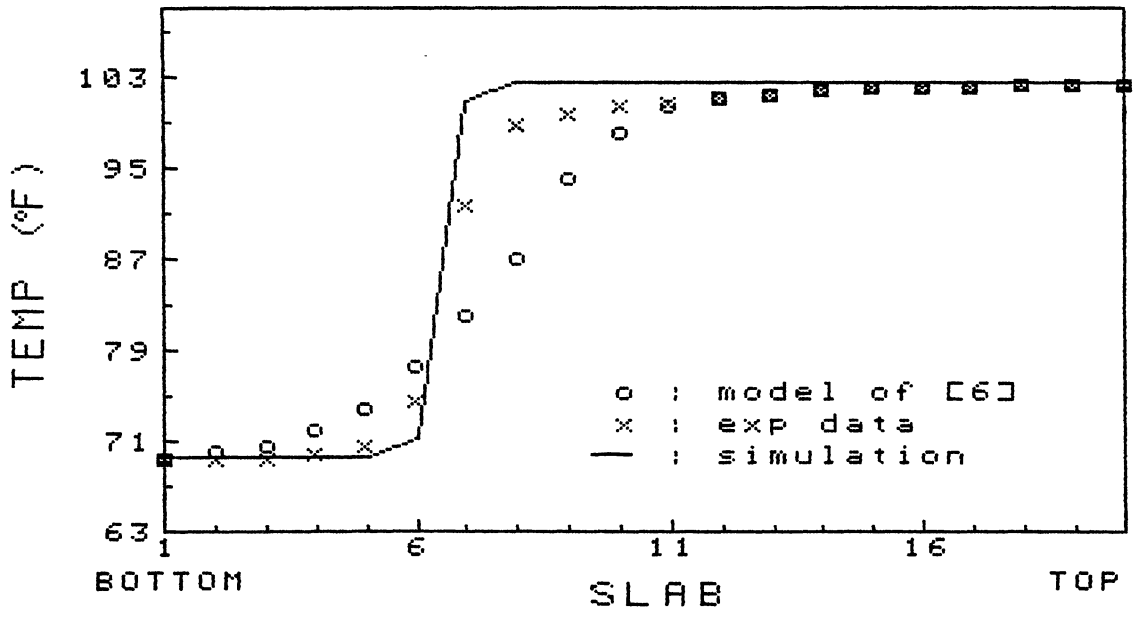

Figure 17. Comparison of Storage Tank Temperature Profiles for the Laminar Case of Curve 2 in Figure 2

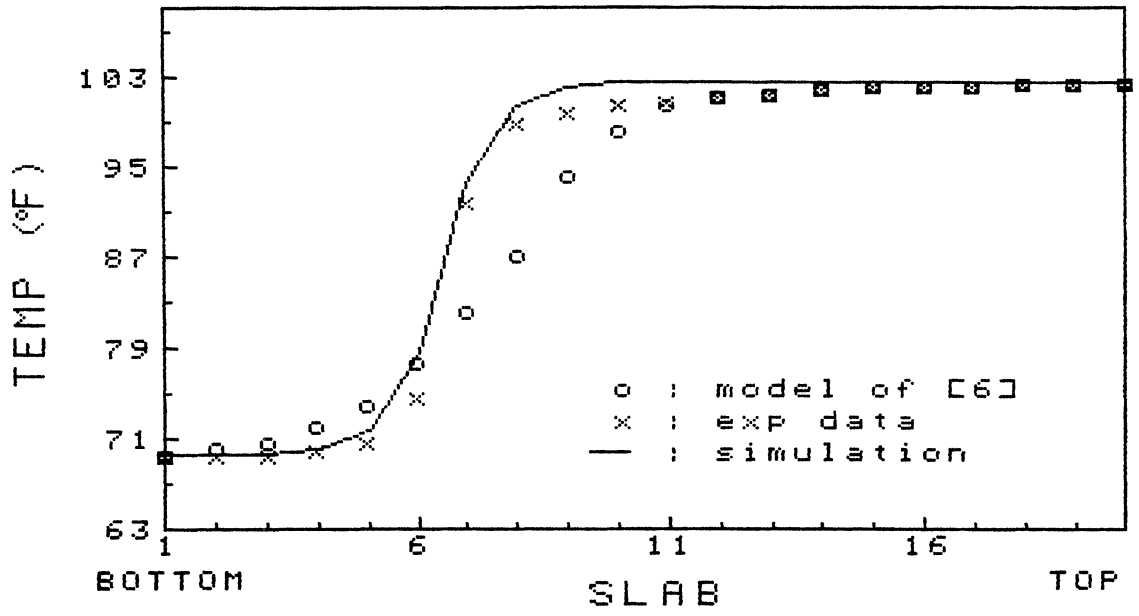

Figure 18. Comparison of Storage Tank Temperature Profiles for the Turbulent Uniform Case of Curve 2 in Figure 2

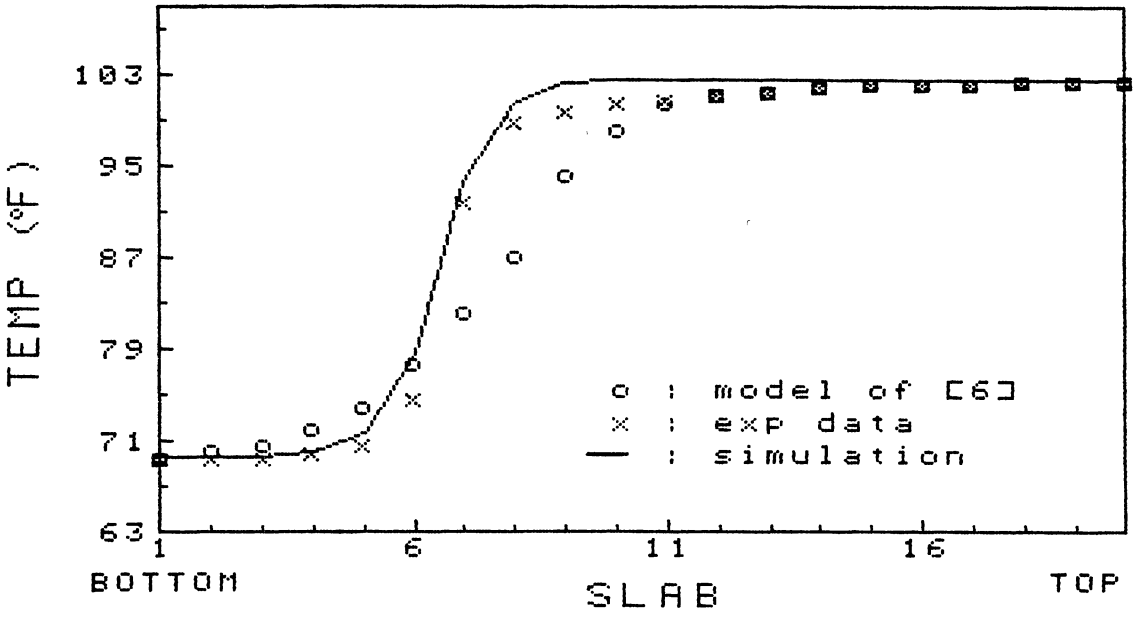

Figure 19. Comparison of Storage Tank Temperature Profiles for the Turbulent Varying Case of Curve 2 in Figure 2

has decreased due to the variation of the inlet temperature, as the authors of [6] have mentioned. If the inlet temperature had remained constant during the experiment, this decrease would not be as noticeable. Figure 19 shows the results of the varying case. Notice that the eddy conductivity values in the four regions of the tank for the varying case of the second curve were not changed from the values of the first curve. Both the uniform and varying simulated profiles match the experimental profiles except at the location above the thermocline for the reasoning mentioned above.

In comparing our one-dimensional model with their one-dimensional model, note that our model simulated results that consistently lay on or near the thermocline, whereas their one-dimensional model produced a thermocline wider and flatter than the experimental thermocline. This suggests that their model did not consider enough mixing in the portion of the tank near the inlet. Table III summarizes the results of both curves. Observing this table along with the temperature plots, the eddy conductivity factor is shown to vary from a maximum value at the inlet to a minimum value at the outlet as the thermocline moves from its development at the inlet to its depletion at the exit.

4.2 Eddy Conductivity Variation

The previous results indicate that turbulent mixing does occur and that it decreases in some fashion from the inlet to the exit. Therefore, there are two unknowns that still exist; the amount of mixing and how it decreases. In order to eliminate one of the unknowns concerning the variation of the eddy conductivity factor from inlet to the exit, define three types of functions which decrease from the inlet

TABLE III

SIMULATION RESULTS OF EXPERIMENTAL DATA FROM [6]

Fig.	Case	Eddy Conductivity Factor Used	Allowable Range of Eddy Conductivity
14	Laminar Uniform	1	-
15	Turbulent Uniform	20	15-25
16	Turbulent Varying	(1) 25* (2) 15 (3) 5 (4) 1	-
17	Laminar Uniform	1	-
18	Turbulent Uniform	10	5-15
19	Turbulent Varying	(1) 25* (2) 15 (3) 5 (4) 1	-

* Eddy conductivity factors used in the four regions of the tank (turbulent varying case) where, 1 refers to the region next to the inlet and 4 refers to the region near the exit of the tank.

to the outlet: linear, hyperbolic, and exponential. These three functions are presented in Equation (4.1) for linear, Equation (4.2) for hyperbolic, and Equation (4.3) for exponential.

LINEAR:

$$EDDY = A(ISLAB) + B \tag{4.1}$$

where

FLOW INTO BOTTOM

$$A = \frac{E_{INLET} - 1}{1 - NSLAB}$$

$$B = E_{INLET} - A$$

FLOW INTO TOP

$$A = \frac{1 - E_{INLET}}{1 - NSLAB}$$

$$B = 1 - A$$

HYPERBOLIC:

$$EDDY = A\left(\frac{1}{ISLAB}\right) + B \tag{4.2}$$

where

FLOW INTO BOTTOM

$$A = \frac{E_{INLET} - 1}{1 - \frac{1}{NSLAB}}$$

$$B = E_{INLET} - A$$

FLOW INTO TOP

$$A = \frac{1 - E_{INLET}}{1 - \frac{1}{NSLAB}}$$

$$B = 1 - A$$

EXPONENTIAL:

$$EDDY = A\ e^{-(ISLAB)} + B \qquad (4.3)$$

where

FLOW INTO BOTTOM

$$A = \frac{E_{INLET} - 1}{e^{-1} - e^{-NSLAB}}$$

$$B = E_{INLET} - A\ e^{-1}$$

FLOW INTO TOP

$$A = \frac{1 - E_{INLET}}{e^{-1} - e^{-NSLAB}}$$

$$B = 1 - A\ e^{-1}$$

Figure 20 shows how each of the above functions decrease from the inlet to the outlet. Once the proper function is determined, then the only unknown to determine is the value of the inlet eddy conductivity, for that particular function. Knowing this inlet eddy conductivity value and the decreasing function defines the eddy conductivity values throughout the tank.

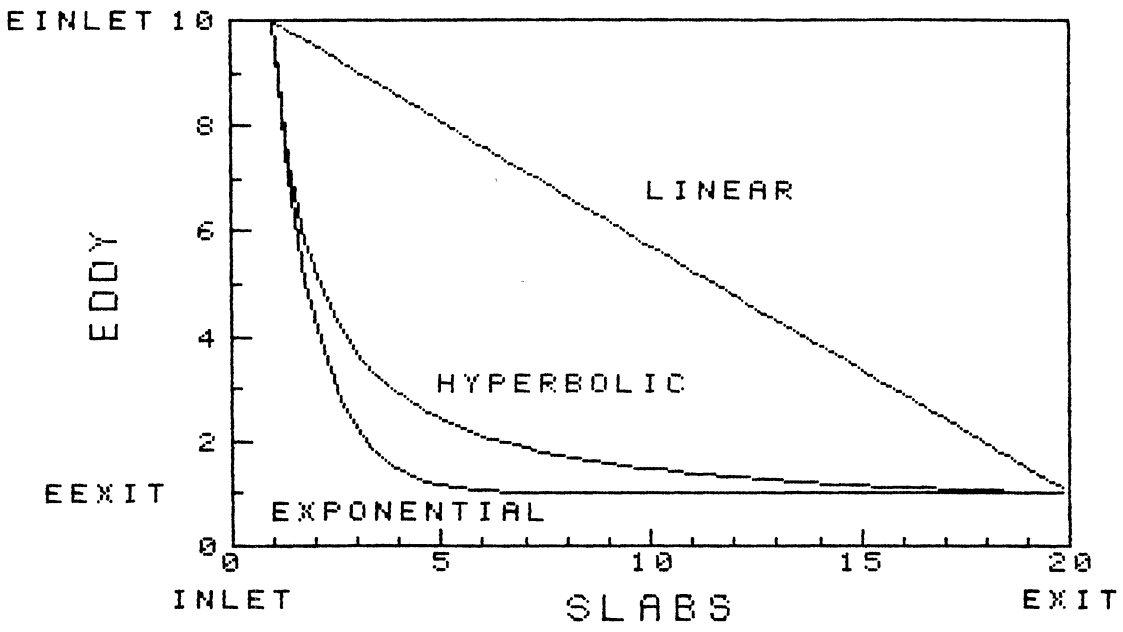

SLAB	LINEAR	HYPERBOLIC	EXPONENTIAL
1	10.00	10.00	10.00
2	9.53	5.26	4.31
3	9.05	3.68	2.22
4	8.58	2.89	1.45
5	8.11	2.42	1.16
6	7.63	2.11	1.06
7	7.16	1.88	1.02
8	6.68	1.71	1.01
9	6.21	1.58	1.00
10	5.74	1.47	1.00
11	5.26	1.39	1.00
12	4.79	1.32	1.00
13	4.32	1.26	1.00
14	3.84	1.20	1.00
15	3.37	1.16	1.00
16	2.89	1.12	1.00
17	2.42	1.08	1.00
18	1.95	1.05	1.00
19	1.47	1.02	1.00
20	1.00	1.00	1.00

Figure 20. Eddy Conductivity Variation Inside the Tank for Linear, Hyperbolic, and Exponential Functions

Adoly's work [7] contains a plot of outlet temperature versus time for several different flow rates with approximately the same temperature difference between the inlet water and initial water in the tank. Using this available data, the function which best represents the variation of eddy conductivity from inlet to exit may be obtained for different flow rates. For each of the three functions, the best inlet eddy conductivity factor was obtained. Figures 21 through 29 show the results of using the three functions for three different flow rates from Adoly's paper ranging from high, medium, to low flow rates.

The decreasing linear function produced good results at high flow rates but did not perform well for the lower flow rates indicating that the eddy conductance decreases sharper away from the inlet than the linear function predicts. The decreasing exponential function produced better results than the linear function indicating that indeed the eddy conductance drops off sharply away from the inlet value. Yet the decreasing exponential function failed to predict the smooth transition at the beginning of thermocline. The decreasing hyperbolic function performed the best for all the flow rates. Note that the hyperbolic function also predicts a sharp decay from the inlet eddy conductivity value, although not as dramatic as the decreasing exponential function. Therefore the hyperbolic function can predict the smooth transition at the beginning of thermocline better than the decreasing exponential function.

After establishing the best decreasing function, the prediction of the inlet eddy conductivity for this decreasing function remains to be evaluated. Figures 30 and 31 show the remaining two experiments from Adoly's paper that were simulated. Table IV presents the summary of the

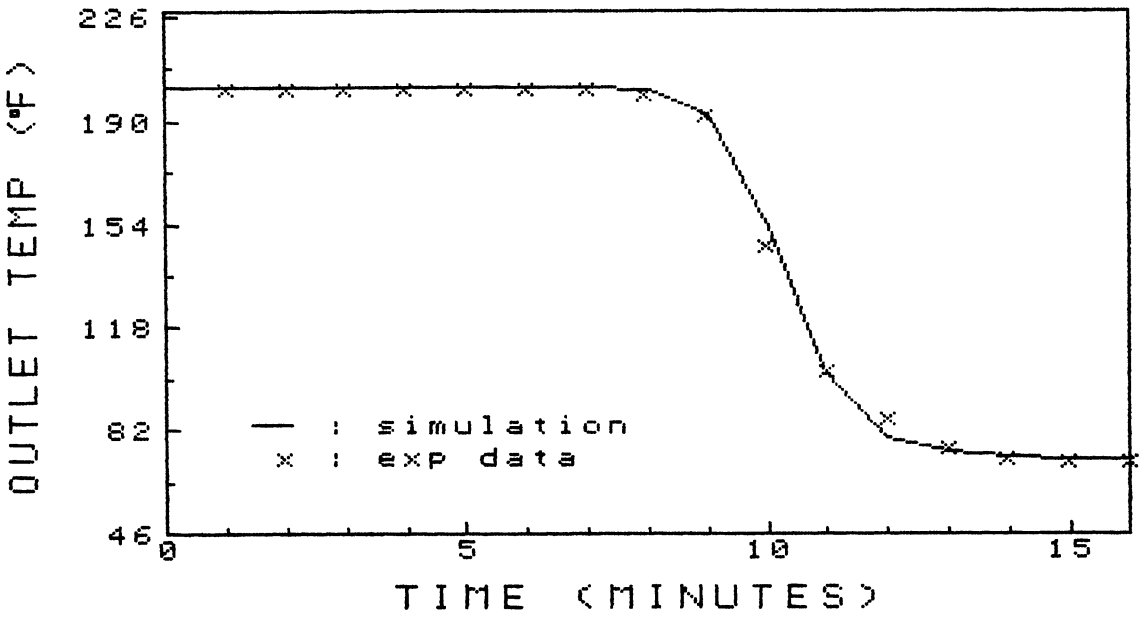

Figure 21. Simulation of Experimental Data in [7] for 2.0 gpm and 130 ^{0}F ΔT Using the Linear Function

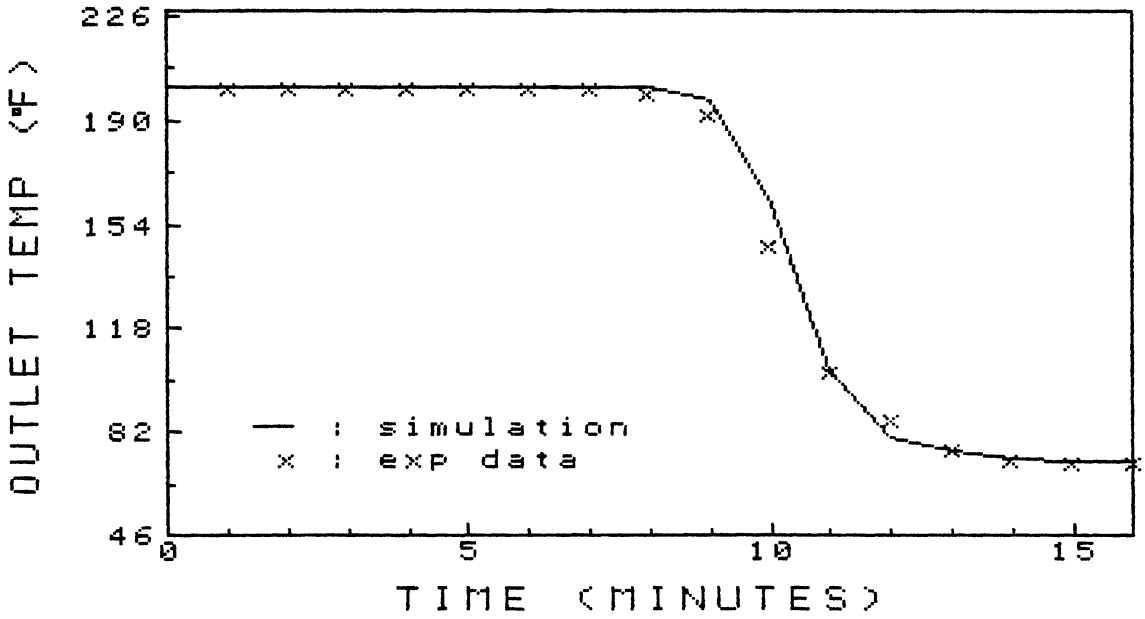

Figure 22. Simulation of Experimental Data in [7] for 2.0 gpm and 130 ^{0}F ΔT Using the Hyperbolic Function

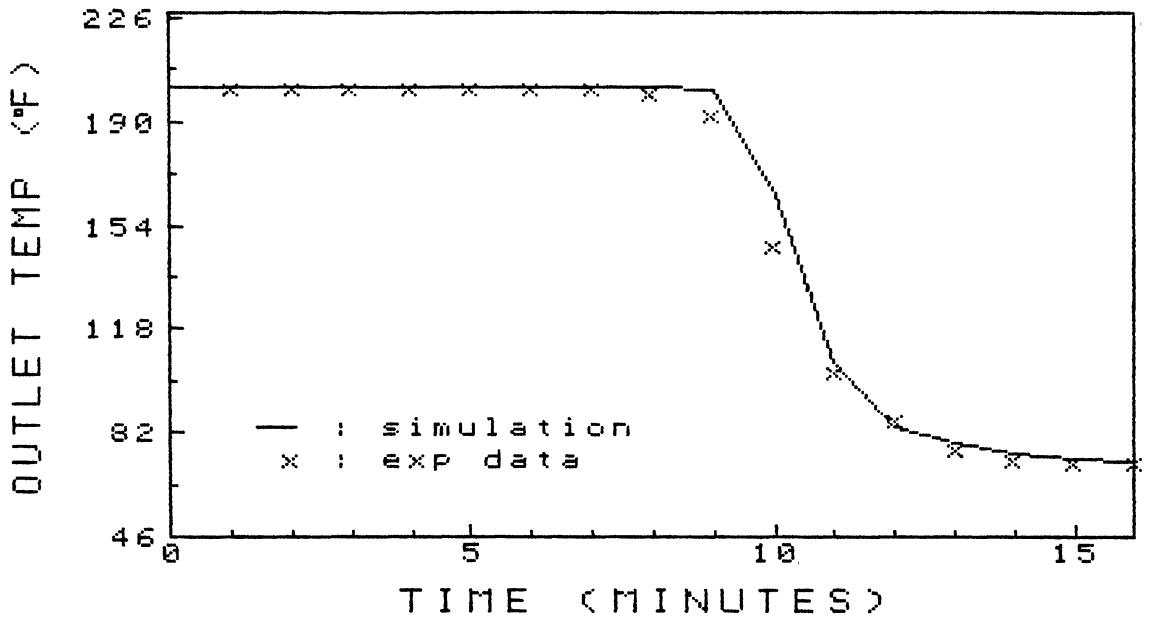

Figure 23. Simulation of Experimental Data in [7] for 2.0 gpm and 130 ^{0}F ΔT Using the Exponential Function

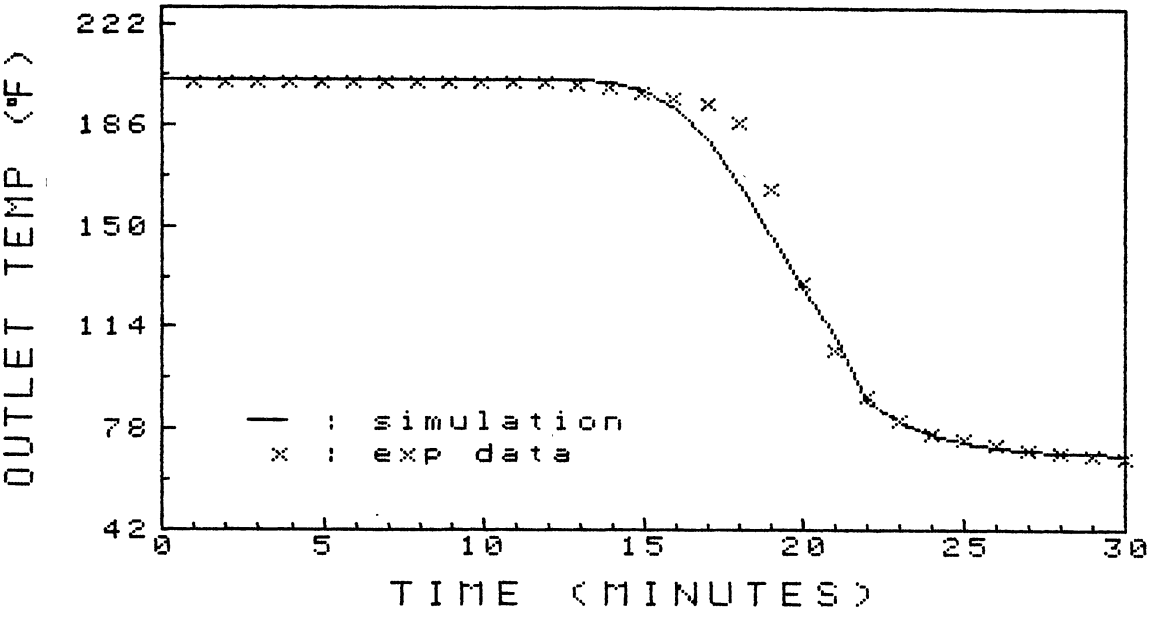

Figure 24. Simulation of Experimental Data in [7] for 1.09 gpm and 133.5 ^{0}F ΔT Using the Linear Function

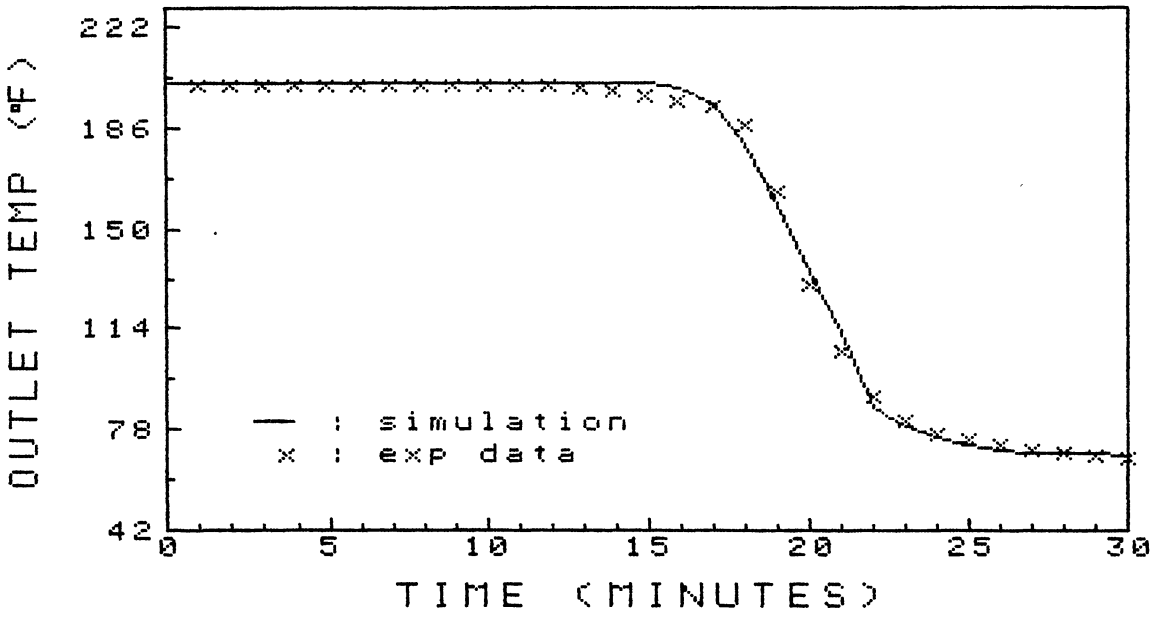

Figure 25. Simulation of Experimental Data in [7] for 1.09 gpm and 133.5 ^{0}F ΔT Using the Hyperbolic Function

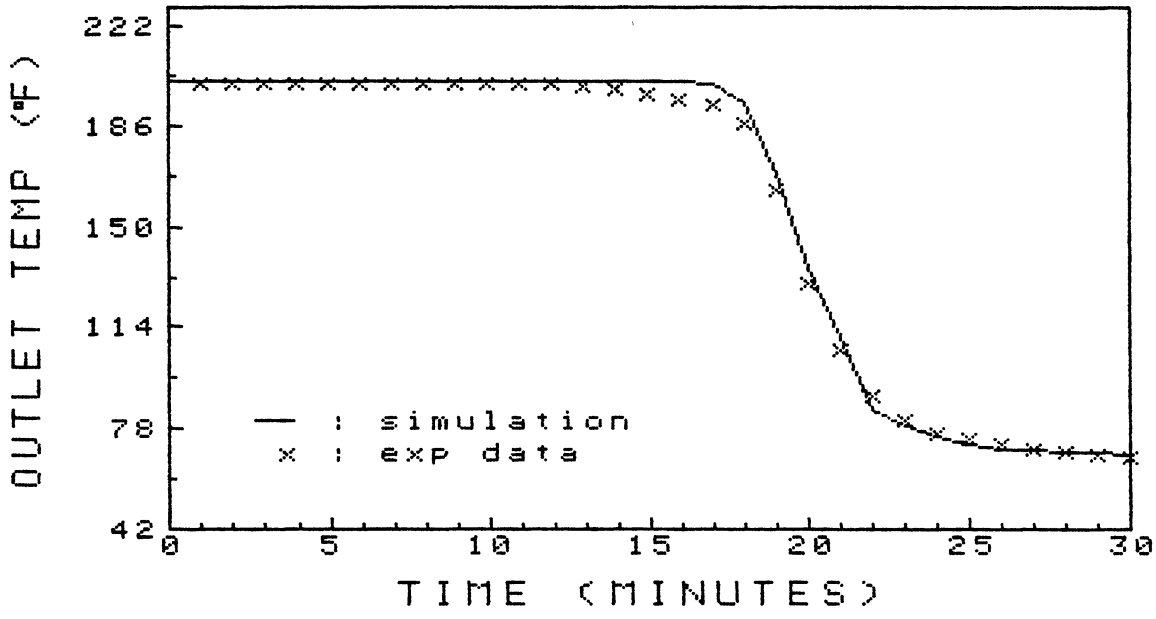

Figure 26. Simulation of Experimental Data in [7] for 1.09 gpm and 133.5 ^{0}F ΔT Using the Exponential Function

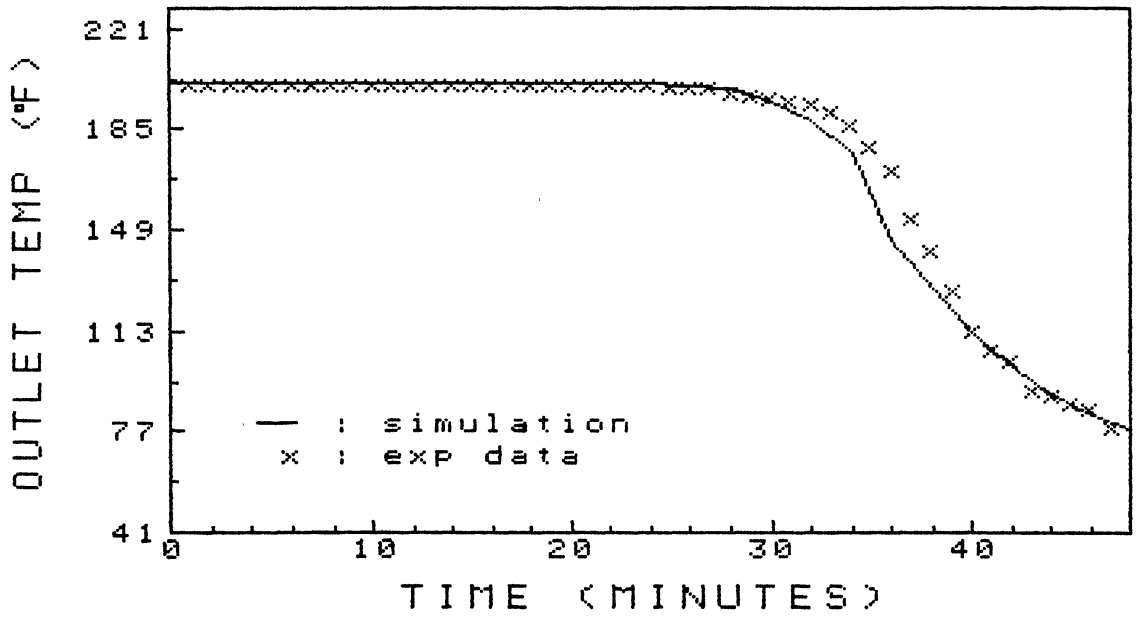

Figure 27. Simulation of Experimental Data in [7] for 0.55 gpm and 134 ^{0}F ΔT Using the Linear Function

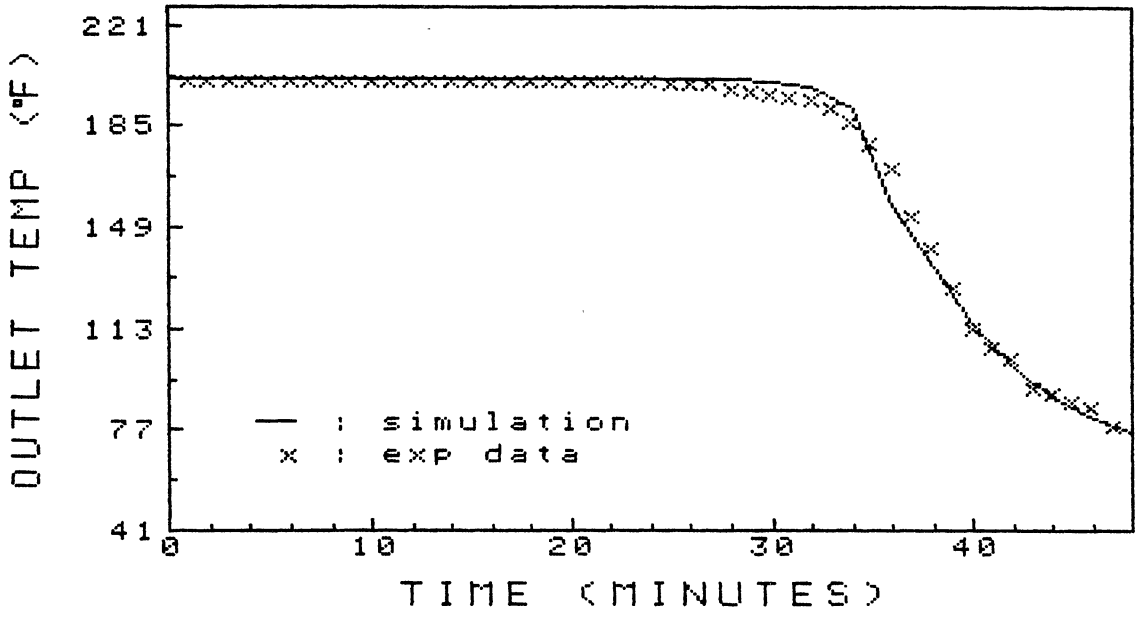

Figure 28. Simulation of Experimental Data in [7] for 0.55 gpm and 134 ^{0}F ΔT Using the Hyperbolic Function

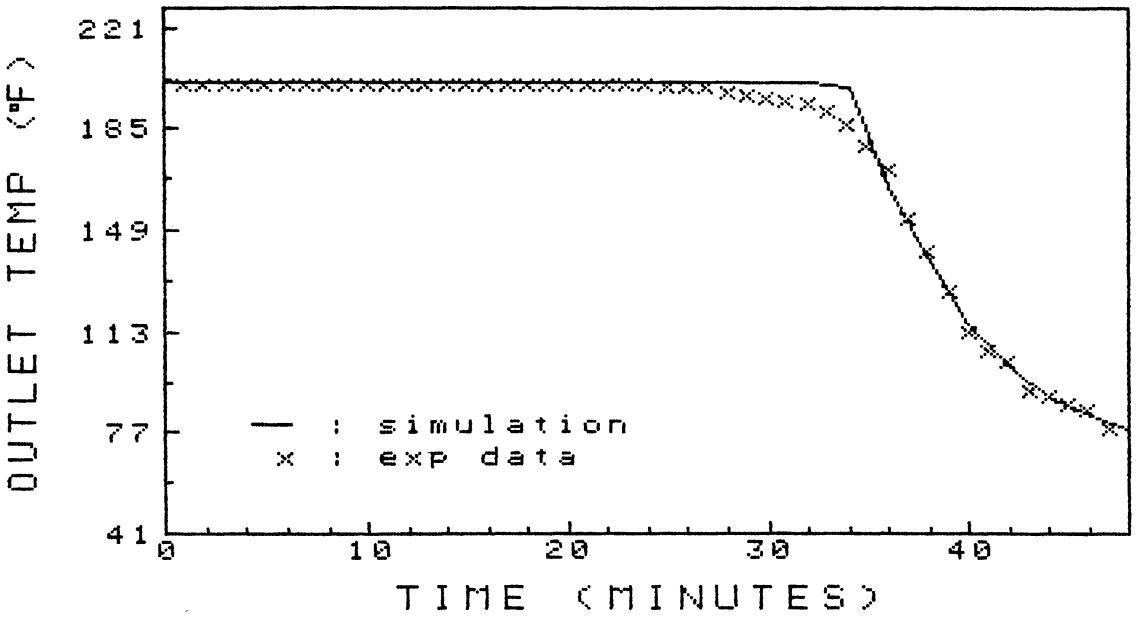

Figure 29. Simulation of Experimental Data in [7] for 0.55 gpm and 134 ^{0}F ΔT Using the Exponential Function

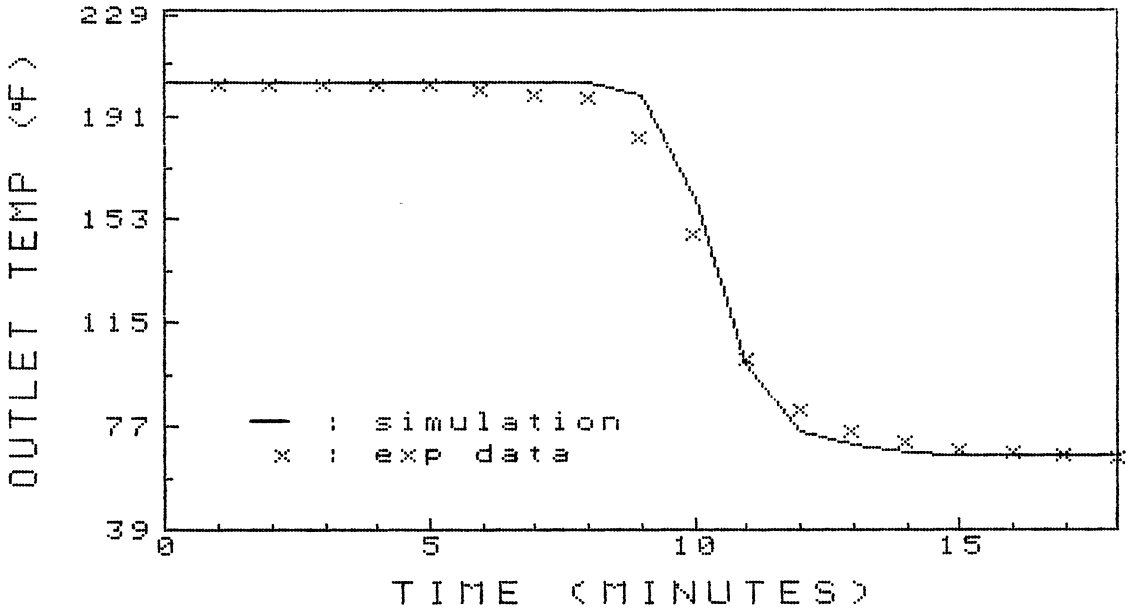

Figure 30. Simulation of Experimental Data in [7] for 2.0 gpm and 137 ^{0}F ΔT Using the Hyperbolic Function

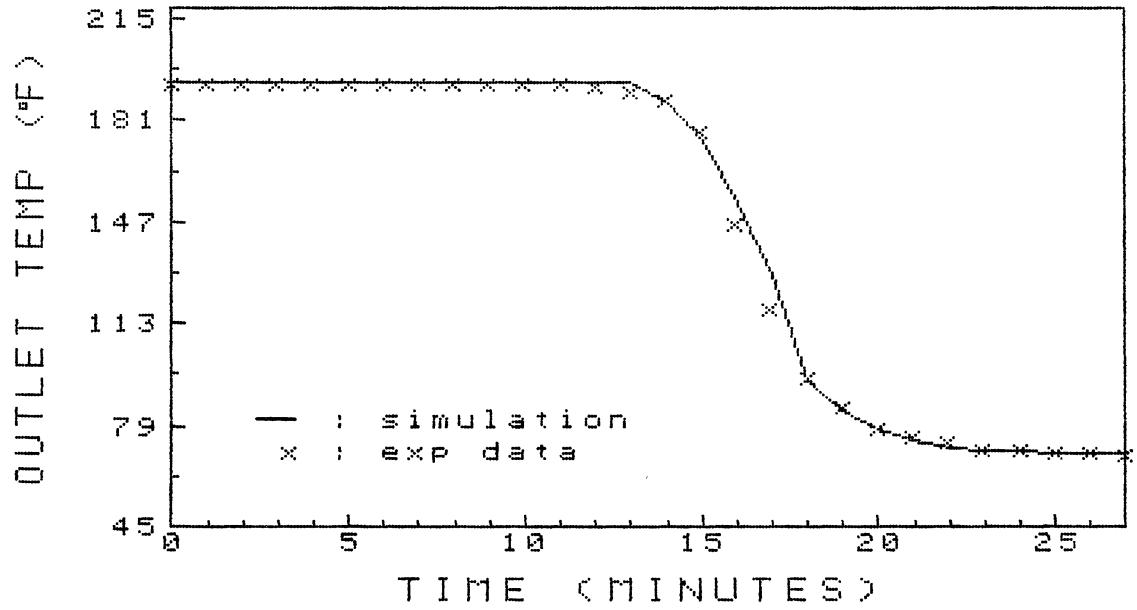

Figure 31. Simulation of Experimental Data in [7] for 1.28 gpm and 124 ^{0}F ΔT Using the Hyperbolic Function

TABLE IV

SIMULATION RESULTS OF EXPERIMENTAL DATA FROM [7] FOR THE DECREASING HYPERBOLIC FUNCTION

Figure	Inlet Eddy Conductivity Factor	Inlet Temperature ^{o}F	Initial Temperature ^{o}F	Volumetric Flow Rate gpm	Reynolds Number	Richardson Number
22	1000	72	202	2	1000	90,3000
25	800	68.5	202	1.09	529	30,740
28	500	67.5	201.5	0.55	263	1,204,000
30	1000	66	203	2	946	92,940
31	900	70	194	1.28	616	203,000

five experiments simulated with the decreasing hyperbolic function along with the corresponding Reynolds and Richardson numbers. The characteristic length in the Reynolds number is based on the inside tank diameter. The characteristic length in the Richardson number is based on the effective tank height (i.e. height between inlet and outlet). The velocity in both the Reynolds and Richardson numbers is the tank velocity (i.e. the ratio of the volumetric flow rate over tank cross-sectional area).

4.3 Inlet Geometry Dependency

Cole's paper [8] contains a plot of outlet temperature versus time for several different inlets keeping the flow rate and temperature difference constant as shown in Figure 3. The side-inlet-outlet and dual radial diffusers were investigated in order to determine the magnitude of the eddy conductance on inlet geometry. The simulated results for side-inlet-outlet and dual radial diffusers are shown in Figures 32 and 33, respectively. The side-inlet-outlet geometry required twice the amount of eddy conductance as did the dual radial diffusers for this particular flow rate. This indicates that the eddy conductivity is definitely dependent upon the type of inlet geometry.

The lack of available experimental data for a range of flow rates and temperature differences for different inlet configurations restricts further investigation concerning the eddy conductivity functional relationship with the inlet geometry. This topic should be analyzed in more detail; thus requiring the need for more experimental data for different inlets.

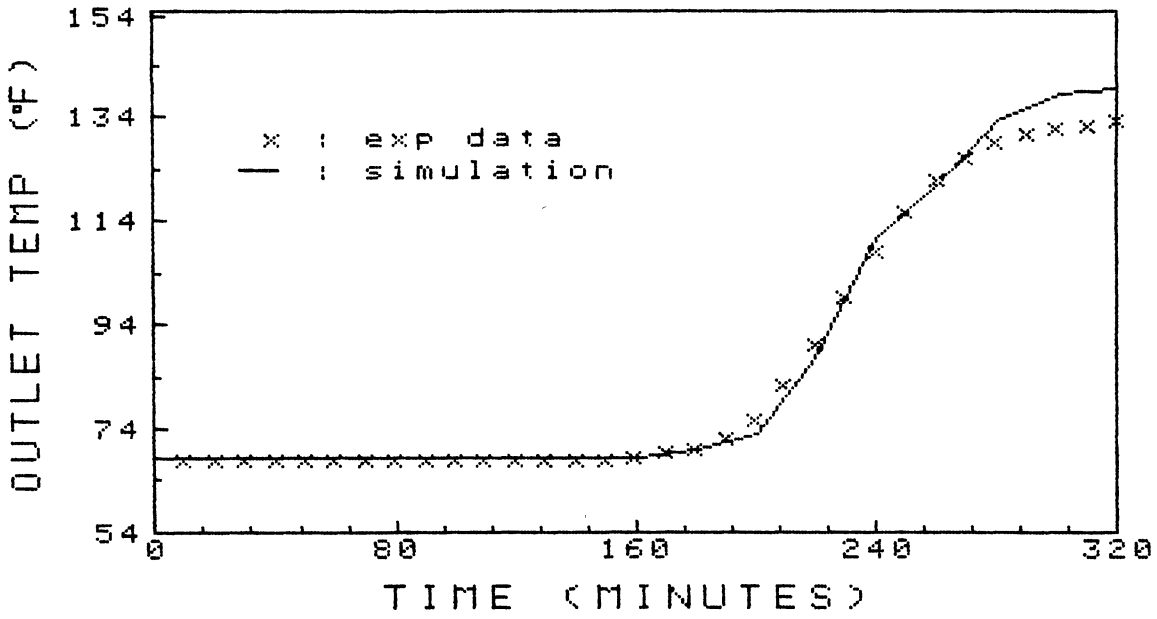

Figure 32. Simulation of Experimental Data in [8] for 0.75 l/min and 40 ^{0}C ΔT Using the Hyperbolic Function with the Side-Inlet-Outlet Design

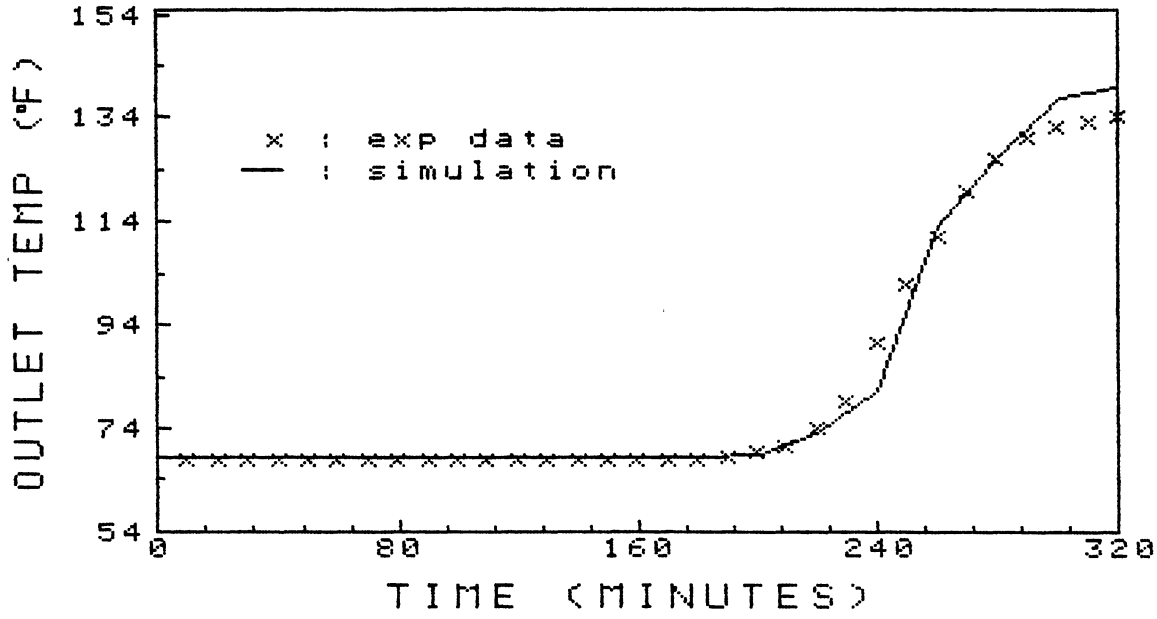

Figure 33. Simulation of Experimental Data in [8] for 0.75 l/min and 40 ^{0}C ΔT Using the Hyperbolic Function with the Dual Radial Diffuser Design

CHAPTER V

OSU EXPERIMENTATIONS

The results from the literature survey supplied sufficient information for only one particular inlet with different Reynolds and Richardson numbers. Most of the sources only presented one set of experimental data for their inlet design. No experimental data were found on the variation of Richardson number for a given Reynolds number or vice versa. Therefore to complete the analysis it was necessary to produce experimental data for different Reynolds and Richardson numbers for a different type of inlet design. This chapter describes the experimental work performed at Oklahoma State University. Salt was used to simulate the density difference between the hot and cold water. Several experiments were conducted for the solid circular plate used as the inlet diffuser. Simulation of this experimental data provided the needed information for completion of the analysis.

5.1 Experimental Setup

Instead of trying to establish a setup consisting of hot water tanks and insulated tanks in order to produce hot and cold water, the setup at Oklahoma State University used salt water and tap water at the same temperature to replace the hot and cold water. The density difference between the salt water and tap water represents the same density difference between the hot and cold water to be tested. With

the use of salt, the prototype tank did not need to be insulated. Since the salt cannot penetrate through the tank walls, the corresponding thermal analogy of our model would assume that no heat is transferred through the tank walls. Another benefit of using salt is that flow visualization of the thermocline development can easily be examined since the tank is not covered with insulation.

A schematic of the setup is presented in Figure 34 and the test tank is shown in Figure 35. The setup consisted of the following. A 23.5 gallon cylindrical plexiglass tank with an inside diamter of 11 7/16 inches, height of 52.8 inches, and a 1/4 inch wall thickness, was used as the prototype test tank. A side-outlet was located 50.1 inches above the bottom of the tank which correspondes to an effective tank capacity of 22.3 gallons. The inlet geometry contained a vertical inlet with a solid circular diffuser plate with a diameter of 11 1/4 inch and a 3/8 inch clearance between the tank wall and the diffuser. The plate was located 2 1/8 inches above the bottom of the tank. A 150 gallon head tank containing the salt water was elevated in order to generate the flow rate. A 150 gallon mixing tank was used to mix the salt solution. A centrifugal pump was used only to pump the salt solution up to the head tank. A 30 gallon tank was used to collect the water flowing out of the test tank. Several valves were used to control the flow. The tubing used to connect the tanks consisted of 1.5 inch PVC pipes. Two flowmeters for high and low flow rates were used to determine the flow rate. The flowmeter calibration curves are shown in Figures 36 and 37.

The flow visualization setup required a camera, a tripod, a stopwatch, a background grid system on the test tank with markings

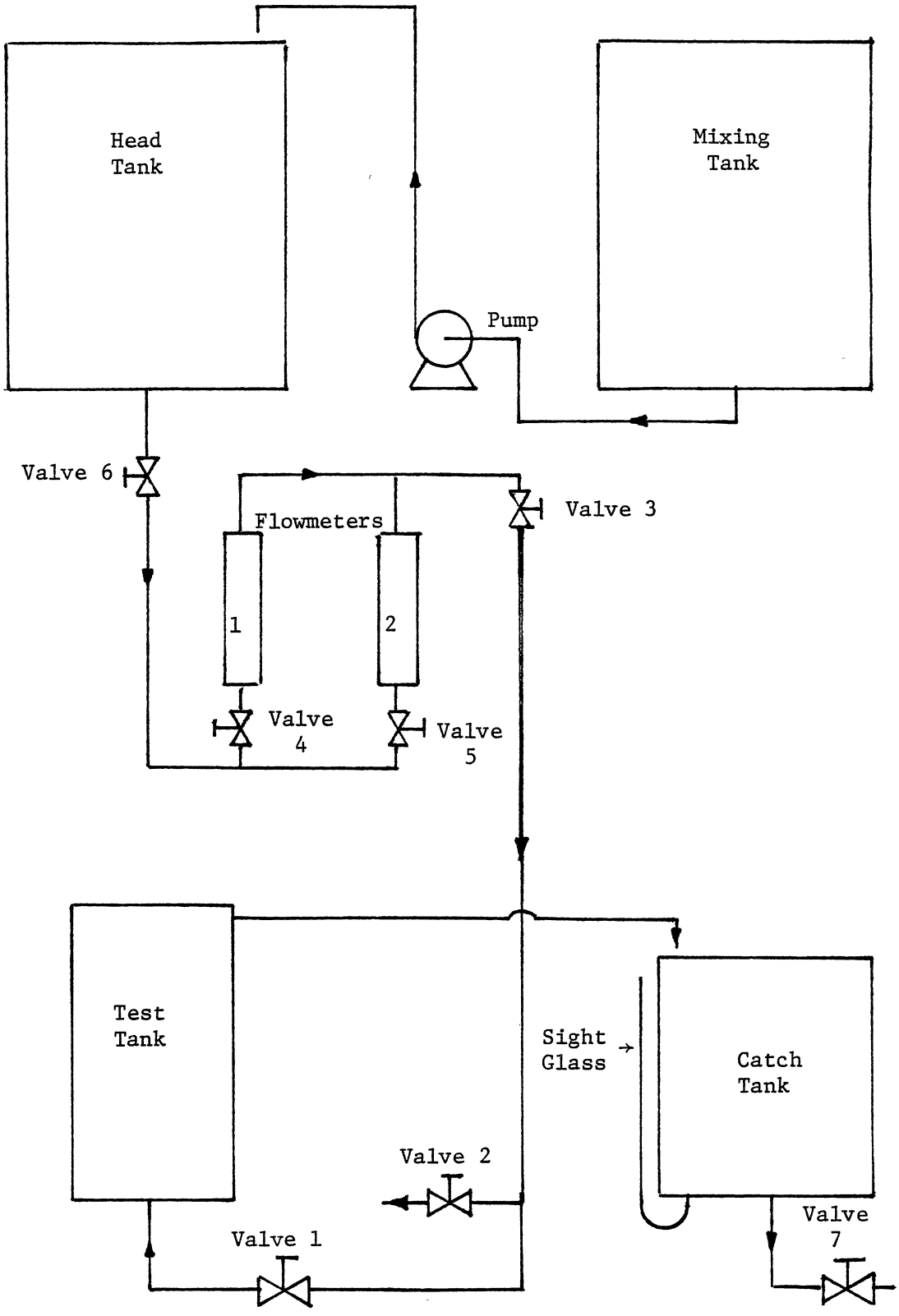

Figure 34. Schematic Diagram of OSU Experimental Setup

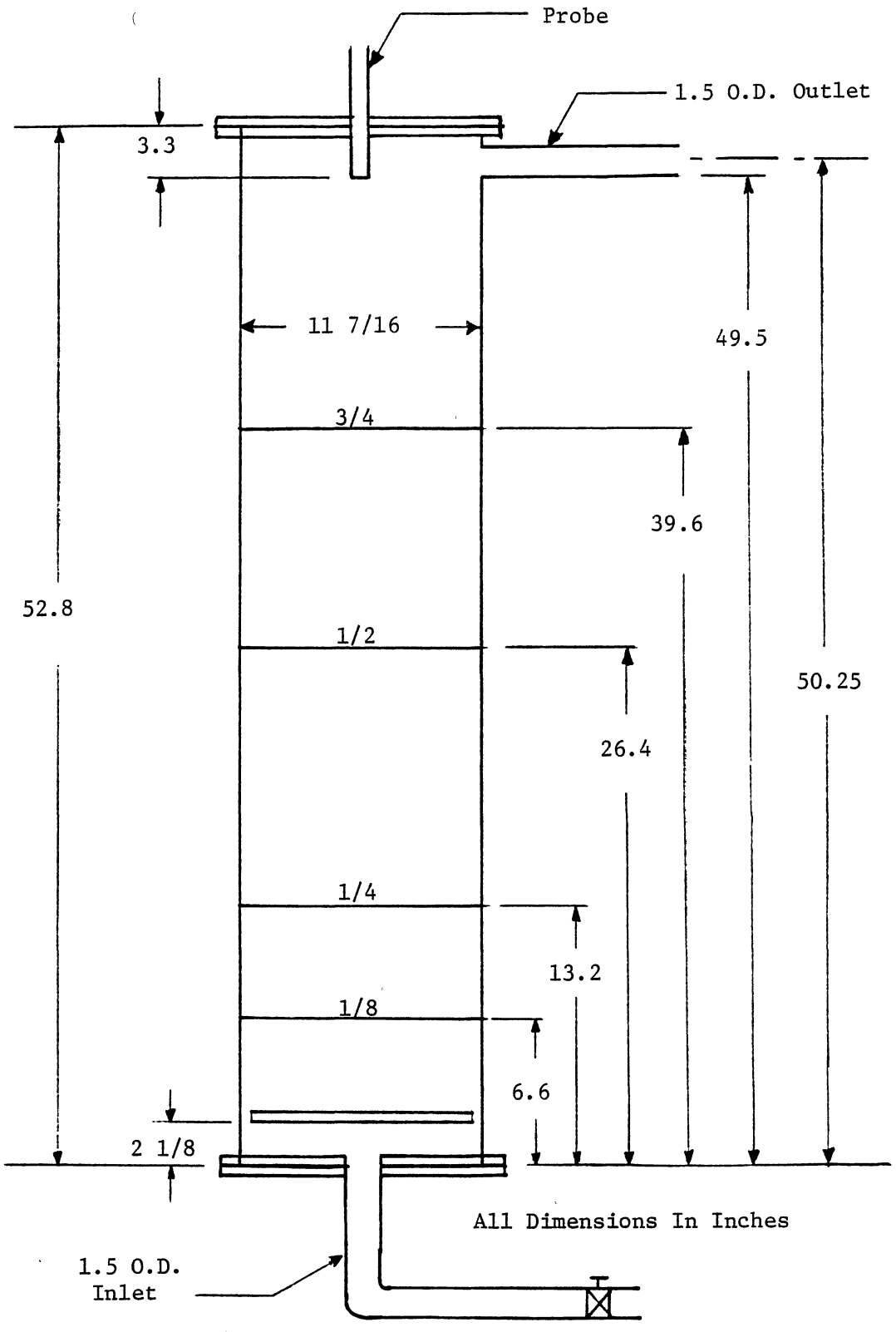

Figure 35. Prototype Test Tank Used in the OSU Experimental Setup

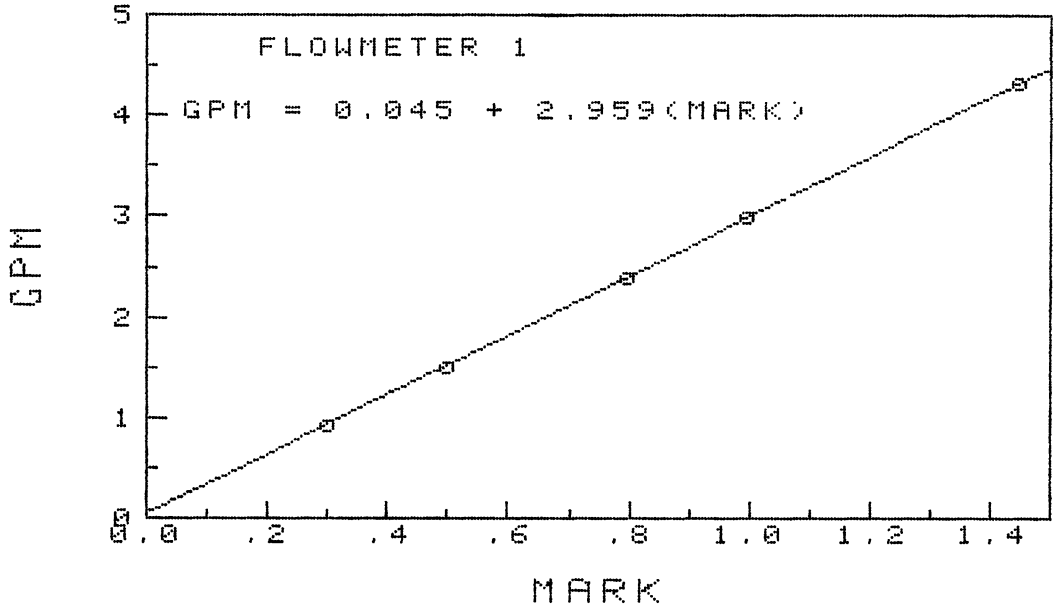

Figure 36. Calibration Curve for Flowmeter 1 (High Flow Rate Meter)

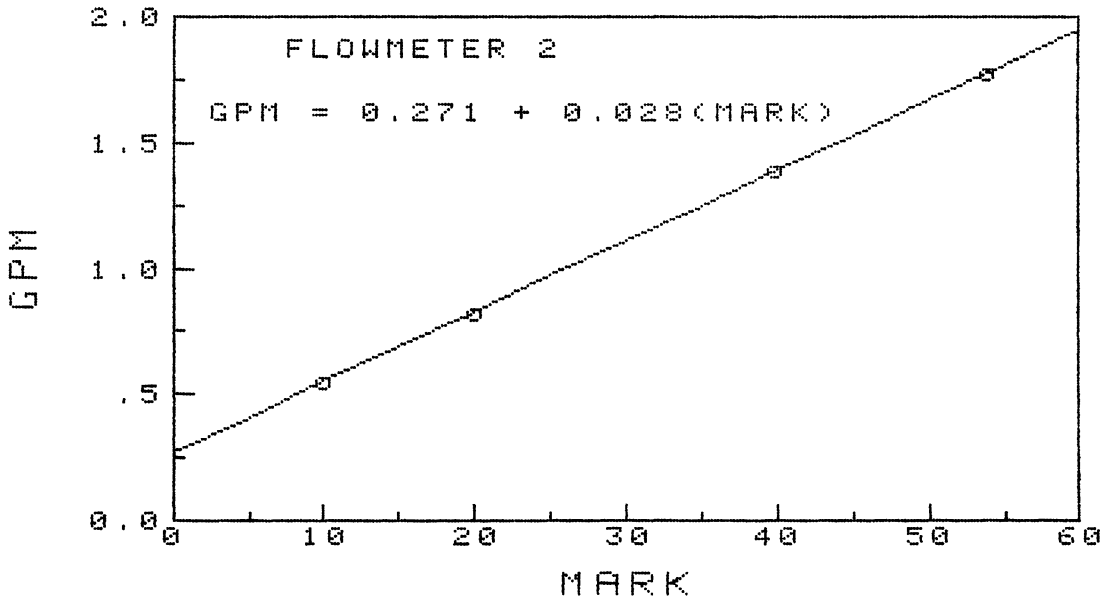

Figure 37. Calibration Curve for Flowmeter 2 (Low Flow Rate Meter)

located at every 6.6 inches corresponding to 1/16 of the total volume of the test tank (1.57 gallons), and a sight glass attached to the 30 gallon tank which was used to determine the amount of water that had been flushed out of the test tank. The dye, consisting of green food coloring, was added to the salt solution so that the thermocline development could be observed, where the green salt solution represented the cold water and the fresh water represented the hot water.

A conductivity probe obtained from Cole-Parmer Instrument Company was used to measure the salt in the test tank. The accuracy of this probe produced results within 1 % of its cell constant which was 1.0 ohm/ohm-cm. The probe was located next to the outlet of the tank. The probe required an AC power source, a wheatstone bridge, and an AC voltmeter to detect the voltage output from the probe. The input voltage to the bridge was approximately 4.86 volts rms. A circuit diagram is presented in Figure 38. The wheatstone bridge was balanced in the fresh tap water initially in the test tank so that the output voltage was approximately zero. As the incoming salt approached the probe, the voltage registered by the voltmeter started to increase. A calibration curve of percent salt concentration versus voltage based on a solution temperature of 60 ^{o}F is presented in Figure 39. In order for the calibration curve to remain correct, the temperature of the salt solution and tap water must remain near 60 ^{o}F while the data was being recorded. This problem was resolved by filling the tanks with tap water out of the faucet just before running the experiment. The water from the faucet was approximately 60 ^{o}F. The temperature in the tanks during the experiment did not change more than one degree while the experiments were conducted.

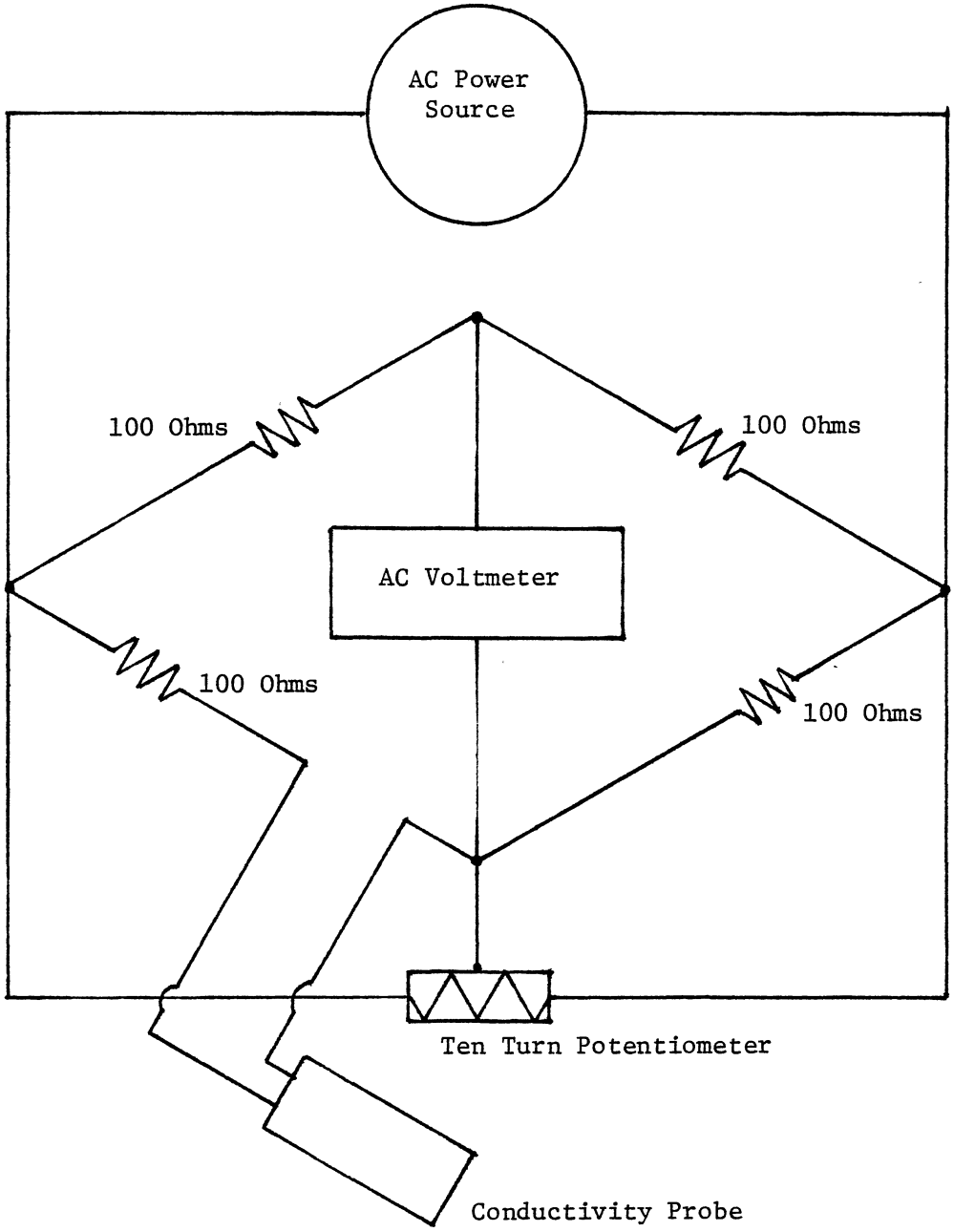

Figure 38. Circuit Diagram Of Wheatstone Bridge for Conductivity Probe

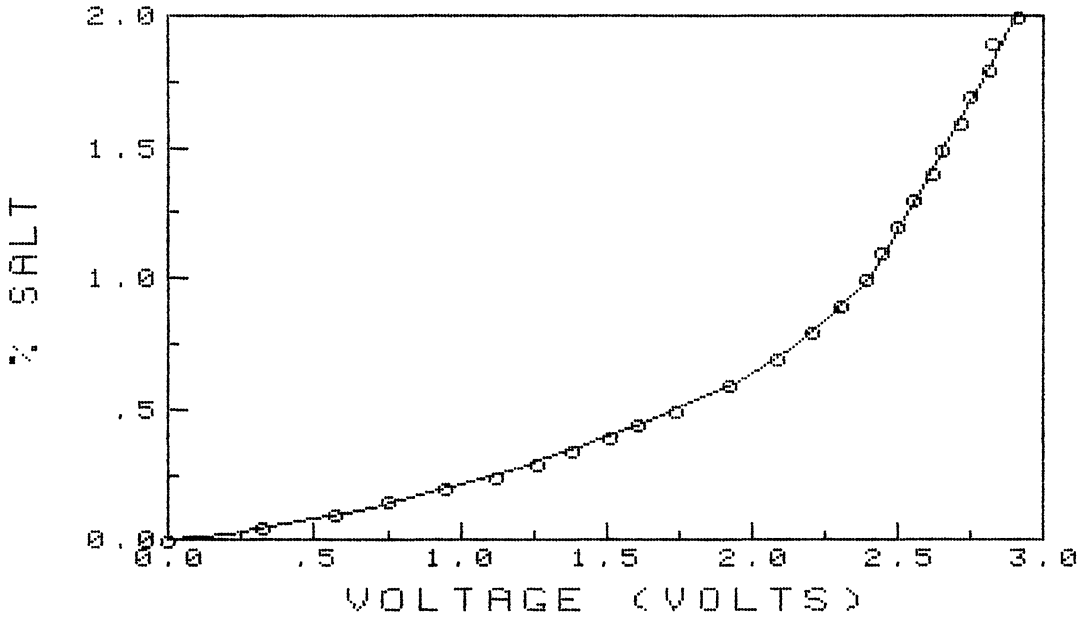

EOUT	%SALT	%SALT FIT	%DIF
.330	.050	.049	2.1
.580	.100	.100	.4
.755	.150	.143	5.2
.954	.200	.199	.6
1.126	.250	.254	1.6
1.269	.300	.304	1.4
1.392	.350	.351	.2
1.515	.400	.400	.1
1.620	.450	.445	1.1
1.740	.500	.499	.2
1.924	.600	.590	1.7
2.093	.700	.705	.7
2.210	.800	.805	.7
2.304	.900	.898	.2
2.395	1.000	.998	.2
2.450	1.100	1.102	.2
2.497	1.200	1.190	.9
2.551	1.300	1.292	.6
2.622	1.400	1.429	2.1
2.656	1.500	1.496	.3
2.715	1.600	1.614	.9
2.753	1.700	1.691	.6
2.819	1.800	1.826	1.4
2.826	1.900	1.841	3.2
2.911	2.000	2.019	1.0

Figure 39. Conductivity Probe Calibration Curve for 60 ^{0}F Solution Temperature

5.2 Experimental Procedure

A total of nine experiments were conducted. Three different salt solutions were used (2%, 1%, 0.5%). For each salt solution, three different flow rates were conducted (3.3 gpm, 1.8 gpm, 0.8 gpm). Approximately 130 gallons of salt solution was placed in the mixing tank. The conductivity probe was used to determine the amount of salt needed for the salt solution. One milliliter of dye was added for every 25 gallons of salt solution. After sufficiently mixing the solution, it was pumped from the mixing tank up to the supply tank. The prototype test tank initially contained fresh tap water. In order to alleviate the air bubbles which might be trapped within the pipes, the following steps were executed: (1) While filling the test tank with tap water, open valve 1 and 2 to allow the water to flow out the bottom of the tank into the drain. Then, close valve 2 first and close valve 1 next. (2) Open valve 2 and 3 to allow the salt solution to flow into the drain. Close valve 2 to stop the flow and leave valve 3 open. This will eliminate the air bubbles trapped in the pipes.

Before starting the experiment, the 30 gallon catch tank should contain enough water so that the sight glass level is at zero. The high flow rate experiments are conducted first; therefore, open valve 4 and close valve 5 so that Flowmeter 1 can be used. Open valve 2 to start the experiment. Adjust the float on the 1.1 mark corresponding to 3.3 gpm. Start the stopwatch when the green dye has just entered the test tank at the bottom. When the sight glass on the catch tank reaches the 1/8 mark, take a picture and record the time. Note that the markings on the catch tank include the amount of water in the entrance pipe from valve 1 to the bottom of the test tank; so that when the 1/8 mark is

reached in the catch tank, exactly 1/8 of the test tank volume has flown out. Continue to take pictures and record the time at the 1/4, 1/2, and 3/4 marks. As the thermocline approaches the probe, record the voltage readings every 5 seconds until the 1 1/8 mark is reached in the catch tank. Also record the time for the outlet and 1 1/8 mark. Close valve 3 to stop the experiment. Drain the test tank and fill it up with tap water again taking into consideration the above steps to alleviate the air bubbles. The medium flow rate experiment is conducted next: therefore, open valve 5 and close valve 4 so that Flowmeter 2 can be used. Start the experiment and adjust the float on the 55 mark corresponding to 1.8 gpm. Take pictures and data as mentioned above. Then perform the low flow rate experiment and use Flowmeter 2 again with the float located on the 20 mark corrseponding to 0.8 gpm. While running the above experiments, make sure to occasionly monitor the input voltage so that it does not drift from the 4.86 value.

5.3 Experimental Results

The flow visualization experiments show how the incoming salt solution (green dye solution which represents cold water) mixes with the fresh water (clear solution which represents hot water) inside the tank. The mixing occurs based on two principles; diffusion of the salt from the salt solution to the fresh water caused by the density difference between the two solutions which is analogous to thermal conduction, and fluid movement of the salt solution into the fresh water analogous to thermal convection. The mixing trends observed from the flow visualization are shown in Figures 40 through 42. In Figure 40, the flow rate changed from approximatedly 0.83 gpm to 3.3 gpm for a

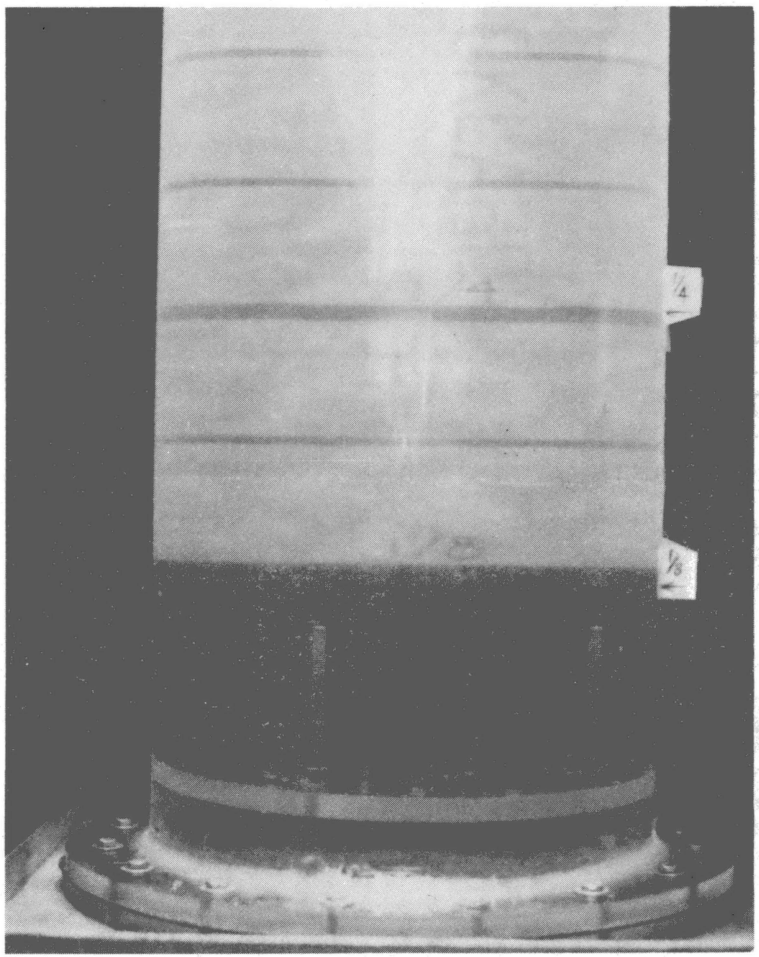

0.83 gpm

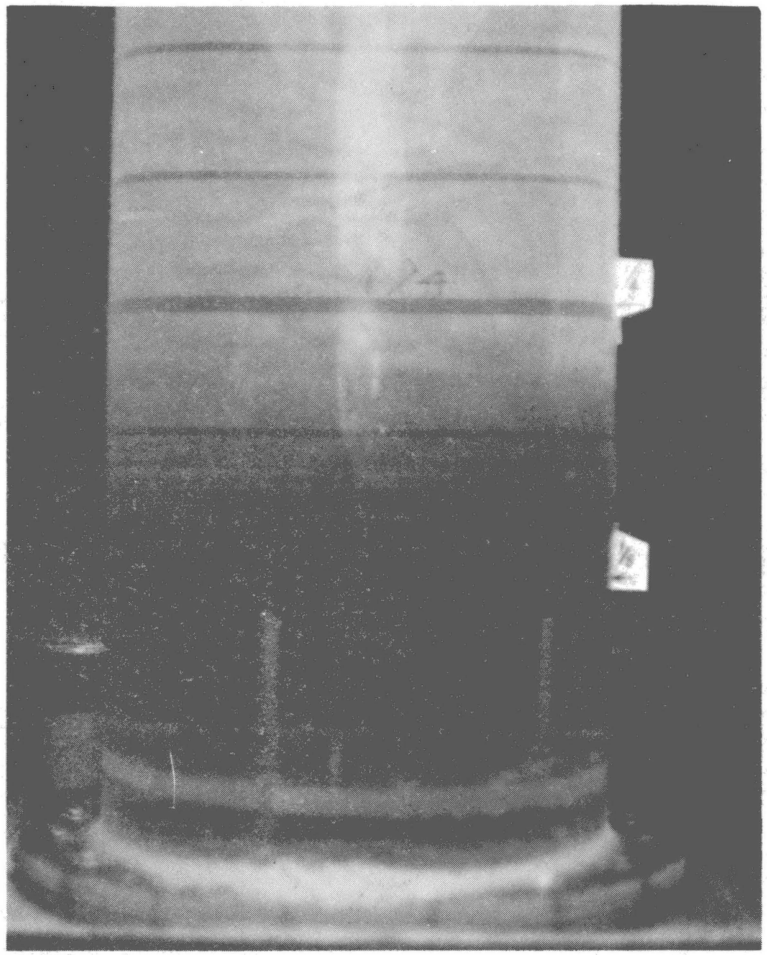

3.33 gpm

Figure 40. Visualization of Thermocline Location at the 1/8 Position for 1 % Salt Concentration.

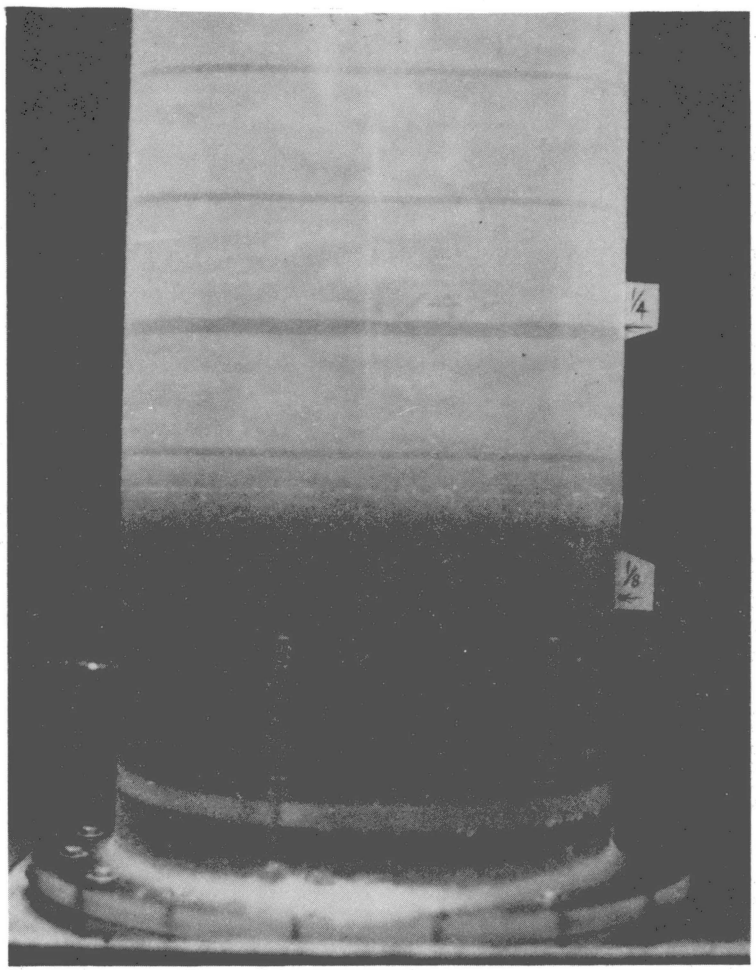

0.5 % Salt

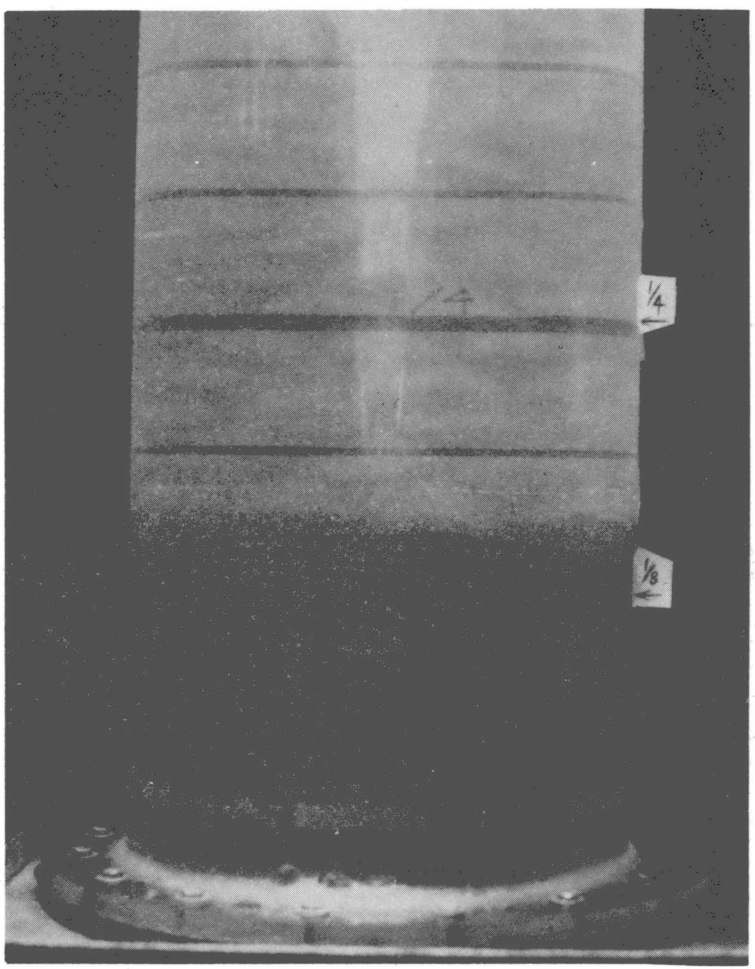

2 % Salt

Figure 41. Visualization of Thermocline Location at the 1/8 Position for 1.83 gpm.

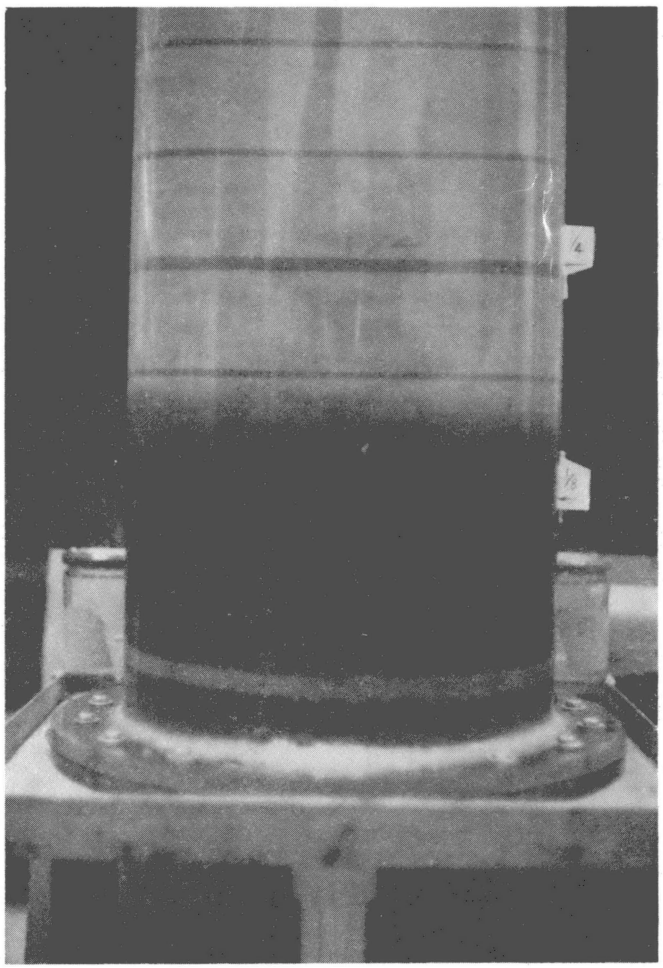

1/8 Position

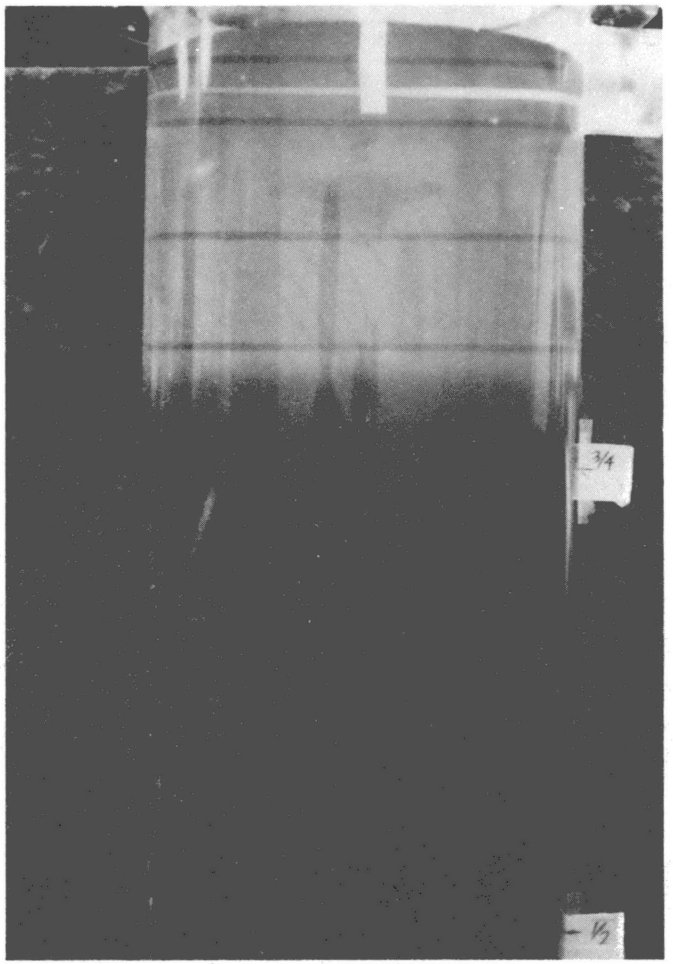

3/4 Position

Figure 42. Visualization of Thermocline Movement Through the Tank for 1 % Salt Concentration.

constant salt concentration of 1 %. The pictures were taken at the 1/8 mark in the tank; therefore if no mixing occurred, the green salt solution would be exactly at the 1/8 mark. For the low flow rate, the thermocline was located very near the 1/8 mark, thus the turbulent mixing was small. For the high flow rate, the thermocline spread beyond the 1/8 mark indicating that more turbulent mixing is occurring. In Figure 41, the flow rate (approximately 1.83 gpm) remained constant while the salt concentration changed from 0.5 % to 2 %. Again, the pictures were taken at the 1/8 mark in the tank for comparison. The amount of turbulent mixing occurring in the 2 % solution is a little less than 0.5 % solution. The amount of increase in the flow rate in Figure 40 was the same as the amount of increase in the salt concentration in Figure 41. Yet changing the flow rate increased the turbulent mixing much more than changing the salt concentration. Figure 42 indicates that the thermocline thickness does not change much from its initial development at the inlet as it moves toward the exit. The thermocline location above the 1/8 mark is approximately the same as the thermocline location above the 3/4 mark (see Figure 42). This indicates that most of the turbulent mixing occurs at the inlet and does not contribute as much away from the inlet. This supports the form of the decreasing hyperbolic function used to predict the variation of the mixing occurring in the tank in Chapter IV.

The data obtained from the probe measurement relates the outlet temperature to time. Appendix C explains how the temperatures were obtained from the voltage readings registered on the voltmeter. Simulating this experimental data with the computer model developed in Chapter III will determine the eddy conductivity values for the nine

experiments. Figures 43 through 51 present both the experimental data and the simulated temperature profile.

The lower flow rate experiments possess a sharper transition from the inlet temperature to the thermocline for the experimental data than the simulated temperature profile. This could be due to the fact that the mass diffusion of salt is not of the same magnitude as conduction of heat. Otherwords, the Lewis number (ratio of thermal diffusivity to molecular diffusivity) is not equal to one. The diffusion of salt is slower than the the conduction of heat; thus resulting in a sharper transition from the inlet value. The bulk transfer of salt into the fresh water is approximately the same as the convection of heat from the cold to hot water. Therefore, the salt experiments predict the convection of heat but may have underestimated the conduction of heat. This may be noticed in the higher flow rate experiments where convection of heat contributes the most in the mixing of the fluids. As seen in the high flow rate experiments, the simulated profile predicts the experimental profile both before and on the thermocline region. Notice that in some of the experiments, the simulated and experimental profiles deviate somewhat from each other near the end of the profile. This is probably due to the input power voltage fluctuations during the operation of the experiment. This does not affect the thermocline as much since the probe is very sensitive to smaller salt concentrations. The probe is less sensitive to higher salt concentrations; thus the effect of the input voltage could be more substantial as the tank fills up with the salt solution toward the end of the experiment. Overall, the simulated thermocline matches the experimental data adequately

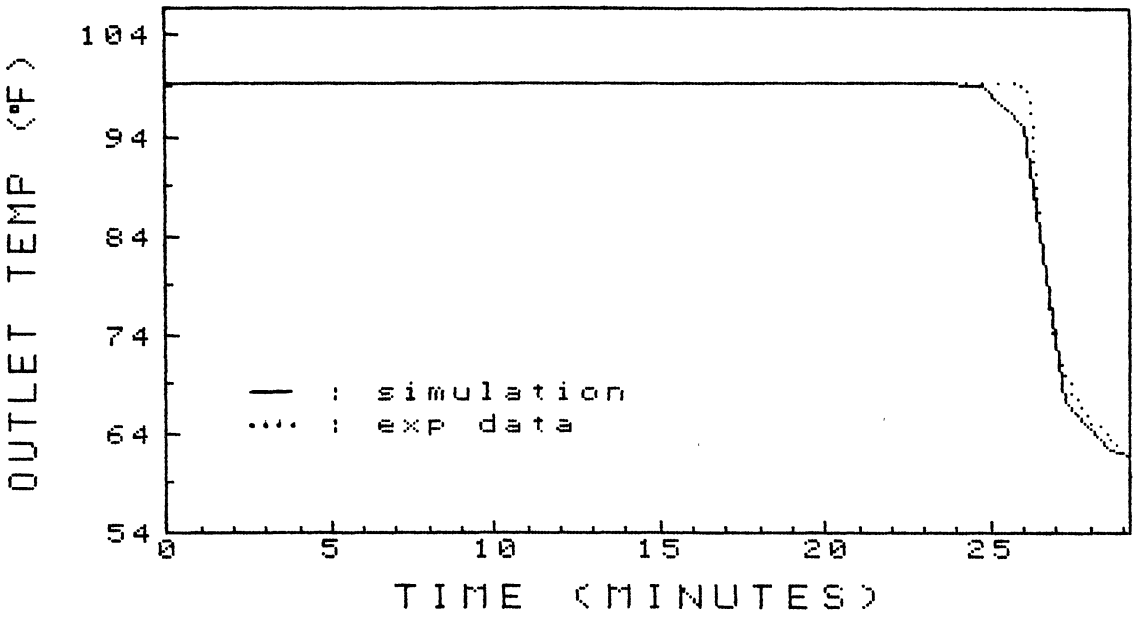

Figure 43. Simulation of OSU Experimental Data for 0.5 % Salt and 0.83 gpm Using the Hyperbolic Function

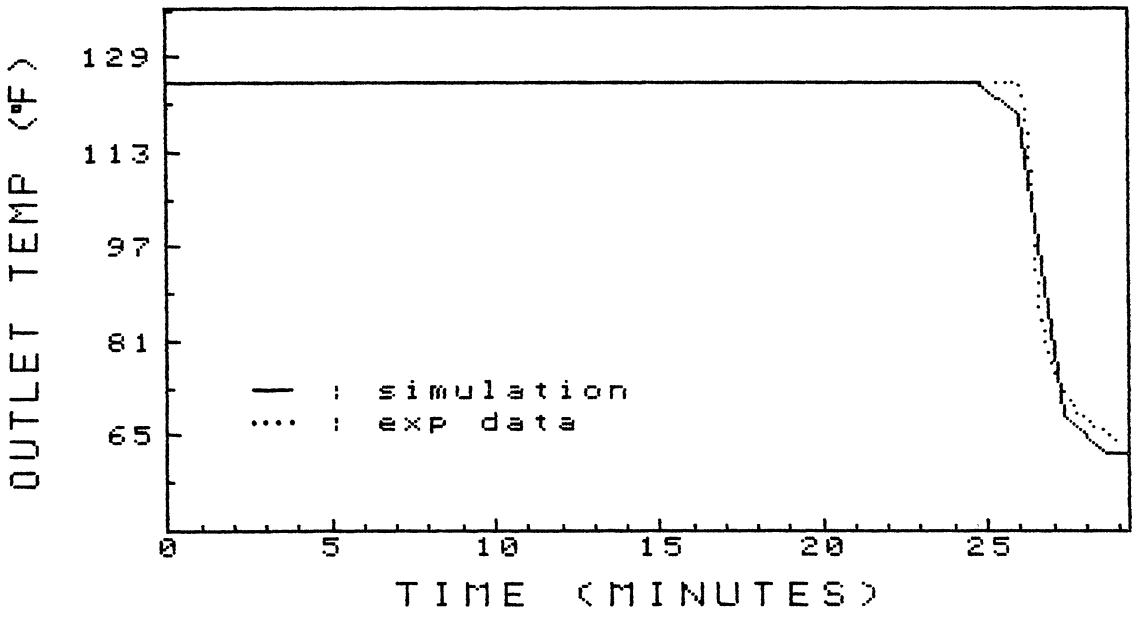

Figure 44. Simulation of OSU Experimental Data for 1.0 % Salt and 0.83 gpm Using the Hyperbolic Function

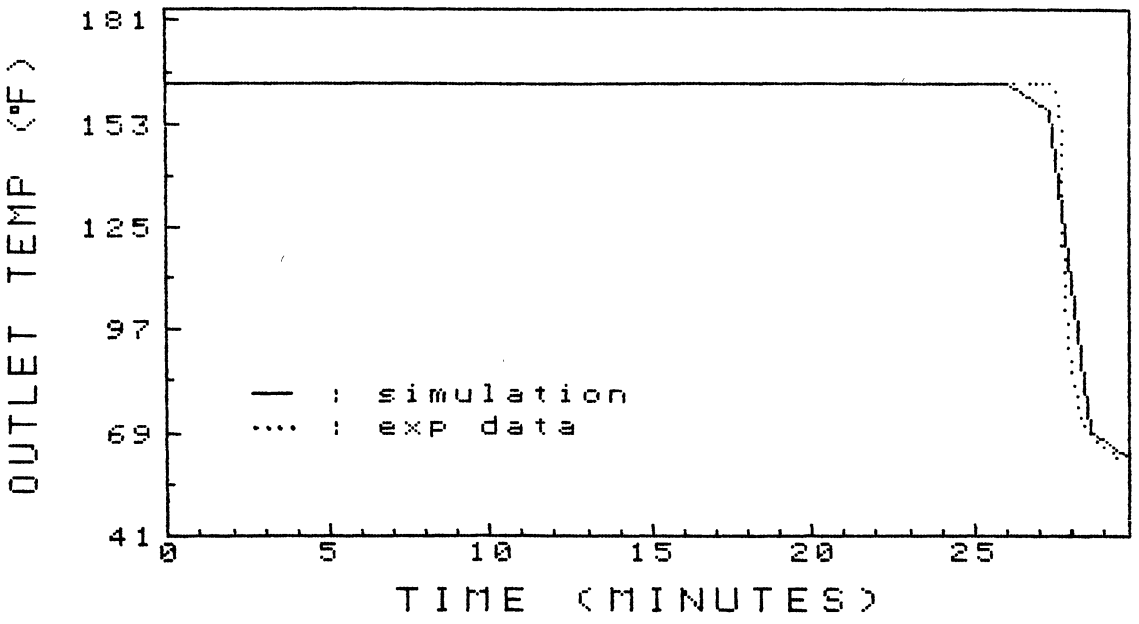

Figure 45. Simulation of OSU Experimental Data for 2.0 % Salt and 0.80 gpm Using the Hyperbolic Function

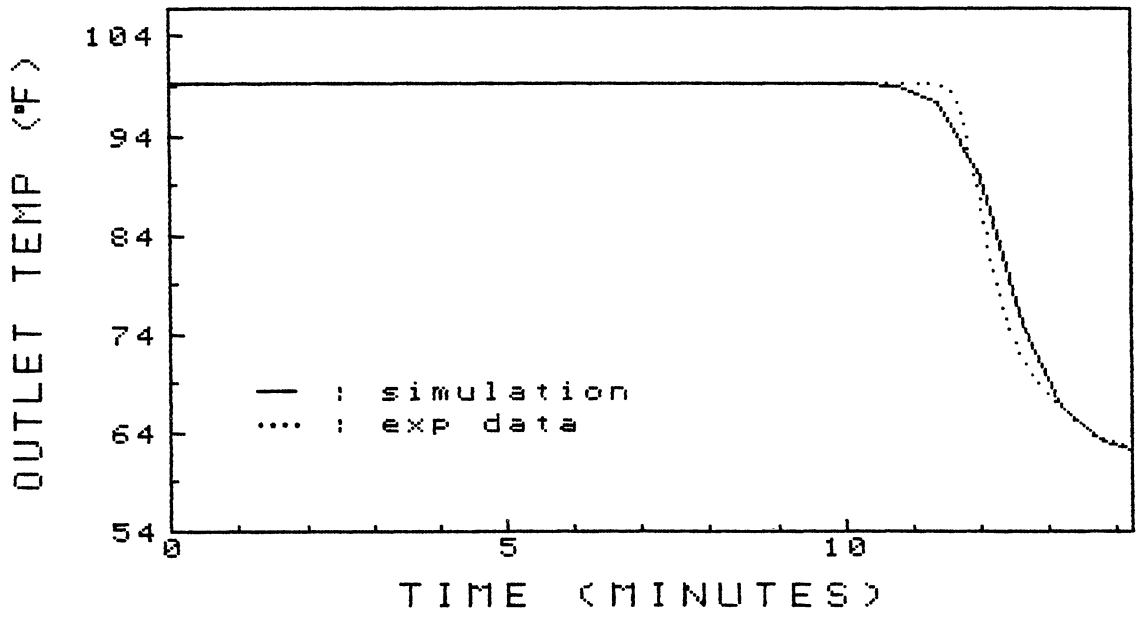

Figure 46. Simulation of OSU Experimental Data for 0.5 % Salt and 1.84 gpm Using the Hyperbolic Function

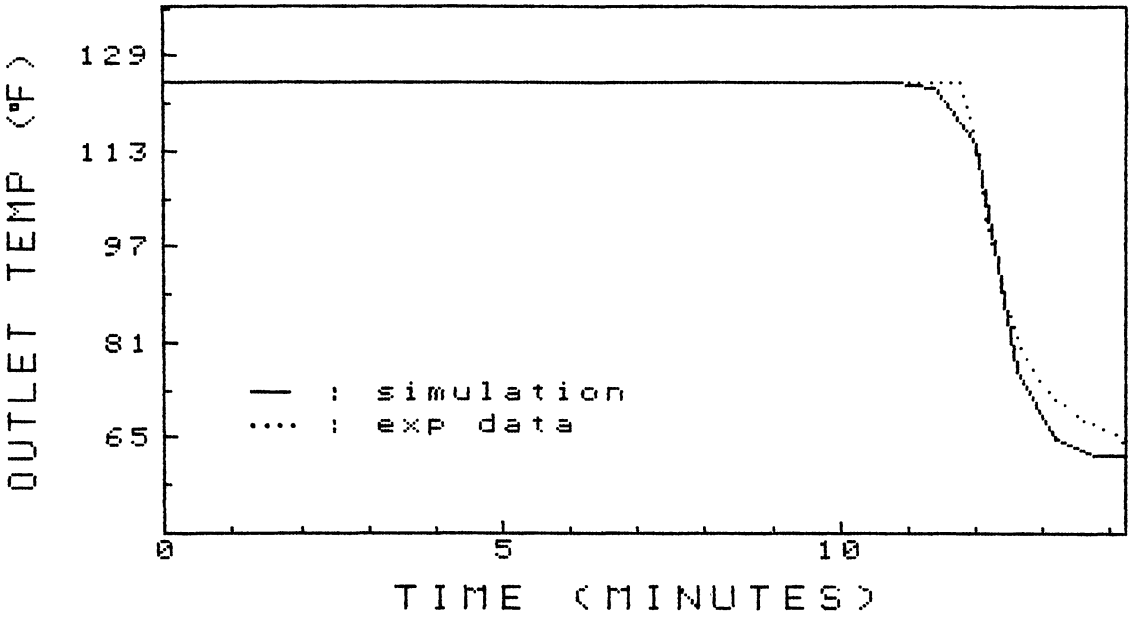

Figure 47. Simulation of OSU Experimental Data for 1.0 % Salt and 1.83 gpm Using the Hyperbolic Function

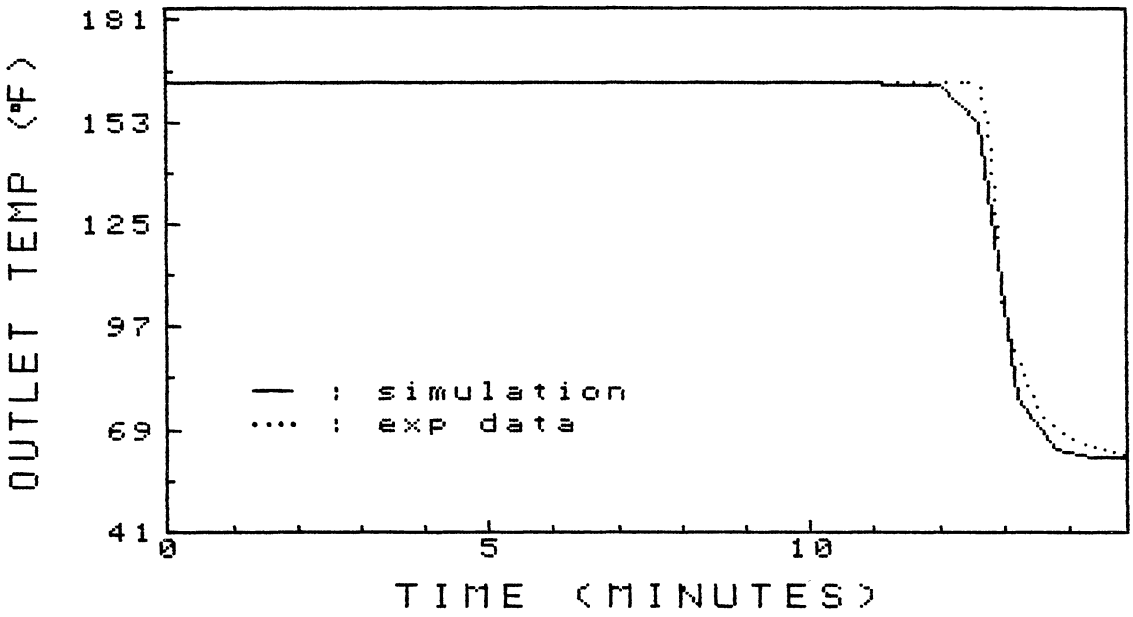

Figure 48. Simulation of OSU Experimental Data for 2.0 % Salt and 1.76 gpm Using the Hyperbolic Function

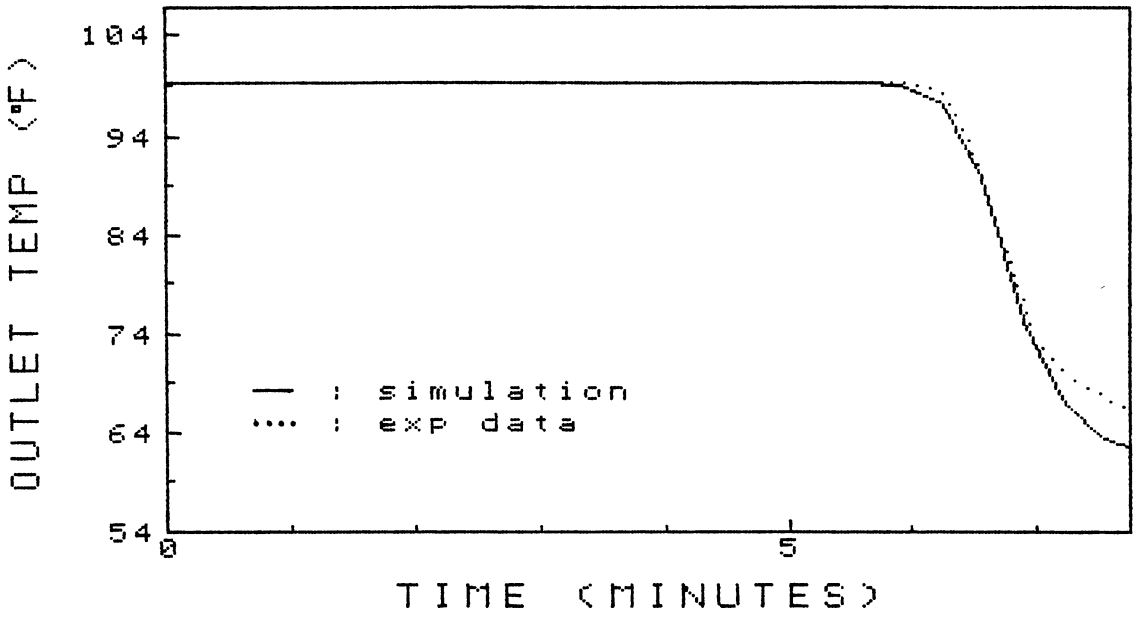

Figure 49. Simulation of OSU Experimental Data for 0.5 % Salt and 3.38 gpm Using the Hyperbolic Function

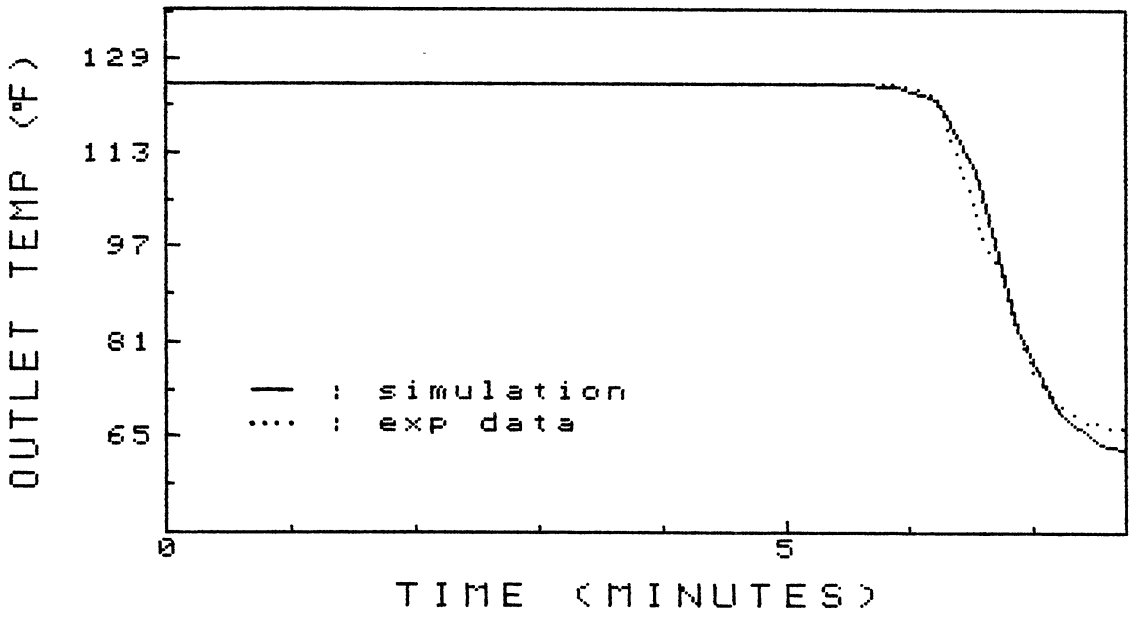

Figure 50. Simulation of OSU Experimental Data for 1.0 % Salt and 3.40 gpm Using the Hyperbolic Function

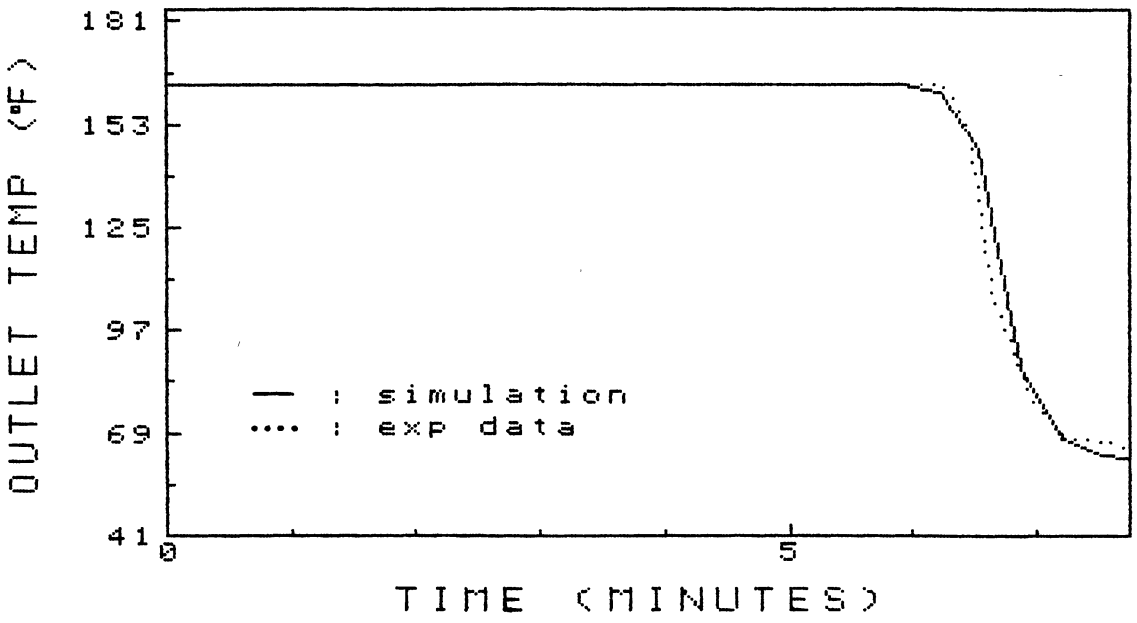

Figure 51. Simulation of OSU Experimental Data for 2.0 % Salt and 3.38 gpm Using the Hyperbolic Function

except at the locations mentioned above. Table V summarizes the eddy conductivity factors, Reynolds number, and Richardson number for each experiment.

TABLE V

SIMULATION RESULTS OF OSU EXPERIMENTAL DATA FOR THE DECREASING HYPERBOLIC FUNCTION

Figure	Inlet Eddy Conductivity Factor	Inlet Temperature ^{o}F	Initial Temperature ^{o}F	Volumetric Flow Rate gpm	Reynolds Number	Richardson Number
43	20	61	99	0.83	250	110,000
44	10	61	99	0.83	280	226,000
45	5	61	99	0.80	280	507,000
46	250	61	124	1.84	570	22,200
47	100	61	124	1.83	610	46,600
48	50	61	124	1.76	640	104,000
49	700	61	164	3.38	1040	6,600
50	500	61	164	3.40	1140	13,500
51	200	61	164	3.38	1220	28,000

CHAPTER VI

INLET EDDY CONDUCTIVITY RELATIONSHIP

After obtaining the values of the eddy conductivity factor for the inlet in Chapter IV from Reference [7] and the inlet in Chapter V, the next step is to determine the inlet eddy conductivity relationship with Reynolds number and Richardson number for both inlets. Knowing the inlet eddy conductivity factor, the eddy conductivity variation from the inlet to the outlet inside the tank is calculated from Equation (4.2). This chapter presents the general form of the two dimensionless numbers used to obtain an equation for the inlet eddy conductivity factor as a function of these dimensionless numbers for the inlets investigated.

6.1 OSU Data Correlation

The relationship between the inlet eddy conductivity factor and the two dimensionless numbers will first be examined for the experimental data obtained from the Oklahoma State experiments. A logarithmic plot of inlet eddy conductivity factor versus Richardson number is shown in Figure 52. Notice that there is a family of three curves containing the three Reynolds numbers for the corresponding high, medium, and low flow rates. Each curve represents a nearly constant Reynolds number. If the three curves could be collapsed on one curve by grouping the Reynolds number and Richardson number together in some fashion, then a functional relationship would exist between the inlet eddy conductivity factor and

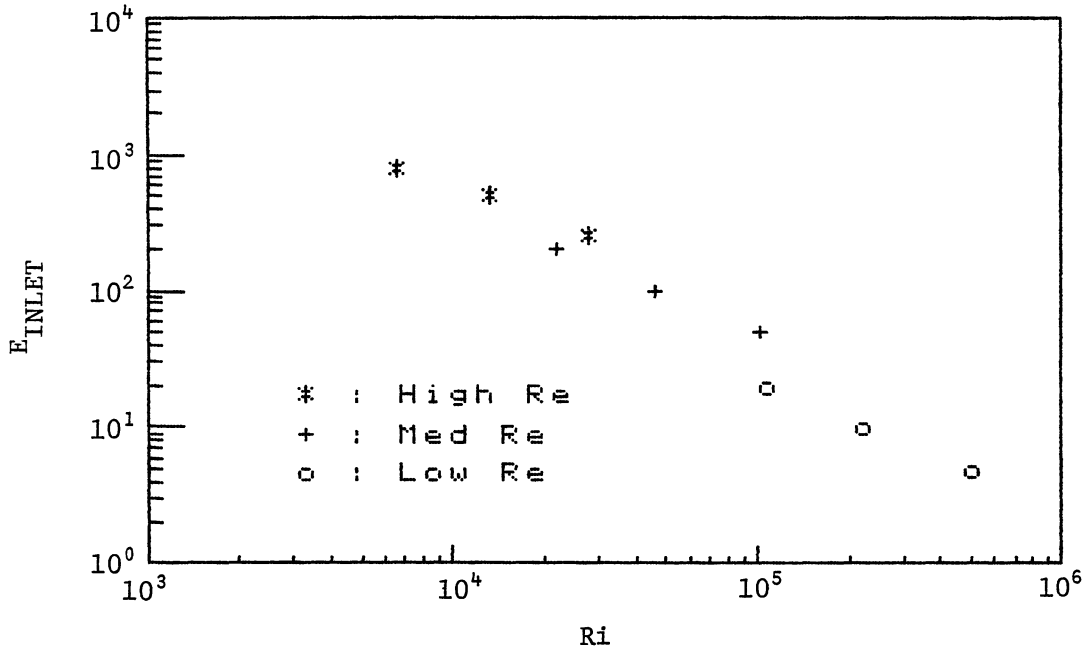

Figure 52. Inlet Eddy Conductivity Versus Richardson Number for OSU Experimental Data

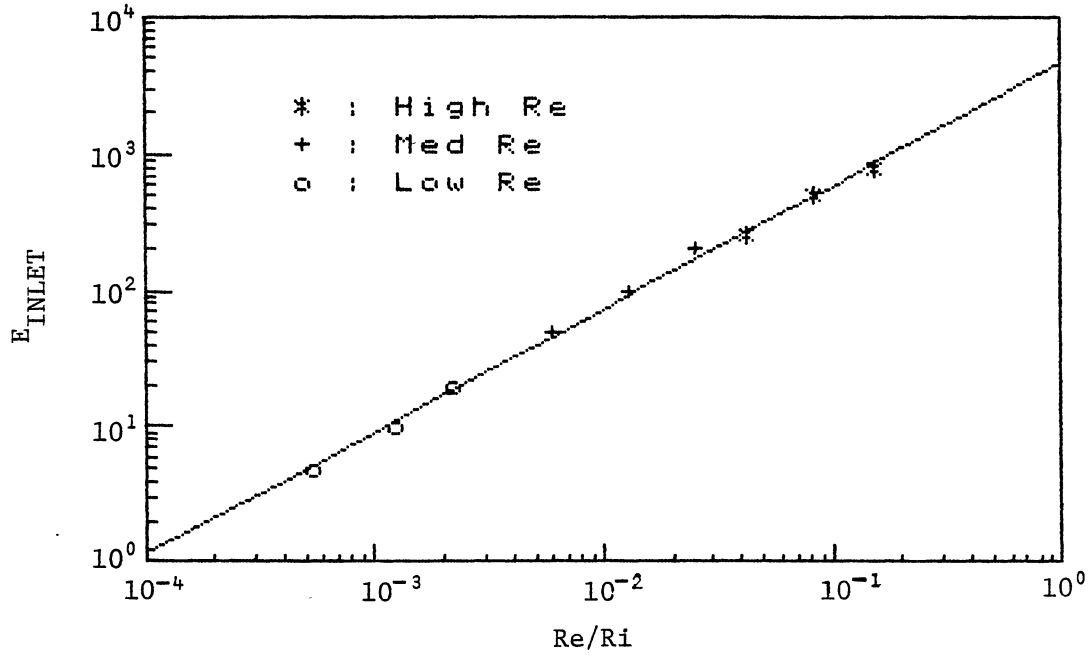

Figure 53. Inlet Eddy Conductivity Versus Reynolds Number Over Richardson Number for OSU Experimental Data

the two dimensionless numbers.

Several relationships of Reynolds number and Richardson number were examined. The best relationship proved to be the ratio of Reynolds number over Richardson number. A logarithmic plot of inlet eddy conductivity factor versus the ratio of Reynolds number over Richardson number is presented in Figure 53. This relationship produced a straight line through all three groups of Reynolds numbers on a logarithmic plot given by Equation (6.1).

$$E_{INLET} = M(Re/Ri)^{N} \tag{6.1}$$

Thus a successful relationship has been determined between the inlet eddy conductivity factor and the two dimensionless numbers. Performing a least squares fit for the straight line through the nine experimental data points produces two coefficients in Equation (6.1), namely the slope (N) and intercept (M) as shown below.

$$M = 4700$$

$$N = 0.905$$

A functional relationship has been established for the inlet geometry used in this work. The value of the inlet eddy conductivity factor can now be calculated for any given Reynolds number and Richardson number. After obtaining this inlet value, Equation (4.2) can predict the eddy conductivity variation from the inlet to outlet inside the tank.

6.2 Adoly's Experimental Data Correlation

In order to test the form of the relationship developed, it would be interesting to see if other experimental data for different inlets obey the same relationship. A logarighmic plot of Adoly's [7] results is presented in Figure 54. All of the five experimental points lie near the straight line just as the Oklahoma State University experiments did. Therefore, the form of the relationship of Reynolds number to Richardson number is the same for both cases as shown in Equation (6.1). A least squares fit produces two coefficients for the inlet used in Adoly's paper as presented below:

$$M = 2320$$

$$N = 0.176$$

Only the coefficients in Equation (6.1) have changed for the two different inlets.

6.3 Future Improvements

The results discovered in this chapter are very encouraging. A general relationship seems to hold true for the two different inlets. In order to verify this relationship, more experimental data for different inlets must be obtained. If the results hold true for several other different inlets, then this new dimensionless number consisting of Reynolds number over Richardson number may be used in predicting the amount of mixing occurring in a stratified storage tank. Only the adjustments of the coefficents obtained from the least squares fit need to be considered for the different inlets.

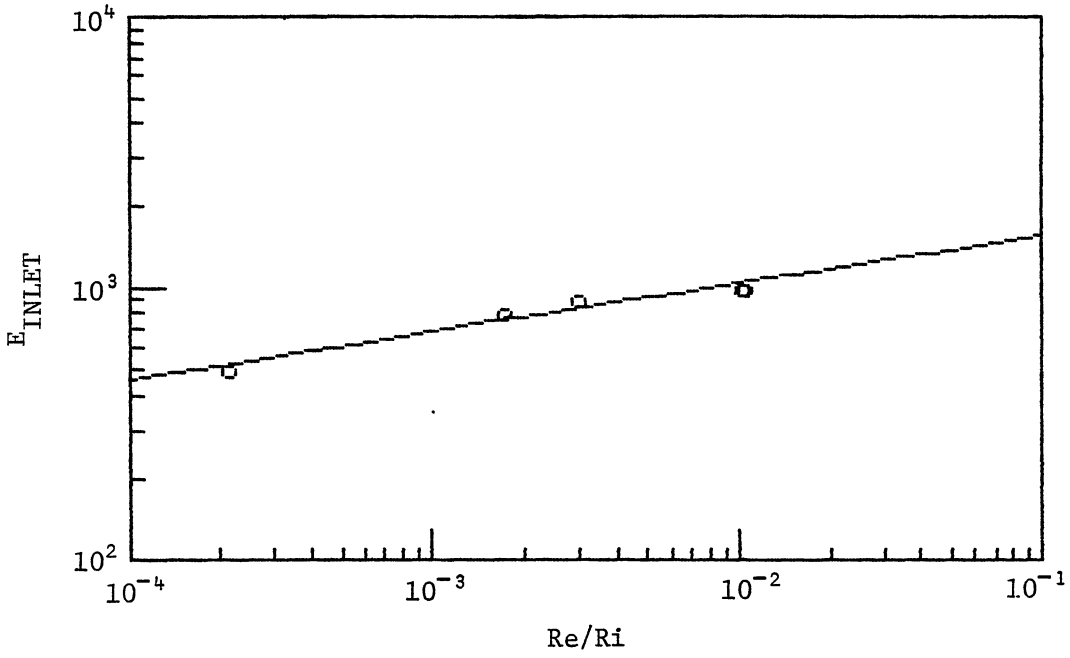

Figure 54. Inlet Eddy Conductivity Versus Reynolds Number Over Richardson Number for Experimental Data in [7]

CHAPTER VII

SUMMARY, CONCLUSIONS, AND RECOMMENDATIONS

7.1 Summary and Conclusions

The results show that a very simple numerical model can accurately simulate a stratified storage tank. The only precaution which proved to be necessary was to separate the conduction and convection algorithms in order to eliminate the gradual "smearing" of the temperature profiles in the convection-only case. The conduction algorithm was applied at each time step and the convection algorithm was applied whenever the buffer tank contained one slab volume. A variable integer relationship between time steps was achieved by means of conceptual buffer tanks.

Turbulent mixing was included with conduction by introducing an eddy conductivity factor. The eddy conductivity factors decreased from a maximum value at the inlet to a minimum value at the outlet. The decreasing hyperbola function predicted the best variation of the eddy conductivity factors inside the tank. A general relationship between the inlet eddy conductivity factor and the ratio of Reynolds number over Richardson number was found to exist for two different inlet configurations. Only two coefficients, M and N, change for the different inlets.

The model developed in Chapter III adequately predicted the experimental data found in the literature and the experimental data obtained in this work. Thus the model is flexible enough to be used for

different inlet configurations. Also the flow visualization experiments help to verify the mixing trends occurring inside the tank.

This one-dimensional model is efficient enough to be incorporated in simulations of complex chilled-water systems such as our campus-wide air conditioning at Oklahoma State University. At the same time, it proved to be more accurate than the one-dimensional model reported in the literature, because of the care taken with the points mentioned above.

7.2 Recommendations

The author's recommendation for future consideration consists of examining the following points:

(1) Picking the most efficient value of NSALB in order to reduce the computational time yet still obain satisfactory results. A larger NSLAB value will reduce the size of the buffer tank volume and more accurately predict the experimental data. A smaller amount of fluid will be accumulated in the buffer tank thus flushing the buffer tank more often.

(2) Determining the relationship between salt diffusion and heat conduction in order to obtain a correction factor for the low flow rate experiments using salt. This may be determined experimentally by executing a thermal test experiment using thermocouples to measure the temperature. For example, fill the tank half full of 60 ^{o}F water and half full of 90 ^{o}F water. Then monitor the erosion of the thermocline with no flow through the tank. Next fill the tank half full of fresh water and half full of salt water with the same density difference. Monitor the salt diffusion with the conductivity probe to determine the

diffusion of salt across the thermocline.

(3) Examine the effects of different inlets in the laboratory in order to see if the general relationship developed for the two dimensionless numbers exist, Richardson number and Reynolds number.

(4) Obtain the coefficients from the least squares fit for all the inlets that are examined and try to determine a relationship for the coefficients versus inlet geometry.

(5) Modify the analytical model for variable inlet temperature that may be between the extreme temperatures inside the tank.

(6) Examine how the heat loss through the wall in an uninsulated tank contributes to the blending of the temperatures inside the tank. This contribution may be added to the turbulent mixing inside the tank to obtain the overall effect of mixing on the temperatures.

REFERENCES

1. Sha, W. T., and Lin. "Three-Dimensional Mathematical Model of Flow Stratification in Thermocline Storage Tanks." Proceedings of the 3rd Southeastern Conference on Solar Energy, 1978, pp. 185-201.

2. Lavan, Z., and J. Thompson. "Experimental Study of Thermally Stratified Hot Water Storage Tanks." Solar Energy, Vol. 19, No. 5, (1977), pp. 519-524.

3. Sliqinski, B. J., A. R. Mech, and T. S. Shih. "Stratification in Thermal Storage During Charging." Proc. 6th Int. Heat Transfer Conference, Toronto, (1978).

4. Cabelli, A. "Storage Tanks - A Numerical Experiment." Solar Energy, Vol. 19, (1977), pp. 45-54.

5. Han, S. M., and S. T. Wu. "Computer Simulation of a Solar Energy System with an Entrainment Energy Storage Tank Model." Proceedings of the Third Southeastern Conference on Application of Solar Energy, Huntsville, Alabama, (April 1978).

6. Sharp, M. K. "Thermal Stratification in Liquid Sensible Heat Storage." (M.S. thesis, Colorado State University, Spring 1978.)

7. Adoly, M. A. "Thermal Stratification in Storage Tanks." (Ph.D. dissertation, University of Texas at Dallas, 1981.)

8. Cole, R. L., and F. O. Bellinger. "Natural Thermal Stratification in Tanks, Phase 1. Final Report." ANL 82-5.

9. Chaney, S. R., J. A. C. Humphrey, L. Month, and A. Shah. "Flow and Heat Transfer of A Stably-Stratified Fluid Through an Enclosure." ASME 83-WA/HT-75.

10. Chow, Chuen-Yen. An Introduction to Computational Fluid Mechanics. Seminole Publishing Company, Boulder, Colorado, 1983, pp. 331-336.

APPENDIX A

LITERATURE REVIEW

A.1 THERMALLY STRATIFIED TANKS - DESIGN AND NUMERICAL METHODS

1. Baines, W. D., W. W. Martin, and L. A. Sinclair. "On the Design of Stratified Thermal Storage Tanks." ASHRAE Transactions, Vol. 88, Part 2, (1982), pp. 426-439.

2. Baines, W. D., W. W. Martin, and D. M. Smith. "Development of Stratification in a Rectangular Tank by Horizontal Inflow." Journal of Fluids Engineering, Vol. 105, No. 1, (March 1983), pp. 59-64.

3. Braun, M. J., and O. W. Durrant. "The Application of Thermal Energy Storage Systems to Power Generation and Process Industries." ASME 82-WA/HT-74.

4. Cabelli, A. "Storage Tanks - A Numerical Experiment." Solar Energy, Vol. 19, (1977), pp. 45-54.

5. Calobrisi, Gary, James Henderson, Dr. Harry Brown, and Dr. Bernard Hand. "Comparison of Performance and Computer Simulation of a Thermal Storage System for Commerical Buildings." ASHRAE Transactions, Vol. 86, Part 1, pp. 336.

6. Chan, A. M. C., P. S. Smereka, and D. Giusti. "A Numerical Study of Transient Mixed Conversion Flows in a Thermal Storage Tank." Journal of Solar Energy Engineering, Vol. 105, (August 1983), pp. 246-253.

7. Chaney, S. R., J. A. C. Humphrey, L. Month, and A. Shah. "Flow and Heat Transfer of A Stably-Stratified Fluid Through an Enclosure." ASME 83-WA/HT-75.

8. Cole, R. L., and F. O. Bellinger. "Natural Thermal Stratification in Tanks, Phase 1. Final Report." ANL 82-5.

9. Cole, R. L., and F. O. Bellinger. "Thermally Stratified Tanks." ASHRAE Transactions, Vol. 88, Part 2, (1982), pp. 1005-1017.

10. Gopal, Raj. "Potential for Thermal Storage With an Organic Phase Change Material Using a Self-Contained Supercooling Suppressant Design." ASHRAE Transactions, Vol. 85, Part 1, (1979), pp. 145-155.

11. Gross, R.J., C. E. Hickox, and C. E. Hackett. "Numerical Simulation of Dual Media Thermal Energy Storage Systems." Journal of Solar Energy Engineering, Vol. 102, (November 1980), pp. 287-293.

12. Han, S. M., and S. T. Wu. "Computer Simulation of a Solar Energy System with an Entrainment Energy Storage Tank Model." Proceedings of the Third Southeastern Conference on

Application of Solar Energy, Huntsville, Alabama, (April 1978).

13. Hess, C. R. and C. W. Miller. "An Experimental and Numerical Study on the Effect of the Wall in a Thermocline - Cylindrical Enclosure - Type II." Solar Energy, Vol. 28, No. 2, (1982), pp. 153-161.

14. Hopfinger, E. J. and P. F. Linden. "Formation of Thermoclines in Zero-Mean-Shear Turbulence Subjected to a Stabilizing Bouyancy Film." Journal of Fluid Mechanics, Vol. 114, (1982), pp. 157-173.

15. Jaluria, Y. and S. K. Gupta. "Decay of Thermal Stratification in a Water Body For Solar Energy Storage." Solar Energy, Vol. 28, (1982), pp. 137-143.

16. Kennedy, M. J., S. J. Sersen, and S. M. Rossi. "Comparison of Liquid Solar Thermal Storage Subsystems in the National Solar Data Network." ASME 80/WA/SOL-36, (November 1980).

17. Klein, S. A. "TRNSYS, a Transient Simulation Program." ASHRAE Transactions, Vol. 82, (1976), pp. 623-633.

18. Loehrke, R. I., J. C. Holzer, H. N. Gari, and M. K. Sharp. "Stratification Enhancement in Liquid Thermal Storage Tanks." Journal of Energy, Vol. 3, No. 3, (1979), pp. 129.

19. Matsudaira, Hideo and Yasuo Tanaka. "Dynamic Characteristics of a Heat Storage Water Tank - Part 1." ASHRAE Transactions, Vol. 85, Part 1, (1979), pp. 110-124.

20. Matsudaira, Hideo, Yasuo Yanaka, and Hikoshi Takahashi. "Dynamic Characteristics of a Heat Storage Water Tank - Part II." ASHRAE Transactions Vol. 85, Part 1, (1979), pp. 125-144.

21. Phillips, W. F., and R. N. Dave. "Effects of Stratification on the Performance of Liquid - Based on Solar Heating Systems." Solar Energy, Vol. 29, No. 2, (1982), pp. 111-120.

22. Phillips, W. F., and R. A. Pate. "A Hot Liquid Energy Storage System Utilizing Natural Circulation." ASME 74-WA/HT-16, (1974).

23. Phillips, W. F., and R. D. Cook. "Natural circulation from a Flat Plate Collector to a Hot Liquid Storage Tank." ASME 75-HT-53, (August 1975).

24. Sha, W. T., and Lin. "Three-Dimensional Mathematical Model of Flow Stratification in Thermocline Storage Tanks." Proc. 3rd Southeastern Conf. on Solar Energy, (1978).

25. Sharp, M. K. "Thermal Stratification in Liquid Sensible Heat Storage." (M.S. thesis, Colorado State University, Spring 1978.)

26. Sharp, M. K., and R. I. Loehrke. "Stratified Thermal Storage in Residential Solar Energy Applications." Journal of Energy, Vol. 3, No. 2, (1979), pp. 106.

27. Sharp, M. K., and R. I. Loehrke. "Stratified Versus Well-Mixed Sensible Heat Storage in a Solar Space Heating System." ASME 78-HT-49 (1978).

28. Tambly, Robert T. "Thermal Storage: Resisting Temperature Blending." ASHRAE Journal, Vol. 22, No. 1, (January 1980), pp. 65-70.

29. Talaat, M. E., and E. Colucci. "Thermal Storage Performance Calculations by Closed Form and Finite Difference Solutions." ASME 82-HT-52.

30. Van Koppen, C. W. J., L. S. Fischer, and A. Dijmans. "Stratification Effects in the Short and Long Term Storage of Solar Heat." Presented Int. Solar Energy Cong., New Delhi, (1978).

31. Veryeri, E. "A Theoretical and Experimental Study of a Thermally Conducting Wall on a Stratified Fluid in a Cylinder with a Step Increase Temperature at the Top." (M.S.thesis, University of California, Berkeley 1978.)

32. Wildin, M. W., M. P. Witkofsky, P. G. Stromberg, and J. M. Noble. "Performance of Labyrinth-Stratified Water Storage Tanks for Heating and Cooling the Mechanical Engineering Building at The University of New Mexico." The University of New Mexico College of Engineering Bureau of Engineering Research Report No. ME-115(81), October 1981.

33. Yang, Wen-Jei, and C. P. Lee. "Dynamic Response of Solar Heat Storage Systems." ASME 74-WA/HT-22, (1974).

34. Young, M.F., and J.B. Bergquam. "Performance Characteristics of a Themosyphon Solar Domestic Hot Water System." Journal of Solar Energy Engineering, Vol.103, (August 1981), pp 193-200.

A.2 THERMALLY STRATIFIED TANKS - EXPERIMENTAL DATA

1. Abdoly, M. A. "Thermal Stratification in Storage Tanks." (Ph.D. dissertation, University of Texas at Dallas, 1981.)

2. Abdoly, M. A., and D. Rapp. "Theoretical and Experimental Studies of Stratified Thermocline Storage of Hot Water." Energy Convers. Mgmt., Vol. 22, (1982), pp. 275-285.

3. Hess, C. F., and C. W. Miller. "An Experimental and Numerical Study on the Effect of the Wall in a Thermocline - Cylindrical Enclosure - Type I." Solar Energy, Vol. 28, No. 2, (1982), pp. 145-152.

4. Lavan, Z., and J. Thompson. "Experimental Study of Thermally Stratified Hot Water Storage Tanks." Solar Energy, Vol. 19, No. 5, (1977), pp. 519-524.

5. Miller, C. W. "The Effect of a Thermally-Conducting Wall on a Stratified Fluid in a Cylinder." Heat Transfer and Thermal Control Systems Progress in Astronautics and Aeronautics, Vol. 60, (1977), pp. 190.

6. Tanaka, T., T. Tani, S. Sawata, K. Sakuta, and T. Horigome. "Fundamental Studies on Heat Storage of Solar Energy." Solar Energy, Vol. 19, (1977), pp. 415-419.

7. Wildin, M. W., M. P. Witkofshy, J. M. Noble, R. E. Hopper Jr, and P. G. Stromberg. "Experience with Thermal Storage in Tanks of Stratified Water for Solar Heating and Load Management." ASHRAE Transactions, Vol. 88, Part 2, (1982), pp. 1018-1027.

8. Young, M. F., and J. W. Baughn. "An Investigation of Thermal Stratification in Horizontal Storage Tanks." Journal of Solar Energy Engineering, Vol. 103, (November 1981), pp. 286-290.

A.3 INLET DISCHARGES, MANIFOLDS, AND BOTTOM WITHDRAWALS

1. Brooks, N. H., and R. C. Y. Koh. "Selective Withdrawal from Density Stratified Reservoirs." Journal of the Hydraulics Division, Vol. 95, No. HY4, Proc. Paper 6702, (July 1969), pp. 1369-1400.

2. Cederwall, Klas. "Gross Parameter Solution of Jets and Plumes." Journal of Hydraulics, Vol. 101, (May 1975), pp. 489.

3. Darden, Rufus B., Jorg Imberger, and Hugo B. Fischer. "Jet Discharge into a Stratified Reservoir." Journal of Hydraulics, Vol. 101, (September 1975), pp. 1211.

4. Dodge, Franklin T., and Edgar B. Bowles. "Draining of Tanks With Submerged Outlets Without Vacuum-Relief." Journal of Fluids Engineering, Vol. 104, No. 1, (March 1982), pp. 67-71.

5. Elder, R. A., and W. O. Wunderich. "The Prediction of Withdrawal Layer Thickness in Density Stratified Reservoirs." Proceedings 13th Congress, IAHR, Kyoto, Japan, Vol. 2, (Sept. 1969), pp. 309-316.

6. Gari, H. N., and R. I. Loehrke. "A Controlled Buoyant Jet for Enhancing Stratification in a Liquid Storage Tank." Journal of Fluids Engineering, Vol. 104, No. 4, (December 1982), pp. 475-481.

7. Gari, H. N., R. I. Loehrke, and J. C. Holzer. "Performance of an Inlet Manifold for a Stratified Storage Tank." ASME Heat Transfer Conference, Paper No. 70-HT-67, (August 1979).

8. Henderson - Sellers, Brian. "Forced Plumes in a Stratified Reservoir." Journal of Hydraulics, Vol. 104, (April 1978), pp. 487.

9. Kao, Timothy W. "Selective Withdrawal Criteria of Stratified Fluids." Journal of Hydraulics, Vol. 102, (June 1976), pp. 717.

10. Lin, E. I. H., and W. T. Sha. "Effects of Baffles on Thermal Stratification in Thermocline Storage Tanks." Proc. 1979 Int. Solar Energy Conference, Atlanta (1979).

11. Loehrke, R. I. "A Passive Technique for Enhancing Thermal Stratification in Liquid Storage Tanks." ASME 78-HT-50 (1978).

12. Sliqinski, B. J., A. R. Mech, and T. S. Shih. "Stratification in Thermal Storage During Charging." Proc. 6th Int. Heat Transfer Conf., Toronto, (1978).

13. Walesh, Stuart G. and Peter L. Monkmeyer. "Bottom Withdrawal of Viscous Stratified Fluid." Journal of Hydraulics, Vol. 99, (September 1973), pp. 1401.

14. Wright, Steven, and Roger B. Wallace. "Two-Dimensional Buoyant Jets in Stratified Fluid." Journal of Hydraulics, Vol. 105, (November 1979), pp. 1393.

A.4 TEMPERATURE AND MIXING EFFECTS

1. Busnaina, Ahmed A., David Lilley, and Peter Moretti. "Local Destratification of Lakes." Journal of Hydraulics, Vol. 107, (March 1981), pp. 259.

2. Gill, A. E., and A. Davey. "Instabilities of a Buoyancy Driven System." Journal of Fluid Mechanics, Vol. 25, (1969), pp. 775-798.

3. Harleman, Donald R. F. "Hydrothermal Analysis of Lakes and Reservoirs." Journal of Hydraulics, Vol. 108, (March 1982), pp. 301.

4. Holliday, D., and M. E. McIntyre. "On Potential Energy Density in an Incompressible Stratified Fluid." Journal of Fluid Mechanics, Vol. 107, (1981), pp. 221-225.

5. Jirka, Gerhard H. and Masataka Watanabe. "Thermal Structure of Cooling Ponds." Journal of Hydraulics, Vol. 106, (May 1980), pp. 701.

6. Lam Lau, Y., and B. C. Krishnappan. "Modeling Transverse Mixing in Natural Streams." Journal of Hydraulics, Vol. 107, (February 1981), pp. 209.

7. Nicholas, V. M. and James G. Rodger. "Vertical Mixing in Stratified Tidal Flows." Journal of Hydraulics, Vol. 104, (March 1978), pp. 337.

8. Schinkel, W. M. M., S. J. M. Linthorst, and Hoogendoorn. "The Stratification in Natural Convection in Vertical Enclosures." Journal of Heat Transfer, Vol. 105, No. 2, (May 1983), pp. 267-272.

9. Shaaban, A. H., and M. N. Ozisik. "The Effect of Nonlinear Density Stratification on the Stability of a Vertical Water Layer in the Conduction Regime." Journal of Heat Transfer, Vol. 105, No. 1, (1983), pp. 130-137.

10. Spalding, D. B., U. Svensson. "The Development and Erosion of the Thermocline." Heat Transfer and Turbulent Buoyant Convection, Hemisphere Publishing Corporation, (1977), pp. 113-122.

11. Stefan, Heinz, and Dennis E. Ford. "Temperature Dynamics in Dimictic Lakes." Journal of Hydraulics, Vol. 101, (January 1975), pp. 97.

12. Uzzell, Jr., James and M. Necatti Ozisik. "Three-Dimensional Temperature Model for Shallow Lakes." Journal of Hydraulics, Vol. 104, Part 2, (December 1978), pp. 1635.

13. Zob, A. P. "Significance of Temperature Stratification in Liquid Storage Tanks for Solar Applications." Proc. Solar Energy Storage Options Conference, San Antonio (1979).

A.5 STRATIFIED FLOW

1. Benjamin, T. B. "Steady Flows from a Stably Stratified Reservoir." Journal of Fluid Mechanics, Vol. 106, (1981), pp. 245-260.

2. Cook, Robert E. "Effects of Stratification in Performance and Control of Residential Electric Water Heaters." ASHRAE Transactions, Vol. 86, Part 1, (1980).

3. Findikakis, Angelos and Robert L. Street. "Finite Element Simulation of Stratified Turbulent Flow." Journal of Hydraulics, Vol. 108, (August 1982), pp. 904.

4. French, Richard H. "Stratification and Open Channel Flow." Journal of Hydraulics, Vol. 104, (January 1978), pp. 21.

5. Hyden, Hans "Water Exchange in Two Layer Stratified Waters." Journal of Hydraulics, Vol. 100, (March 1979), pp. 345.

6. Jaluria, Y., and B. Gebhart. "Stability and Transition of Buoyancy-Induced Flows in a Stratified Medium." Journal of Fluid Mechanics, Vol. 66, (1974), pp. 593-612.

7. Meyer, Zygmunt. "Vertical Circulation in Density Stratified Reservoir." Journal of Hydraulics, Vol. 108, (July 1983), pp. 853.

8. Wang, John. "Finite Element Model of 2-Dimensional Stratified Flow." Journal of Hydraulics, Vol. 105, (December 1979), pp. 1473.

A.6 METHOD OF TESTING STORAGE TANKS

1. Hill, James E., George Kelly, and Bradley Peavy. "A Method of Testing for Rating Thermal Storage Devices Based on Thermal Performance." Solar Energy, Vol. 19, (1977), pp. 721-732.

2. Hunt, Bernard J, Thomas E. Richtmyer, James E. Hill, and Elizabeth A. Franklin. "Testing of Water Tanks for Thermal Storage According to ASHRAE Standard 94-77." ASHRAE Transactions, Vol. 85, Part 1, (1979), pp. 481-501.

APPENDIX B

COMPUTER NOMENCLATURE AND COMPUTER PROGRAM

COMPUTER NOMENCLATURE

A -- Above diagonal term in TDMA

AREA -- Cross-sectional area of tank, ft^2

ACCUMB -- Bottom buffer tank

ACCUMT -- Top buffer tank

AMIX -- Dimensionless mixing constant

AMIXEX -- Value of AMIX at the exit

AMIXI -- AMIX value based on inlet properties

AMIXIN -- Value of AMIX at the inlet

AMIXL -- Laminar value of AMIX (EDDY = 1)

AMIXO -- AMIX value based on initial properties

B -- Below diagonal term in TDMA

C -- Right side term in TDMA

CLOSS -- Conduction heat loss to environment

CHOICE -- Used to select the type of given experimental temperature profile

D -- Diagonal term in TDMA

DIA -- Inside diameter of tank, ft

DIFUS -- Average thermal diffusivity between initial and inlet properties, ft^2/min

DIFIN -- Thermal diffusivity based on inlet temperature, ft^2/min

DIFO -- Thermal diffusivity based on initial temperature, ft^2/min

DELR -- Density difference between initial and inlet, lbm/ft^3

DELT -- Time interval in subprogram TANK, minutes

DELTM -- Time interval in main program, minutes

DELX -- Distance between slabs in the tank, ft

DIR -- Direction of flow where DIR = 1 flow into bottom, DIR = -1 flow into top, and DIR = 0 no flow

EDDY -- Eddy conductivity factor

EEXIT -- Exit eddy conductivity factor which is 1

EINLET -- Inlet eddy conductivity factor

EMAX -- Maximum inlet eddy conductivity factor

ERROR -- Summation of error between experimental and simulated data

ETEST -- Error test variable

FINISH -- Termination value for program, minutes

FLOW -- Dimensionless flow parameter

GPM -- Volumetric flow rate, gpm

HD -- Tank height over inside tank diameter ratio

HEIGHT -- Height of water in tank between inlet and outlet, ft

IEND -- Total number or experimental data points

ISLAB -- Position of slab I

NSLAB -- Number of slabs in the tank

NSLAB1 -- NSLAB - 1

PICK -- Used to select the type of function for eddy variation

POS1 -- Calculated position value for beginning thermocline location

POS2 -- Calculated position value for ending thermocline location

QMAX -- Maximum volumetric flow rate, ft^3/min

QVOL -- Volumetric flow rate, ft^3/min

REY -- Average Reynolds number between inlet and initial properties

REYIN -- Reynolds number based on inlet properties

REYO -- Reynolds number based on initial properties

RICH -- Average Richardson number between inlet and initial properties

RICHIN -- Richardson number based on inlet properties

RICHO -- Richardson number based on initial properties

ROW -- Average density of fluid between inlet and initial, lbm/ft^3

ROWIN -- Density of fluid based on inlet temperature, lbm/ft^3

ROWO -- Density of fluid based on initial temperature, lbm/ft^3

SLOPE -- Multiplication factor in eddy variation equation

SINLET -- Variable used to store best EINLET value during run

SEXIT -- Variable used to store best EEXIT value during run (Always 1)

T -- Temperature, ^oF

TENVIR -- Temperature of the environment, ^oF

TEST -- Test the direction of flow for previous time level

TEST1 -- Test value for beginning thermocline position

TEST2 -- Test value for ending thermocline position

TEXP -- Experimental temperature, ^oF

TNEW -- Temperature variable used to store temperatures at new time level, ^oF

TIME -- Time, minutes

TIN -- Temperature of incoming flow, ^oF

TO -- Initial temperature in the tank, ^oF

TOUT -- Temperaure of exiting flow, ^oF

VALUE1 -- Percentage of beginning thermocline wanting to test

VALUE2 -- Percentage of ending thermocline wanting to test

VEL -- Velocity of water in the tank, ft/min

VMAX -- Maximum velocity of water in tank, ft/min

XI -- Conversion of integer variable ISLAB to real variable

XINCEP -- Intercept value in eddy variation equation

XMIN -- Variable used to store the minimum error during run

XNSLAB -- Conversion of integer variable NSLAB to real variable

XNU -- Average kinematic viscosity between inlet and initial temperature, ft^2/sec

XNUIN -- Kinematic viscosity based on inlet temperature, ft^2/sec

XNUO -- Kinematic viscosity based on initial temperature, ft^2/sec

Computer Program

```
C*********************************************************************
C                                                                     *
C                                                                     *
C     THIS PROGRAM WILL DETERMINE THE BEST CONSTANTS FOR A FUNCTION   *
C     VARIATION OF EDDY CONDUCTION FACTORS FROM MAXIMUM AT THE        *
C     INLET TO MINIMUM AT THE EXIT.                                   *
C                                                                     *
C          EINLET  -  MAXIMUM VALUE AT THE INLET                      *
C          EEXIT   -  VALUE AT THE EXIT WHICH IS 1                    *
C                                                                     *
C     SELECT THE TYPE OF FUNCTION VARIATION OF FACTORS                *
C                                                                     *
C          PICK = 1   -  LINEAR VARIATION                             *
C          PICK = 2   -  HYPERBOLIC VARIATION                         *
C          PICK = 3   -  EXPONENTIAL NEGATIVE VARIATION               *
C                                                                     *
C     SELECT THE TYPE OF COMPARISONS                                  *
C                                                                     *
C          CHOICE = 1  -   OUTLET TEMP  VERSUS  TIME                  *
C          CHOICE = 2  -   TEMP PROFILE VERSUS  SLABS IN TANK         *
C                               FOR SPECIFIC TIME DESIRED             *
C                                                                     *
C*********************************************************************
C                                                                     *
      COMMON
     1/VAR/A(50),B(50),C(50),D(50),ACCUMT,ACCUMB,AMIX,AMIXL,AMIXIN,
     2     AMIXEX,DELT,DELTM,DELX,DIR,EINLET,EEXIT,FLOW,ISLAB,NSLAB,
     3     NSLAB1,PICK,T(50),TEST,TEXP(50),TIN,TIME,TNEW(50),TOUT(200)
C
C   READ THE FOLLOWING INFORMATION FROM A DATA FILE
C
C     GPM    -    VOLUMETRIC FLOW RATE IN GPM
C     NSLAB  -    NUMBER OF SLABS, INTEGER VALUE
C     DIR    -    1 (FLOW INTO BOT), -1 (FLOW INTO TOP), 0 (NO FLOW)
C     DELT   -    MINUTES AND MUST BE MULTIPLE OF DELTM
C     DELTM  -    MINUTES
C     HEIGHT -    FEET
C     DIA    -    FEET
C     TO     -    FAHRENHEIT
C     TIN    -    FAHRENHEIT
C     IEND   -    NUMBER OF DATA POINTS, INTEGER VALUE
C
      READ(8,31) GPM,NSLAB,DIR,DELT,DELTM,HEIGHT,DIA
      READ(8,32) TO,TIN,IEND
      DO 10 I = 1, IEND
  10       READ(8,33) TEXP(I)
      DO 20 I = 1, NSLAB
  20       T(I) = TO
C
C   SELECT DESIRED CHOICE
```

```
C
      PICK = 2
      CHOICE = 1
      IF (CHOICE.EQ.1) FINISH = IEND * DELTM
      IF (CHOICE.EQ.2) FINISH = DELTM
C
C   DETERMINE POSITION OF THERMOCLINE YOU WANT TO TEST.
C
C     EXAMPLE:  VALUE1 = 0.025  IS  2.5 % OF (TEXP-TO)/(TO-TIN)
C               VALUE2 = 0.025  IS  2.5 % OF (TEXP-TIN)/(TIN-TO)
C
C     SET VALUE1 = 0 , VALUE2 = 0   TO EXAMINE TOTAL THERMOCLINE
C
      VALUE1 = 0.025
      VALUE2 = 0.025
      DO 40 I = 1, IEND
           TEST1 = ABS((TEXP(I)-TO)/(TO-TIN))
           TEST2 = ABS((TEXP(I)-TIN)/(TIN-TO))
           IF (TEST1.LE.VALUE1) POS1 = I
           IF (TEST2.GE.VALUE2) POS2 = I
   40 CONTINUE
C
C   CALCULATE TANK AND FLOW PROPERTIES
C
      XMIN = 1.0E10
      NSLAB1 = NSLAB - 1
      ACCUMT = 0.0
      ACCUMB = 0.0
      TEST = 0.0
      TIME = 0.0
      PI = 3.141593
      AREA = PI * DIA**2/4.0
      HD = HEIGHT/DIA
      DELX = HEIGHT / FLOAT(NSLAB)
      ROWIN = 62.267+9.1402E-3*TIN-1.3489E-4*TIN**2+1.7632E-7*TIN**3
      ROWO = 62.267+9.1402E-3*TO-1.3489E-4*TO**2+1.7632E-7*TO**3
      ROW = (ROWIN + ROWO) / 2.0
      DELR = ABS (ROWIN - ROWO)
      QVOL = GPM / 7.48
      VEL = QVOL / AREA
      FLOW = VEL * DELT / DELX
      DIFIN = 8.093E-5+2.134E-7*TIN-4.670E-10*TIN**2+5.472E-13*TIN**3
      DIFO = 8.093E-5+2.134E-7*TO-4.670E-10*TO**2+5.472E-13*TO**3
      DIFUS = (DIFIN + DIFO) / 2.0
      AMIXI = DIFIN * DELT / DELX**2
      AMIXO = DIFO * DELT / DELX**2
      AMIXL = DIFUS * DELT / DELX**2
      XNUIN = 2.9693E-5-4.1657E-7*TIN+2.4105E-9*TIN**2-4.95E-12*TIN**3
      XNUO = 2.9693E-5-4.1657E-7*TO+2.4105E-9*TO**2-4.95E-12*TO**3
      XNU = (XNUIN + XNUO) / 2.0
      RICHIN = DELR * 32.174 * HEIGHT / (ROWIN * (VEL/60.0)**2)
      RICHO = DELR * 32.174 * HEIGHT / (ROWO * (VEL/60.0)**2)
      RICH = DELR * 32.174 * HEIGHT / (ROW * (VEL/60.0)**2)
      REYIN = VEL/60.0 * DIA / XNUIN
```

```
      REYO = VEL/60.0 * DIA / XNUO
      REY = VEL/60.0 * DIA / XNU
      WRITE(6,13) POS1,POS2
      WRITE(6,26) GPM,DIR,TO,TIN,DELT,DELTM
      WRITE(6,21)
      WRITE(6,22)
      WRITE(6,23) REY,REYIN,REYO,RICH,RICHIN,RICHO,AMIXL,AMIXI,AMIXO,
     +            FLOW
      WRITE(6,24)
      WRITE(6,22)
      WRITE(6,25) VEL,DIFUS,DIFIN,DIFO,XNU,XNUIN,XNUO,
     +            ROW,ROWIN,ROWO
      WRITE(6,27)
      WRITE(6,28) HEIGHT,DIA,HD,NSLAB,DELX,AREA
      WRITE(6,29)
      WRITE(6,4) (TEXP(I), I = 1, IEND)
      WRITE(6,14)
C
C  START LOOPING TO FIND THE BEST INLET EDDY CONDUCTIVITY
C
      EEXIT = 1
      AMIXEX  = EEXIT * AMIXL
      DO 100 EINLET = 1, 2000, 100
           AMIXIN = EINLET * AMIXL
           WRITE (6,1) EINLET,EEXIT
           DO 300 M = 1, NSLAB
  300           T(M) = TO
           ACCUMT = 0.0
           ACCUMB = 0.0
           TEST = 0.0
           TIME = 0.0
           FLAG = 1.0
  400      TIME = TIME + DELTM
           CALL TANK
           IF (TIME.LT.FINISH) GO TO 400
C
C     SUM UP THE ERROR BETWEEN THE EXPERIMENTAL VALUE AND
C          SIMULATED VALUE AT EACH POINT
C
           ERROR = 0.0
           DO 500 N = 1, IEND
                IF (CHOICE.EQ.1) THEN
                     IF ((N.GE.POS1).AND.(N.LE.POS2)) THEN
                          ERROR=ERROR+ABS(TEXP(N)-TOUT(N))
                     END IF
                ELSE
                     IF ((N.GE.POS1).AND.(N.LE.POS2)) THEN
                          ERROR=ERROR+ABS(TEXP(N)-T(N))
                     END IF
                END IF
  500      CONTINUE
           WRITE (6,5) ERROR,XMIN
C
C     PERFORM ERROR TEST TO SEE IF ACCUMULATED ERROR HAS DECREASED
```

```
C          IF SO, SAVE EINLET AND ERROR VALUE
C
           IF (ERROR.GT.XMIN) THEN
                ETEST = 0.25 * XMIN + XMIN
                IF (ERROR.GT.ETEST) GO TO 900
                GO TO 100
           ELSE
                IF (CHOICE.EQ.1) THEN
                    WRITE (6,4) (TOUT(II), II = 1, IEND)
                ELSE
                    WRITE (6,4) (T(II), II = 1, IEND)
                END IF
                XMIN = ERROR
                SINLET = EINLET
                SEXIT = EEXIT
                WRITE (6,2) ERROR,SINLET,SEXIT
           END IF
  100 CONTINUE
  900 IF (PICK.EQ.1) WRITE (6,6)
      IF (PICK.EQ.2) WRITE (6,8)
      IF (PICK.EQ.3) WRITE (6,12)
      WRITE (6,2) XMIN,SINLET,SEXIT
   26 FORMAT (/,1X,'FLOW RATE = ',E10.3,' GPM',17X,'DIR = ',F3.0,
     +       /,1X,'TO = ',E10.3,' F',26X,'TIN = ',E10.3,' F',/,1X,
     +       'DELT = ',E10.3,' MIN',22X,'DELTM = ',E10.3,' MIN',//)
   21 FORMAT (40X,'DIMENSIONLESS NUMBERS',/)
   22 FORMAT (30X,'AVG TEMP',15X,'INLET TEMP',15X,'INITIAL TEMP',/)
   23 FORMAT (1X,'REYNOLDS NO :',15X,E10.3,13X,E10.3,15X,E10.3,/,1X,
     +         'RICHARDSON NO :',13X,E10.3,13X,E10.3,15X,E10.3,/,1X,
     +         'AMIX LAMINAR :',14X,E10.3,13X,E10.3,15X,E10.3,/,1X,
     +           'FLOW VALUE :',16X,E10.3,///)
   24 FORMAT (40X,'FLOW PROPERTIES',/)
   25 FORMAT (1X,'VELOCITY  FT/MIN :',10X,E10.3,/,1X,
     +   'DIFUSIVITY  SQ.FT/MIN :',5X,E10.3,13X,E10.3,15X,E10.3,/,1X,
     +    'VISCOSITY  SQ.FT/SEC :',6X,E10.3,13X,E10.3,15X,E10.3,/,1X,
     +      'DENSITY  LBM/CU.FT :',8X,E10.3,13X,E10.3,15X,E10.3,///)
   27 FORMAT (40X,'TANK PROPERTIES',/)
   28 FORMAT (1X,'HEIGHT = ',E10.3,' FT',10X,'DIA = ',E10.3,' FT',
     +        10X,'HD = ',E10.3,/,1X,'NSLAB = ',I4,20X,'DELX = ',
     +        E10.3,' FT',9X,'AREA = ',E10.3,' SQ.FT',///)
   29 FORMAT (25X,'EXPERIMENTAL TEMPERATURE DATA',///)
   13 FORMAT (/,10X,'SIMULATION OF EXPERIMENTAL DATA FOR ',
     +     'ADOLY EXP61',/,15X,
     +     'ERROR TEST BETWEEN ',F4.0,'  AND  ',F4.0,///)
   14 FORMAT (////,25X,'DETERMINE THE BEST INLET EDDY CONDUCTIVITY',/)
    1 FORMAT (//,1X,'EINLET = ',F7.2,15X,'EEXIT = ',F7.2)
    2 FORMAT (/,10X,'*********',8X,'ERROR = ',E11.4,8X,'*********',
     +        /,10X,'SINLET = ',F7.2,6X,'SEXIT = ',F7.2,/)
    4 FORMAT (8(3X,F6.2))
    5 FORMAT (/,8X,'ERROR = ',E11.4,10X,'XMIN = ',E11.4,/)
    6 FORMAT (///,5X,'THE BEST EINLET FOR LINEAR FUNCTION IS:')
    8 FORMAT (///,5X,'THE BEST EINLET FOR HYPERBOLIC FUNCTION IS:')
   12 FORMAT (///,5X,'THE BEST EINLET FOR EXP NEG FUNCTION IS:')
   31 FORMAT (F7.3,2X,I3,3X,F6.2,2X,F7.3,2X,F7.3,2X,F9.5,2X,F9.5)
```

```
   32 FORMAT (F8.3,2X,F8.3,2X,I3)
   33 FORMAT (F7.2)
      END
C
C
C ***************************************************************************
C                                                                            *
C          SUBROUTINE TANK TO CALCULATE TEMPERATURES                         *
C                                                                            *
C ***************************************************************************
C
      SUBROUTINE TANK
C
C --- PRELIMINARIES
C
      COMMON
     1/VAR/A(50),B(50),C(50),D(50),ACCUMT,ACCUMB,AMIX,AMIXL,AMIXIN,
     2     AMIXEX,DELT,DELTM,DELX,DIR,EINLET,EEXIT,FLOW,ISLAB,NSLAB,
     3     NSLAB1,PICK,T(50),TEST,TEXP(50),TIN,TIME,TNEW(50),TOUT(200)
C
C   INITIALIZATION OF PARAMETERS
C
  10  DONE = TIME
      XINC = TIME - DELTM
      IF (DIR.LT.0.0) GO TO 1
      IF (DIR.GT.0.0) GO TO 2
      IF (TEST.GT.0.0) GO TO 2
C
C   UPDATE FOR FLOW INTO TOP, DIR = -1
C
    1 ACCUMT = ACCUMT + ABS(FLOW)
C
C   TEST IF FULL, THEN PULSE, AND REPACKAGE
C
      IF (ACCUMT.LT.1.0) GO TO 12
      ACCUMT = ACCUMT - 1
      TNEW(NSLAB) = TIN
      DO 100 ISLAB = NSLAB1, 1, -1
 100       TNEW(ISLAB) = T(ISLAB+1)
      DO 101 ISLAB = 1, NSLAB
 101       T(ISLAB) = TNEW(ISLAB)
C
C   APPLY CONDUCTION FOR IMPLICIT FORM FOR FLOW INTO TOP, AND REPACKAGE
C
  12  DO 102 ISLAB = NSLAB, 1, -1
            CALL SELECT
            K = NSLAB - ISLAB + 1
            B(K) =  -AMIX
            D(K) =  1 + 2*AMIX
            A(K) =  -AMIX
 102        C(K) =  T(ISLAB)
      C(1) = (1+AMIXIN) * T(NSLAB)
      C(K) = (1+AMIXEX) * T(1)
C
```

```
C   SOLVE FOR THE TEMPS USING THE TDMA ALGORITHM
C
      CALL TDMA
C
C   REASSIGN TEMP VALUES STORED IN MATRIX C FROM TDMA TO T MATRIX
C
      DO 103 ISLAB = 1, NSLAB
           K = NSLAB - ISLAB + 1
 103       T(ISLAB) = C(K)
      XINC = XINC + DELT
      IF (XINC.LT.DONE) GO TO 1
      GO TO 11
C
C   UPDATE FOR FLOW INTO BOTTOM, DIR = 1
C
   2  ACCUMB = ACCUMB + ABS(FLOW)
C
C   TEST IF FULL, THEN PULSE, AND REPACKAGE
C
      IF (ACCUMB.LT.1.0) GO TO 13
      ACCUMB = ACCUMB - 1
      TNEW(1) = TIN
      DO 104 ISLAB = 2, NSLAB
 104       TNEW(ISLAB) = T(ISLAB-1)
      DO 105 ISLAB = 1, NSLAB
 105       T(ISLAB) = TNEW(ISLAB)
C
C   APPLY CONDUCTION FOR IMPLICIT FORM FOR FLOW INTO TOP, AND REPACKAGE
C
  13  DO 106 ISLAB = 1, NSLAB
           CALL SELECT
           B(ISLAB) = -AMIX
           D(ISLAB) = 1 + 2*AMIX
           A(ISLAB) = -AMIX
 106       C(ISLAB) = T(ISLAB)
      C(1) = (1+AMIXIN) * T(1)
      C(NSLAB) = (1+AMIXEX) * T(NSLAB)
C
C   SOLVE FOR THE TEMPS USING THE TDMA ALGORITHM
C
      CALL TDMA
C
C   REASSIGN TEMP VALUES STORED IN MATRIX C FROM TDMA TO T MATRIX
C
      DO 107 ISLAB = 1, NSLAB
 107       T(ISLAB) = C(ISLAB)
      XINC = XINC + DELT
      IF (XINC.LT.DONE) GO TO 2
  11  INUM = TIME/DELTM
      IF (DIR.GT.0.0) THEN
           TOUT(INUM) = T(NSLAB)
      ELSE
           TOUT(INUM) = T(1)
      END IF
```

```
      IF (DIR.NE.0.0) TEST = DIR
      RETURN
      END
C
C
C ********************************************************************
C                                                                     *
C          SUBROUTINE TO SOLVE FOR TEMPS USING TDMA METHOD            *
C                                                                     *
C ********************************************************************
C
      SUBROUTINE TDMA
C
C --- PRELIMINARIES
C
      COMMON
     1/VAR/A(50),B(50),C(50),D(50),ACCUMT,ACCUMB,AMIX,AMIXL,AMIXIN,
     2     AMIXEX,DELT,DELTM,DELX,DIR,EINLET,EEXIT,FLOW,ISLAB,NSLAB,
     3     NSLAB1,PICK,T(50),TEST,TEXP(50),TIN,TIME,TNEW(50),TOUT(200)
C
C
      DO 10 L = 2, NSLAB
           V = B(L) / D(L-1)
           D(L) = D(L) - V * A(L-1)
  10       C(L) = C(L) - V * C(L-1)
C
C    BACK SUBSTITUTION OF THE TDMA MATRIX
C
      C(NSLAB) = C(NSLAB) / D(NSLAB)
      DO 20 L = NSLAB1, 1, -1
  20       C(L) = (C(L) - A(L) * C(L+1)) / D(L)
      RETURN
      END
C
C ********************************************************************
C                                                                     *
C          SUBROUTINE TO SELECT AMIX FACTORS                          *
C                                                                     *
C ********************************************************************
C
      SUBROUTINE SELECT
C
C --- PRELIMINARIES
C
      COMMON
     1/VAR/A(50),B(50),C(50),D(50),ACCUMT,ACCUMB,AMIX,AMIXL,AMIXIN,
     2     AMIXEX,DELT,DELTM,DELX,DIR,EINLET,EEXIT,FLOW,ISLAB,NSLAB,
     3     NSLAB1,PICK,T(50),TEST,TEXP(50),TIN,TIME,TNEW(50),TOUT(200)
C
C
      XSLAB = NSLAB
      XI = ISLAB
      IF (PICK.EQ.1) THEN
          SLOPE = (EINLET-EEXIT)/(1.0-XSLAB)
```

```
      XINCEP = EINLET - SLOPE
      IF (DIR.EQ.-1) THEN
            SLOPE = -SLOPE
            XINCEP = EEXIT - SLOPE
      END IF
      AMIX = AMIXL * (SLOPE*I + XINCEP)
END IF
IF (PICK.EQ.2) THEN
      SLOPE = (EINLET-EEXIT)/(1.0-1.0/XSLAB)
      XINCEP = EINLET - SLOPE
      IF (DIR.EQ.-1) THEN
            SLOPE = -SLOPE
            XINCEP = EEXIT - SLOPE
      END IF
      AMIX = AMIXL * (SLOPE/XI + XINCEP)
END IF
IF (PICK.EQ.3) THEN
      SLOPE = (EINLET-EEXIT)/(EXP(-1.0)-EXP(-XSLAB))
      XINCEP = EINLET - SLOPE*EXP(-1.0)
      IF (DIR.EQ.-1) THEN
            SLOPE = -SLOPE
            XINCEP = EEXIT - SLOPE*EXP(-1.0)
      END IF
      AMIX = AMIXL * (SLOPE*EXP(-XI) + XINCEP)
END IF
RETURN
END
```

APPENDIX C

TEMPERATURE EVALUATION FROM CONDUCTIVITY PROBE

The temperature evaluation from the voltage produced by the conductivity probe is calculated from the following steps:

(1) Obtain the flow rate and maximum percent salt solution. Equation (C.1) can be used to calculate the maximum density of the salt solution, where density of salt is 134.8 lbm/ft^3 and density of 60 ^oF water is 62.37 lbm/ft^3.

$$\rho_{sol} = 134.8 \left(\frac{\% \text{ SALT}}{100}\right) + 62.37 \left(1 - \frac{\% \text{ SALT}}{100}\right) \qquad (C.1)$$

Next calculate the maximum density difference between the salt solution and the fresh water at 60 ^oF. Equation (C.2) can be used to calculate the maximum density difference.

$$\Delta\rho_{sol} = \rho_{sol} - 62.37 \qquad (C.2)$$

The corresponding thermal density of the initial water in the tank is obtained from Equation (C.3).

$$\rho_o = 62.37 - \Delta\rho_{sol} \qquad (C.3)$$

The initial temperature is obtained from an empirical equation as a function of density derived from the least squares method shown in Equation (C.4). A plot of temperature versus density is presented in Figure 55. Equation (C.4) is used in four different density regions resulting in four sets of coefficients as shown in Table VI.

$$T = X1 + X2 (\rho_{sol}) + X3 (\rho_{sol})^2 \qquad (C.4)$$

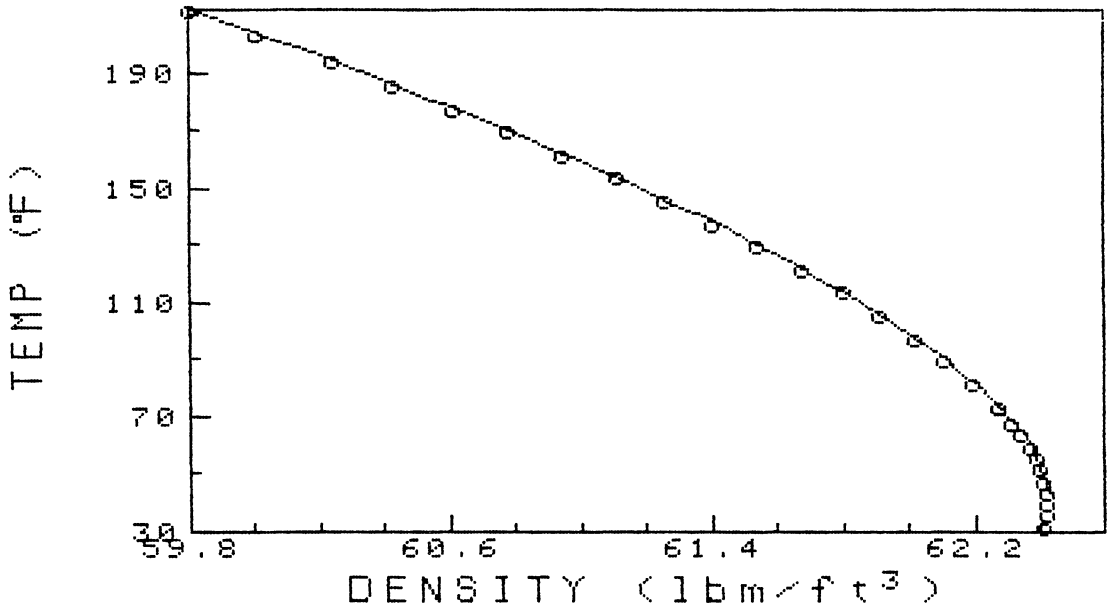

Figure 55. Least Squares Curve of Temperature Versus Density

TABLE VI

LEAST SQUARES COEFFICIENTS FOR TEMPERATURE VERSUS DENSITY

Region	Temperature Range ^{o}F	X1	X2	X3
1	44-60	33167	-777.80	3.9602
2	60-90	-239330	7809.5	-63.671
3	90-150	-62337	2091.4	-17.479
4	150-212	-12938	478.55	-4.3252

The inlet density is assumed as 62.37 lbm/ft^3 corresponding to an inlet temperature of 60 ^oF.

(2) After the inlet and initial properties are evaluated in Step 1, the outlet temperature must be determined from the output voltage. Figure 39 shows a plot of percent salt versus output voltage. An empirical equation for percent salt as a function of output voltage obtained from the least squares method is shown in Equation (C.5). This equation is used in three regions and the coefficients are tabulated in Table VII

$$\% \text{ salt} = Y1 + Y2 \text{ (voltage)} + Y3 \text{ (voltage)}^2 \qquad \text{(C.5)}$$

After obtaining the percent salt from Equation (C.5), the density of the salt solution is calculated from Equation (C.1). The density difference is then obtained from Equation (C.2). Using this density difference and the initial density of the solution obtained from Equation (C.3), the corresponding thermal density is calculated from Equation (C.6)

$$\rho_{sol} = \rho_o + \Delta\rho_{sol} \qquad \text{(C.6)}$$

Once the density is known, the outlet temperature can be obtained from Equation (C.4).

TABLE VII

LEAST SQUARES COEFFICIENTS FOR
PERCENT SALT VERSUS VOLTAGE

Region	% Salt Range	Y1	Y2	Y3
1	0-0.5	1.1599×10^{-3}	0.11157	0.10032
2	0.5-1.0	1.7406	-1.7753	0.61182
3	1.0-2.0	-1.6551	0.39695	0.29726

VITA

Fred John Oppel III

Candidate for the Degree of

Master of Science

Thesis: COMPUTER SIMULATION FOR STRATIFIED THERMAL STORAGE

Major Field: Mechanical Engineering

Biographical:

Personal Data: Born in Kingfisher, Oklahoma, December 13, 1959, the son Mr. and Mrs. Fred J. Oppel, Jr.

Education: Graduated from Kingfisher High School, Kingfisher, Oklahoma, May, 1978; received the Bachelor of Science in Mechanical Engineering degree from Oklahoma State University, May, 1983; completed the requirements for the Master of Science degree at Oklahoma State University, July, 1985.

Professional Experience: Graduate research assistant and teaching assistant, School of Mechanical Engineering, Oklahoma State University, 1983-1985; registered Engineer Intern (EIT), State of Oklahoma.

Professional and Honorary Societies: American Society of Mechanical Engineers; National Society of Professional Engineers; Tau Beta Pi; Pi Tau Sigma.